Maria do Carmo da S. Pereira

Electrochemical Analysis and Histological

Maria do Carmo da Silva Pereira

ELECTROCHEMICAL ANALYSIS AND HISTOLOGICAL EFFECTS OF STAINLESS STEEL CORROSION PRODUCTS IN BLOOD FILTRATION ORGANS: AN EXPERIMENTAL STUDY IN MICE

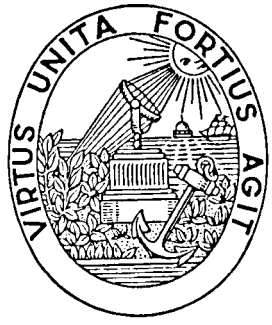

FACULDADE DE ENGENHARIA

UNIVERSIDADE DO PORTO

PORTO 1997

ELECTROCHEMICAL ANALYSIS AND HISTOLOGICAL EFFECTS OF STAINLESS STEEL CORROSION PRODUCTS IN BLOOD FILTRATION ORGANS: AN EXPERIMENTAL STUDY IN MICE

by

Maria do Carmo da Silva Pereira

A thesis submitted to the University of Oporto for the degree of Ph.D. in

Chemical Engineering

Faculty of Engineering

Oporto University

1997

RESUMO

Os iões metálicos podem afectar o bem estar humano de várias formas. Alguns desses metais como o ferro, crómio e níquel têm um papel importante na vida. O organismo regula o seu metabolismo e excreção, uma vez que as suas necessidades são bem estabelecidas. A presença de um implante metálico altera o equilíbrio natural devido à libertação de produtos de corrosão através do organismo que podem acumular em orgãos vitais. Utilizou-se como modelo animal o ratinho, para estudar a acumulação e os efeitos histológicos provocados individualmente pelos produtos de corrosão maioritários do aço inoxidável, isto é, níquel, crómio e ferro, no fígado, rim e baço.

A voltametria de redissolução com adsorção (AdSV) de onda quadrada utilizando microeléctrodos de filme de mercúrio (MFM) foi desenvolvida e optimizada para quantificar a acumulação destes metais nos orgãos dos ratinhos atrás referidos, que foram subcutaneamente injectados com soluções dos metais dissolvidos. A exactidão do método proposto foi verificada comparando os resultados obtidos por espectrometria de absorção atómica (EAA), não se verificando discrepâncias significativas entre eles.

Os resultados analíticos demonstraram uma acumulação significativa destes metais no fígado, rim e baço, comparativamente aos animais controlo. Depois de quatro semanas de tratamento menos de 1% de crómio e níquel injectado é acumulado nos três orgãos enquanto cerca de 22% de ferro ficou retido nestes orgãos.

Da análise histológica, o níquel foi o metal que provocou alterações morfológicas que poderão ser causa de preocupação.

ABSTRACT

Metal ions affect the human well-being in several manners. Some of these metals such as iron, chromium and nickel play an important role in life. The body regulates its metabolism and excretion, once their needs are well established. The presence of a metallic implant changes its natural equilibrium due to the release of corrosion products throughout the body that may accumulate in vital organs. An animal model is used to study the accumulation and the histological effects provoked individually by the stainless steel major corrosion products, *i.e.*, nickel, chromium and iron in the mice liver, kidney and spleen.

Adsorptive stripping voltammetry (AdSV), employing the square wave mode coupled with mercury film microelectrodes (MFM), was developed and optimised to quantify these metal ions accumulation in the referred mice organs, subcutaneously injected with solutions of dissolved metals. The accuracy of the proposed method was checked by comparing the results for the three metals with those obtained by atomic absorption spectrometry (AAS) and no significant discrepancies between both techniques were found.

The analytical results demonstrated a significant accumulation of these metals with time in the liver, kidney and spleen, compared to the control animals. After four weeks of treatment less than 1% of the chromium and nickel injected is accumulated in the three organs whereas for iron near 22% was retained by these organs.

From the histological analysis, nickel was the metal that provoked morphological alterations that may be a cause of concern.

RÉSUMÉ

Les ions métalliques feignent le bien-être humain de diferentes manières. Quelques de ces métaux comme le fer, le chrome et le nickel ont un rôle important pour la vie. L'organisme régle leurs metabolismes et excrétion, car ses nécessités sont bien établies. La présence d'un implant métallique change l'équilibre naturel dû à la libération de produits de corrosion qui peuvent s'accumuler dans des organes vitaux. Un modèle animal a été utilisé pour étudier l'accumulation et ses effets histologiques provoqués individuellement par les produits du l'acier inoxydable, c'est-à-dire, le nickel, le chrome et le fer, dans le foie, le rein et la rate des rats.

La voltametrie par redissolution avec adsortion (AdSV) de onde carré en microélectrodes de filme de mercure (MFM) a été developpée et optimisée pour mésurer l'accumulation de ces métaux dans les organes des rats déjá cités, qui ont été sous-cutanément injectés avec des solutions des métaux dissolus. L'exactitude de la méthode proposée a été verifiée en comparant les résultats obtenus par spectrométrie de absortion atomique (AAS) et aucune différence significative a été registée entre eux.

Les résultats analytiques ont démontré une accumulation significative de ces métaux dans le foie, le rein et la rate, en comparaison avec les animaux de contrôle. Aprés quatre semaines de traitement moins de 1% de chrome et de nickel injecté sont accumulés dans les trois organes cependant presque de 22% de fer est resté accumuler dans ces organes.

Par analyse histologique, le nickel a été le métal qui a provoqué des altérations morphologiques qui pourront être la cause de préoccupation.

ACKNOWLEDGMENTS

I wish to express my sincere gratitude to my supervisor Prof. João Paulo Sousa for his support, understanding and encouragement during these years.

I would also like to thank and express my sincere gratitude to Prof. Maria de Lourdes Pereira from Departamento de Biologia da Universidade de Aveiro for her collaboration and support, as well as her friendship.

Special thanks go to my friend Simone Morais for many "Cientific fruitfull" discussions. I appreciated her company in the experimental work at the INEB. Many thanks to my other friends from INEB for creating a very pleasant work environment.

I would like to express my gratitude to my husband, Pedro and my parents for their love, unconditional support, encouragement and of course lots of patience throughout the work which has led to the present thesis.

My apologises to my daughter, Ana Teresa, for the time that I could not spend with her, during the writing of the thesis.

Finally, I would like to thank to JNICT through Programmes CIENCIA and PRAXIS XXI for the financial support (grant ref. BD/2643/93).

PREFACE

The experimental work presented in this thesis was performed in the INEB-Instituto de Engenharia Biomédica and Departamento de Biologia da Universidade de Aveiro, Portugal, during the period from 1993 to 1996, and the results presented were based and published in the following papers:

M. C. Pereira, J. L. Faria, M. L. Reis and J. P. Sousa, "Nickel quantification in mice organs by adsorptive stripping voltammetry using mercury microelectrodes", *Electroanalysis*, **9** (1997) 150-154.

M. C. Pereira, M. L. Pereira and J. P. Sousa, "Evaluation of nickel toxicity on liver, spleen and kidney of mice after administration of high-dose metal ion", in press at *Journal of Biomedical Materials Research* (1997).

M. C. Pereira, M. L. Pereira and J. P. Sousa, "Adsorptive stripping voltammetric measurements of chromium accumulation in mice organs using mercury film microelectrodes", *Electroanalysis,* **9** (1997) 941-944.

M. C. Pereira, M. L. Pereira and J. P. Sousa, "Individual effects of chromium in the stainless steel implants degradation: an experimental study in mice" submitted (1997).

M. C. Pereira, M. L. Pereira and J. P. Sousa, "Adsorptive stripping measurements of iron accumulation in mice kidney using microelectrodes and histological features", in press at *Journal of Trace Elements in Medicine and Biology* (1997).

M. C. Pereira, M. L. Pereira and J. P. Sousa, "Histological effects of iron accumulation on mice liver and spleen after administration of a metallic solution", submitted (1997).

In addition, the Ph.D. project has resulted in another papers which are only partially included in the thesis:

M. L. Pereira, M. C. Pereira and J. P. Sousa, "Evaluation of nickel effects on mouse liver: tissue response and metal ion accumulation", *Biomedical Letters*, **52** (1995) 235-244.

M. C. Pereira and J. P. Sousa, "Quantification of nickel species in physiological media using microelectrodes", *Portugaliae Electrochimica Acta*, **13** (1995) 477-482.

M. C. Pereira and J. P. Sousa, "Determination of total iron in biological sample solutions with mercury microelectrodes", *Portugaliae Electrochimica Acta*, **14** (1996) 273-278.

M. C. Pereira, M. L. Pereira and J. P. Sousa, "Measurements of chromium accumulation in mice liver by adsorptive stripping voltammetry using mercury film microeletrodes", in *Chemical and Biological Sensors and Analytical Electrochemical Methods*, A. J. Ricco, M. A. Butler, P. Vanysek, G. Horvai and A. F. Silva (eds.), The Electrochemical Society, New Jersey, (1997) 498-503.

CONTENTS

Chapter 1

INTRODUCTION

1

INTRODUCTION

In Europe and in the United States more than 100 million people are over the age of 50 years [1]. With age the quality of skeletal tissues suffer a progressive deterioration and the occurrence of bone diseases, normally osteoarthritis, augment [2] with consequent incidence of broken long bones and joints, especially the hip. Today, the quality of life of people with bone diseases was greatly improved by a large development in the use of orthopaedic implants.

Metallic implants for orthopaedic applications have a remarkable success with thousands being implanted annually [3,4]. The stainless steel AISI 316L became

the standard material of choice for internal fracture fixation devices for short term function or for the life of the patient as in total joint replacements because of its compatibility with body tissues and superior mechanical properties [5]. It is a relatively inexpensive material that can be easily manufactured in different shapes for different applications [6,7]. Its main constituents are iron, chromium and nickel, all of which are biologically essential trace elements to life once they play a significant role in normal metabolic processes [8]. In AISI 316L type stainless steel [9] the proportion of nickel is 10-14% to assure a fully austenitic microstructure, 16-18% of chromium was added in combination with 2-3% of molybdenum to stabilise the passive film of Cr_2O_3 in the presence of chlorides and to improve the resistance of pitting and crevice corrosion [10,11]. The maximum percentage of other constituents present is this alloy are manganese 2.0%, silicon 1.0%, phosphorus 0.045%, carbon 0.03% and sulphur 0.03%. Iron is the balance and corresponds to 61-69% in the alloy [12].

Corrosion of metallic implants

Corrosion could be explained by the destruction of metallic structures by the action of the surrounding medium. Body fluids are highly corrosive saline solutions. Consequently, all metals implanted into the body form corrosion

products [13]. These products range from fine metal particles of varying sizes, metal ions that forms a varieties of salts and complexes with biological elements [14,15,16,17,18]. The rate of corrosion is governed by factors such as material properties, implant design, metal solubility, pH of environment, concentration of the metal, negative ions with special attention to chloride and oxygen [19,20]. It also depends on the surface area of the implant, its surface treatment and passivation by oxygen [21,22] as well as the surgery and the patient conditions [21]. The metallic implant itself responds to corrosive forces by surface and internal metallic structural irregularities called pitting, crevice and fretting corrosion, respectively [21,23,24]. These may weaken the metal or alloy and under mechanical repetitive bending stresses and loads lead to fatigue failure of the implant. It is of clinical practice the immersion of 316L stainless steel implants in solutions of HNO_3 to improve the corrosion resistance by increasing the thickness of the passive film [25].

Despite the high corrosion resistance generally found in stainless steel, there is evidence that metal ions are released and accumulated into adjacent tissues [10,13,26,27,28,29] and may probably initiate systemic effects upon their distribution in the body.

Surface modification of metals, by means of ion implantation and sputter coating are being developed and are a promising to minimise or even eliminate the biodegradation phenomenon [30].

Transport and distribution of corrosion products

The distribution of ions released during the corrosion process of metallic implants will depend on the corrosion rate, their interaction with extracellular proteins, their diffusion through the tissues, their ability to pass through cell membranes, their intracellular toxicity and valence state.

Several studies were done with the intention to clarify the transport and distribution of the corrosion products throughout the body. Some animal models were proposed since it is complicated and sometimes impossible to obtain information about this subject in patients carrying metallic implants. Frequently, in these animal models it is quite difficult to reproduce the slow and continuous release of metal ions into the body. Normally, in the animal models the time of implantation is often very short, at most months or weeks, compared to the implants life-time and usually it employs high dose metal salts or corrosion products administered intramuscularly or subcutaneously. However, useful information were obtained in these studies which are summarised below.

In 1980, Dobbs and Minski [16] determined the concentration of chromium, nickel, iron, cobalt, molybdenum and zinc using neutron activation analysis from an old female at necropsy who had bilateral cobalt-chromium-molybdenum total hip replacements. The measurements indicated that the concentrations of chromium and cobalt in the kidney, spleen, liver and lung were up to fifty times the "Standard Man" values. High values occurred also in the urine and in the hair. Cobalt predominated in the urine whereas chromium predominated near the implants.

Black *et al.* [31] obtained serum from 15 patients before undergoing conventional total hip replacement and for periods up to six months post-operatively. Chromium levels in serum were found to rise to a pronounced post-operative peak and then diminish, but did not fall to normal mean levels by six months. On the other hand serum cobalt levels either remained the same or decreased while serum nickel levels began to rise six weeks after surgery.

The binding of metal ions from salts and corrosion products of stainless steel to blood cells and serum proteins was studied *in vitro* by Merritt *et al.* [32]. Metal salts were added to whole blood and then separated into red cells, white cells and serum. These authors have observed that nickel bound in very small quantities to blood cells. Trivalent chromium bound to cells in very small quantities whereas hexavalent chromium from potassium dichromate and corrosion products showed

very high binding to red cells and some binding to white cells. In a second series of experiments the blood was separated into its components and then the metal salts were added, being the binding pattern identical. Analysis of the serum revealed that almost all of the metals studied were detected in the albumin region indicating strong binding to albumin [33] providing an explanation for the rapid dissemination of metals through the body.

The same authors [34] have done *in vivo* experiments in hamsters intramuscularly injected with metal salts and corrosion products from stainless steel in order to evaluate the transport of metal ions away from the injection site and the binding of the metals to blood cells. After injections the animals were bled at 0 time and 2, 4, 6, 24, 48 and 96 h. The results showed that metals are rapidly transported from the intramuscular site with high levels in the blood by 2 h. The level of metal in the blood varied considerably with nickel being transported in high concentration to the blood and trivalent chromium being transported less to the blood. The highest amount of cell binding was observed with hexavalent chromium.

A series of experiments performed by the same group [35] were conducted to study *in vitro* and *in vivo* metal ion release and the urine excretion of metal ions. Metal salts were injected and corrosion products of stainless steel, obtained by application of a fixed anodic potential, were injected and urine was analysed. The

excretion of metals following salt injection or corrosion products was very similar. All the nickel was rapidly excreted, while only less than 50% of the chromium was excreted.

Other study [36] was conducted to determine the ability of hamsters to eliminate in the urine or store in the organs, large quantities of metal salts given over a period of several months. The results indicated that nickel was rapidly eliminated in the urine and its levels in the liver, kidney, spleen, and lung was similar to that of control animals. Chromium was eliminated in the urine very slowly, being red blood cell associated and the levels were elevated in all the organs compared to control.

In vivo transport and excretion of corrosion products from accelerated anodic corrosion of porous coated F75 alloy (58-63% iron, 27-30% chromium, 5-7% molybdenum and 2.5% nickel), subcutaneously implanted in hamsters was also studied [37,38]. The results demonstrated a rapid and complete excretion of nickel and molybdenum. Most of the cobalt was excreted, with elevation in liver, kidney, and lung. Chromium excretion was much lower due to significant red cell binding and *in vivo* storage especially in the kidney and spleen.

Recent studies performed by the same authors [39,40] have demonstrated that hexavalent chromium is released from the implants containing this metal and became red blood cell associated and was rapidly reduced to the trivalent form.

A model using implanted pins made of 316L stainless steel in rabbits during 28 weeks was developed by Smith and Black [41] to investigate the systemic transport and distribution of iron and chromium corrosion products. The results, obtained by atomic absorption spectrometry, indicate that the iron concentration in plasma is increased and also that elevated iron concentrations were found in liver of rabbits having higher surface areas of implanted 316L. Results from analysis of kidney and liver iron concentrations are consistent with a model of chronic low-level iron overload. Plasma chromium concentrations were likewise significantly elevated, apparently as a function of implanted 316L surface area and duration of implantation. Liver chromium concentrations reflected an ability of the liver to accumulate excess of chromium.

Pereira *et al.* [42] injected mice subcutaneously with stainless steel corrosion products each 72 h for 10 and 14 days. This study showed that chromium, but not iron or nickel had a significant increase in treated mice liver when compared to those from the control animals. No histopathological differences between 10 and 14 days of injected animals were detected. However, massive hepatic degeneration was observed in both groups when compared to the control.

The same group also investigated the accumulation of iron, chromium and nickel in organs associated with blood filtration, following intraperitoneal injections of a stainless steel solution. Mice were sacrificed at 4, 16, 24 h and 1, 2,

4, 8 and 16 weeks [43] after injection. In contrast to a sharp peak of iron detected in kidney after 24 h, the iron accumulated steadily in both the spleen and the liver. High chromium accumulation was observed in the spleen for 2 weeks and in the liver for 6 weeks after which both organs were cleared of this metal. A small amount of chromium was detected in the kidney after 8 weeks. Some nickel was detected in the spleen and the kidney, but after 4 weeks the spleen was clear of this metal.

Systemic effects of corrosion products

Black [13] stated that the corrosion products are biologically active, and that patients exhibit symptoms due to these corrosion products. With prolonged implantation time, the possibility of long term effects due to low level species release from implanted materials was discussed by the same author [21,31,44]. The possible systemic effects detected were metabolic, carcinogenic, immunologic and bacteriologic effects:

a) metabolic effects

The major constituents of stainless steel are essential biological trace elements

that play a very important role in metabolic process. Moreover, all metals are toxic if present in high quantities. The degree of toxicity is dependent of the dose and the oxidation state of the metal. Thus, a systemic alteration in the normal physiological process of an element may manifest itself as a corresponding change in the metabolic process which is intimately dependent upon precise trace element concentration and balance.

b) carcinogenic effects

Nickel and hexavalent chromium are in the list of materials which have proven to be carcinogenic [45]. High iron levels are associated with increased risk of death from cancer [46,47]. These metals are the alloying elements of stainless steel. There have been reports of malignant tumours arising in the tissues adjacent to metallic implants in man after a long implantation time [48,49,50]. Also, remote site tumours have been reported with implantation of clinical metal alloys in rats and these animals showed an apparent relationship between nickel release and tumour incidence [51,52]. Nevertheless, the important preoccupation is the potential carcinogenic effects in the other parts of the body where the tissues are more sensitive to develop tumours.

c) bacteriologic effects

Trace elements are known to be important in bacterial metabolism. It is recognised that one response to systemic infections is a rapid reduction in serum iron concentration [53] negating the access of this metal to the metabolism of bacteria. The presence of implants made of stainless steel produces elevated serum iron concentrations and enhance infection locally and systemically [44].

d) immunologic effects

Activation of the immune system involves recognition of specific invaders named antigens that may be corrosion products. Lymphocytes are the functional units of the immune system and some types of lymphocyte produce antibodies in response to the recognition of a particular antigen. Antibodies bind to antigens to promote destruction of the antigen [54].

There are clear clinical evidences of hypersensitivity to metallic biomaterials [55,56,57,58]. *In vitro* and *in vivo* studies have demonstrated that nickel and iron inhibit the functional activity of human immune cells [59,60].

The cells of the immune system are disseminated throughout the body either as isolated cells, diffuse aggregations or within the lymphoid organs, thymus lymph

nodes and spleen. The remote effects to the site of implant must be taken seriously once several studies have shown that nickel, iron [61] and chromium accumulated in spleen with some histological alterations mainly with metallic nickel [62].

HISTOPHYSIOLOGICAL ASPECTS OF MICE ORGANS

The metal alloys used in implantalogy are constituted by at least three different elements in significant quantities which have different behaviour and properties when released in the body. It is not so easy to correlate specific histological features with the metal ions present in the alloy. The proposed study uses pure metals to differentiate between the histological effects provoked individually by the alloying elements of stainless steel.

For a best understanding of this work, some morphological and functional features of the organs directly related with the blood filtration, *i.e.*, liver, kidney and spleen are presented.

Liver: functions and structure

The liver is the largest gland in the body and is involved in metabolic functions. It is located in the upper right quadrant of the abdominal cavity and, in addition to

the supply of arterial blood from the hepatic arteries, it also receives a major supply of blood from veins of the digestive tube, pancreas and spleen via the hepatic portal vein [63]. The major functions of the liver are the detoxification of metabolic waste products; destruction of spent red cells and recovery of their constituents alone and in conjunction with the spleen, synthesis and secretion of bile into the duodenum via the biliary system and synthesis of the plasma proteins and lipoproteins [64].

The liver is divided into four lobes and surrounded by a capsule of fibrous connective tissue. The *hepatocytes* are the principal cells of this organ, constitutes about 80% of the cell population in the liver, and most of the liver functions are performed by them [63]. The *hepatocytes* are arranged in structures called *lobules*. The *lobules* are roughly hexagonal in shape, reflecting a compact, regular, polyhedral shape in three dimensions (Figure 1.1). It is found at the angles of the polygon the *portal tracts* that are constituted by the portal vein, hepatic artery and bile duct. The central structure of the lobule is the *central vein* and passes across it long axis. The *hepatocytes* are radially arranged in plates of one cell thick from the central vein to the perimeter of the *lobule* and are separated by the *hepatic sinusoids* which are also organised around the *central vein* as the *hepatocytes*. Blood flows between the plates of *hepatocytes*, therefore each cell is bathed by blood at least on two sides [64]. The *hepatic sinusoids* are irregularly dilated vessels whose calibre is larger than the diameter of regular capillaries. These

vessels provide the exchange of substances between the blood and liver parenchyma. *Sinusoids* are lined by phagocytic cells commonly called *Küpffer cells*. The cytoplasm of these cells contains fragments of red blood cells and iron in the form of ferritin, indicative of their functions in the red blood cell breakdown [63].

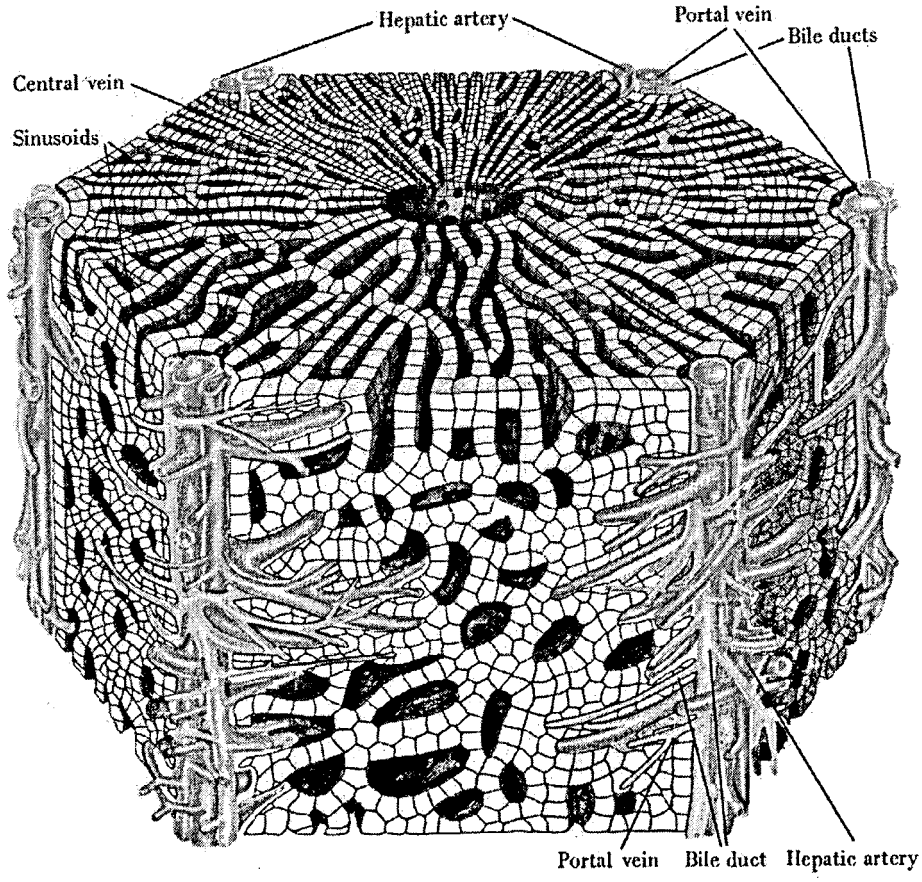

Figure 1.1. Schematic diagram of the liver lobule with the portal tracts at each of the corners [63].

Kidney: functions and structure

The kidneys are highly vascular organs located in the retroperitoneal tissue of the posterior abdominal cavity and is a bean-shaped organ. The kidney functions are related with excretion, electrolyte and water balance. Thus, filtration of most relatively small molecules from blood plasma to form a filtrate, selective reabsorption of most of the water and other molecules from the filtrate, leaving behind excess and waste materials to be excreted and secretion of some excretory products directly from blood into the filtrate occur in this organ. The kidneys are also involved in two homeostatic mechanisms which are mediated via hormones [65,66].

Blood is supplied to each kidney by renal arteries which arise from the aorta and the total blood volume of the body is circulated through the kidneys about 300 times each day [65].

The kidney surface is covered by a thin capsule of firm fibrous tissue. The examination of a longitudinal renal section reveals that it is divided into two distinct regions, the *cortex* located in the outer part and the inner part called *medulla* (Figure 1.2). Approximately 90 to 95% of the blood passing through the kidney is in the cortex region [66].

The functional units of the kidney are the *nephrons*, which components are the *renal corpuscle* and the *renal tubule*.

The *renal corpuscle* is the part of the *nephron* responsible for the plasma filtration and is a spherical structure that include the beginning segment of the *nephron* and contain a unique capillary network, the *glomerulus* which invaginates in the *Bowman's capsule* and the glomerular filtrate passes into the *renal tubule*.

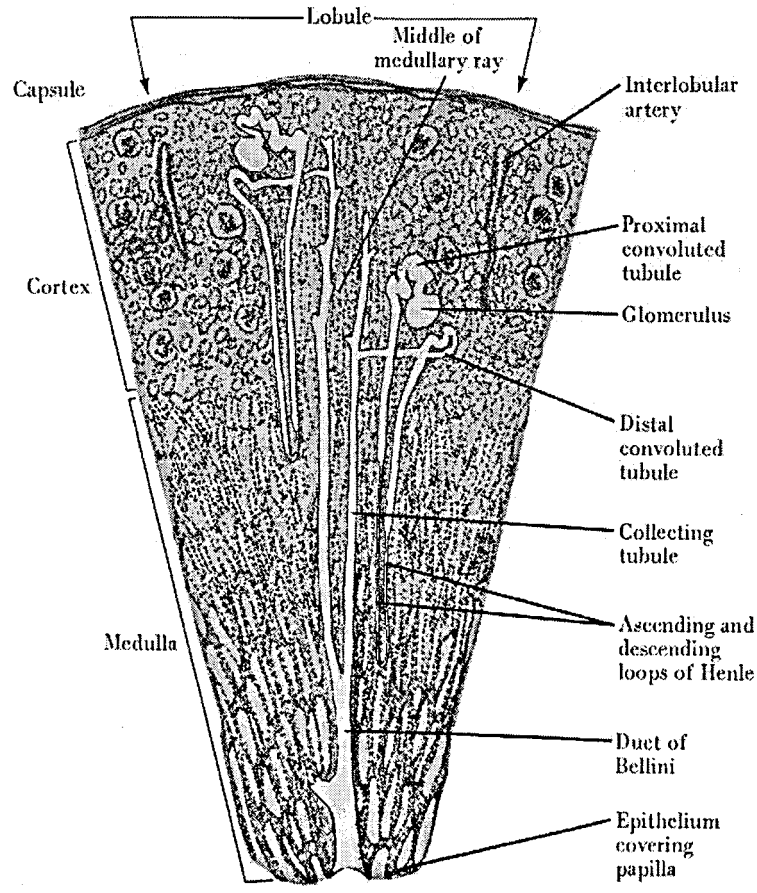

Figure 1.2. Diagram of a section of kidney showing the cortex, the medulla and two nephrons [66].

The functions of the highly convoluted *renal tubule* are the selective reabsorption of water, inorganic ions and other molecules from the glomerular filtrate. It is composed by four distinct histo-physiological zones, each of which has a different role in the renal metabolism. The *proximal convoluted tubule* is the longest and most convoluted section of the *renal tubule*, the *loop of Henle* arises from the *proximal convoluted tubule* as a straight, thin walled limb which descends from the *cortex* into the *medulla*, the *distal convoluted tubule* and in the terminal zone the *collecting tubule* that conducts urine to the collecting ducts which merge to form the large *ducts of Bellini* in the *medulla*.

Spleen: functions and structure

The spleen is a large lymphoid organ situated in the upper left part of the abdomen. It receives a rich blood supply via a single artery, the splenic artery, and is drained by the *splenic vein* into the hepatic portal system [67].

The spleen is involved in removal of particulate matter from circulating blood, production of immunological responses against blood-born antigens, removal and destruction of aged and defective blood cells from circulation and also has the ability to hold large volumes of red blood cells in reserve [67,68].

The spleen has a dense *capsule* of connective tissue from which *trabeculae* extend into the organ (Figure 1.3) containing myofibroblasts [69]. *Trabeculae* conduct larger arteries and veins throughout the spleen and provide major structural support for the fine reticulin network which extends throughout the organ. Macroscopically, the spleen appears to consist of discrete white nodules, called *white pulp*, embedded in a red matrix called the *red pulp*, that constitutes 75% of the volume of this organ [68] and contains large numbers of red blood cells.

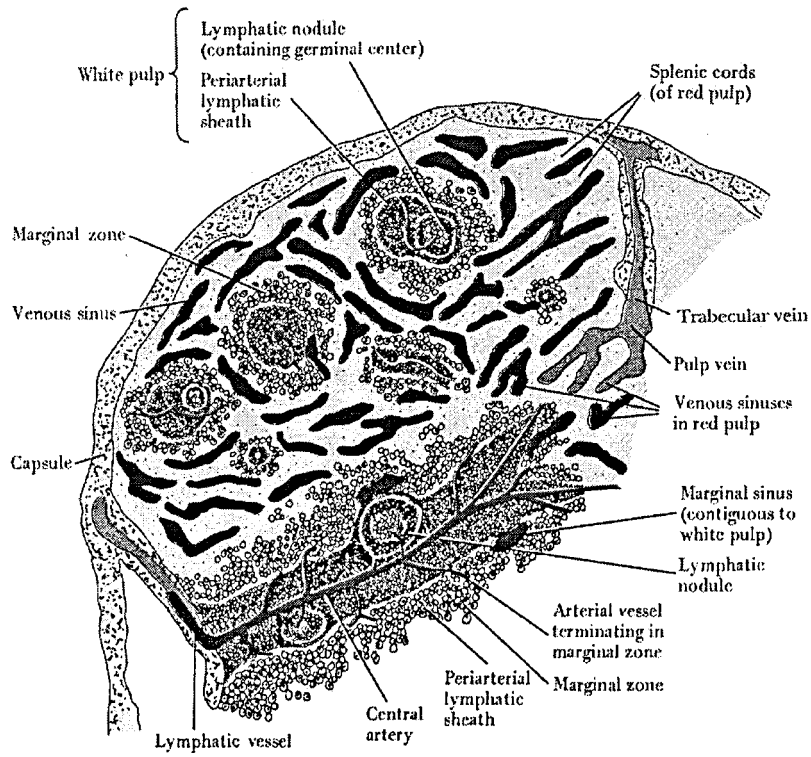

Figure 1.3. Schematic diagram showing the features of the spleen that are evident in a histological section [69].

The *white pulp* consists of a cylindrical mass of lymphatic tissue arranged around a central artery. This mass of lymphocytes constitutes the *periarterial lymphatic sheath* and is surrounded by less densely packed lymphocytes that constitute the *marginal zone*. *Lymphatic nodules* occur along the of the *periarterial lymphatic sheath.*

The red pulp consists of *splenic sinuses* separated by the *splenic cords* or *cords of Billroth.* The *splenic cords* consist of reticular fibres and cells containing large numbers of erythrocytes, macrophages, etc. Many of the macrophages are engaged in the phagocytosis of damaged red blood cells. The iron from degenerating red blood cells is employed in the formation of new red blood cells and the macrophages begin the process of haemoglobin breakdown with the recovery of iron [69].

The *splenic* or *venous sinuses* are special sinusoidal vessels that are lined by unusually shaped endothelial cells [67].

ADSORPTIVE STRIPPING VOLTAMMETRY

Trace analysis requires a sufficient selective and sensitive method with a sufficient high signal-to-noise ratio to determine trace elements of various matrices, sometimes, in the presence of other substances, present in higher

concentrations which may act as interferences suppressing the signal of the element to be analysed. Generally, it is necessary to separate the analyte from the interfering substances by techniques such as extraction, chromatography, *etc.* [70,71] and consequently, the risks of contamination are bigger.

In trace analysis it is often necessary to employ some type of preconcentration step prior to analysis [72]. In the stripping voltammetry techniques this step is done directly in the sample, in which the substance to be determined is concentrated on the measuring electrode and then transferred back into the solution [73]. The improved sensitivity of this procedure has enabled its application to measure very low concentrations of species of biological and pharmaceutical interest in body fluids and tissues [74,75,76]. Other broad advantage of this technique is that the basic instrumentation, normally composed by a potentiostat/galvanostat, is relatively inexpensive and is very flexible. It is very easy to adapt to conventional electrodes or microelectrodes, to chose the type of cells, *etc.*

Bearing this is mind, the method chosen to determine the levels of iron, chromium and nickel in mice organs was adsorptive stripping voltammetry in square wave mode employing mercury film microelectrodes [77,78,79].

In adsorptive stripping voltammetry (AdSV) a spontaneous adsorption process is intentionally used onto the working electrode as a preconcentration step for trace measurements of important species that cannot be accumulated by electrolysis

[80,81]. The resulting voltammetric response of the adsorbed species possessing surface active properties is significantly larger than that of the solution species alone. Hence, the detection limits are improved by several orders of magnitude, *i.e.*, nanomolar concentration range [82], almost solely because the preconcentration step has the ability to enhance substantially the faradaic current component [83,84].

This technique has been successfully applied to the quantification of organic molecules [85,86,87,88] and metal ions through the formation and deposition of surface active and electroactive complexes followed by the subsequent reduction of the metal in the adsorbed complex, *e.g.* nickel with dimetylglioxime ligand [89], iron with catechol [90]. The determination of chromium [91,92,93] and titanium [94,95] can be measured by coupling the adsorption accumulation with catalytic reactions. In this case, the response of accumulated complex is amplified through a catalytic cycle, *e.g.* in the presence of an oxidant to recycle the complex at the electrode surface [96].

In electrochemistry, adsorption means the attachment of molecules or ions from the solution to the surface of electrode due mainly to their hydrophobic character [97]. Adsorption equilibrium is established between the concentration in solution and that on the surface of the electrode and normally it is assumed that adsorption obeys to the Langmuir isotherm which for a given temperature:

$$\Gamma = \Gamma_m \left(\frac{BC}{1+BC} \right) \qquad (1)$$

where Γ is the surface concentration of adsorbate (moles/cm^2), Γ_m the surface concentration corresponding to a monolayer at the surface, C concentration of adsorbate in the bulk and B the adsorption coefficient. When $BC<<1$ equation (1) leads to a linear relationship of the kind:

$$\Gamma = \Gamma_m BC \qquad (2)$$

Thus, at very low concentrations of surface active compounds, the surface concentration onto the electrode is directly proportional to the concentration in solution. From that, the choice of the accumulation time needs special attention to avoid the saturation of the electrode surface with subsequent deviations from linearity [77,79,98].

To achieve maximum sensitivity in the subsequent voltammetric response, optimum conditions for maximum adsorption should be used during the preconcentration step. The amount of surface active compound accumulated on the electrode surface depends of many parameters such as the solvent, electrode material, potential, time, pH, ionic strength, mass transport and temperature. In addition, measurements of metal ions based on the adsorption of their surface active complexes require optimisation of the complexing ligand concentration [79,99]. A ligand concentration higher than required may cause inhibition of the

metal-ligand adsorption through a competitive coverage of the ligand [20]. Optimum conditions for maximum accumulation are usually found by examining the peak current enhancement by varying these parameters. Besides their effect on the peak current enhancement, some of the above parameters may influence other properties of the subsequent voltammetric measurement such as reproducibility and peak shape. A compromise should be made to achieve the desired balance between sensitivity (peak current/concentration) and reproducibility.

The preconcentration should proceed at the potential of maximum adsorption and this potential can be used to improve the selectivity of the technique and minimise interferences [100].

In the stripping process the amplitude, step and frequency should be optimised. These parameters may influence the baseline, the peak shape and reproducibility.

SQUARE WAVE VOLTAMMETRY

Square wave voltammetry (SWV) was conceived by Barker [101] as a result of the necessity to diminish considerably the charging background current. It is a complex differential technique in which a waveform composed of a symmetrical square wave, superimposed on a base staircase potential is applied (E_{app}) to the working electrode [102]. The measured current (i_{meas}) is sampled twice during

each square wave period, once at the end of the forward pulse (i_1) and once at the end of reverse pulse (i_2), (Figure 1.4) and is plotted *versus* the staircase potential [74]. The symmetrical current measurement scheme of this technique provides a significant cancellation from the charging background current and very low detection limits can be attained [96].

The main advantage of square wave voltammetry is the very small analysis time to record voltammograms [102]. The effective scan rate is given by the *frequency* multiplicand by the E_{step} [103].

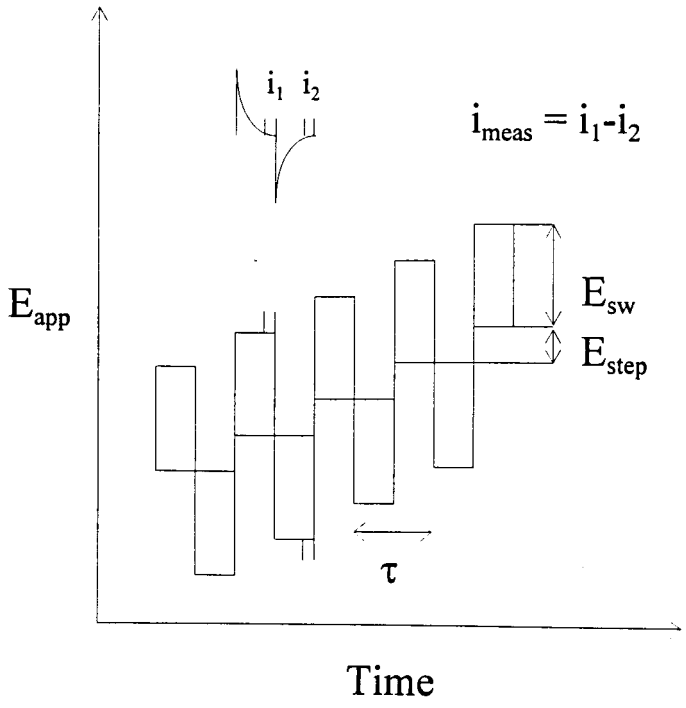

Figure 1.4. Potential-time waveform in SWV. E_{sw}, square wave amplitude; E_{step}, step height; i_1 and i_2 current measurement times and τ square wave period.

Other advantage of this technique is the minimisation of oxygen interference. The possibility to avoid the removal of oxygen, that is time consuming, was studied by Bond [104] and Osteryoung *et al.* [105]. In stripping voltammetry during the preconcentration step the dissolved oxygen is irreversibility reduced at potentials sufficiently negatives and it is depleted from the electrode surface. During the stripping step at elevated scan rates and high frequencies oxygen does not has enough time to reach again the electrode surface.

The features of square wave voltammetry, specifically the speed and sensitivity makes this method exceptionally suitable for the metals envisaged in this study.

MICROELECTRODES

A microelectrode or ultramicroelectrode for some authors [106] is an electrode with at least one dimension small enough that its properties are a function of size [107]. Thus, the term microelectrode is reserved for electrodes with at least one dimension not bigger than 50 μm. Such dimensions offer distinct analytical advantages over conventional electrodes that will be referred along the text.

The use of microelectrodes started by the necessity to have very small electrodes for *in vivo* biological studies as well as from the need to develop new methods capable of probing electrochemical processes on a very short time scale. Davies *et*

al. in 1940s constructed and used a microelectrode to measure oxygen inside biological tissues [108]. However, the large development and the exploration of their properties started in the begin of last decade [107,109,110,111,112,113] owing to the crescent facilities for manufacturing very small electrodes and the increasing performance of the electrochemical equipment. Meanwhile, these small devices extended their applications, *e.g.*, they have been used with success in analysis of trace metals and/or solution volumes less than 30 μL [114], including the exploration of microscopic domains, measurements of local concentrations profiles [115] and detection in microflow systems [116]. Malinski *et al.* [117] made determinations of unbound nickel accumulation in single biological cells: myocytes and rat hepatoma cells, using carbon fibre microelectrodes modified with a conductive polymeric film of porphyrin (< 1-3 μm diameter).

Several geometries are commonly found in literature [106,118,119,120] for these electrodes. By far, the most common geometry used in laboratory is the microdisc [121]. They are constructed by sealing very fine metal wires of platinum, gold, iridium or carbon fibres into a glass capillary or/and epoxy resins, cutting perpendicular to the axis of wire. Finally, the front face of the microelectrode is polished to remove bubbles in the glass and other defects. The good performance of the microelectrode constructed in this way results in proper sealing between the

glass and the microwire. The typical construction scheme of a microdisc electrode is shown in Figure 1.5.

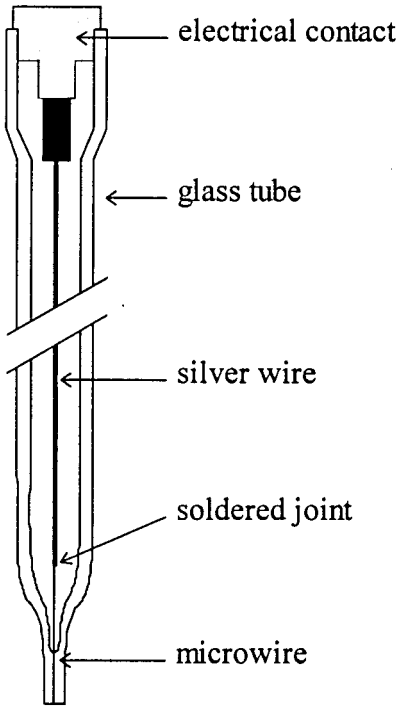

Figure 1.5. Cross-sectional view of a microdisc electrode.

Mass transport at microelectrodes

When electrolysis occurs, a concentration gradient is created between the electrode surface and the bulk solution. For this reason the current measured at the electrode depends on the modes of mass transport that are predominant [122].

Using microelectrodes the mass transfer mode is dominated by diffusion because the flux (as a result of diffusion) is very large and the effects of convection tend to be less apparent than at electrodes of conventional size. Thus, the majority of the theoretical current treatment at this structures of very small dimensions deals with diffusion limited processes.

For simplicity, it is convenient to consider a spherical electrode since the properties derived for the microsphere can be extended to other geometries [107].

A potential step is applied to the electrode immersed in a solution containing only electroactive species and electrolyte. Following the potential step from a value where no electrode reaction occurs to one where the electrochemical reaction is diffusion controlled, the current density, I_d (A/cm^2), is given by

$$I_d = \frac{i_d}{A} = \frac{nFD^{1/2}c^{\infty}}{\pi^{1/2}t^{1/2}} + \frac{nFDc^{\infty}}{r_s} \qquad (3)$$

where r_s is the radius of the sphere (cm), D the diffusion coefficient (cm^2/s), c^{∞} the bulk concentration of electroactive species (mol/cm^3), n the number of electrons involved in the electrode reaction, F the Faraday constant (C/mol), i_d the limiting current (A), A the electrode area (cm^2) and t the time (s). Inspection of equation (3) shows that, the total diffusion-limited current density is composed by the sum of a transient term, which is known as the Cottrell equation [123] and of a steady state term where the current is time independent. Hence, depending on the

time scale of the experiment (*i.e.*, the scan rate) the same microelectrode may exhibit two distinct limiting diffusion regimes. First, at short times, the transient term dominates leading to

$$I_d = \frac{nFD^{1/2}c^{\infty}}{\pi^{1/2}t^{1/2}} \qquad (4)$$

were semi-infinite linear diffusion at the microelectrode takes place (I changes linearly with $t^{-1/2}$). The diffusion is mostly normal to the electrode surface. The microelectrode behaves like a large planar electrode and the traditional concepts and equations developed may be used. The voltammogram response for this time scale is peak-shaped (Figure 1.6a).

Second, at long times, a quasi-spherical diffusion field leads to a steady state current:

$$I_d = \frac{nFDc^{\infty}}{r_s} \qquad (5)$$

From equation (5) the limiting current density is independent of time and inversely proportional to the electrode radius. Therefore, the decrease in the radius increases the limiting current density. Scanning the potential at sufficiently slow scan rates the microelectrode exhibit steady-state (sigmoidal) voltammograms (Figure 1.6b) and the limiting current will be proportional to the radius but is independent of time scale experiment.

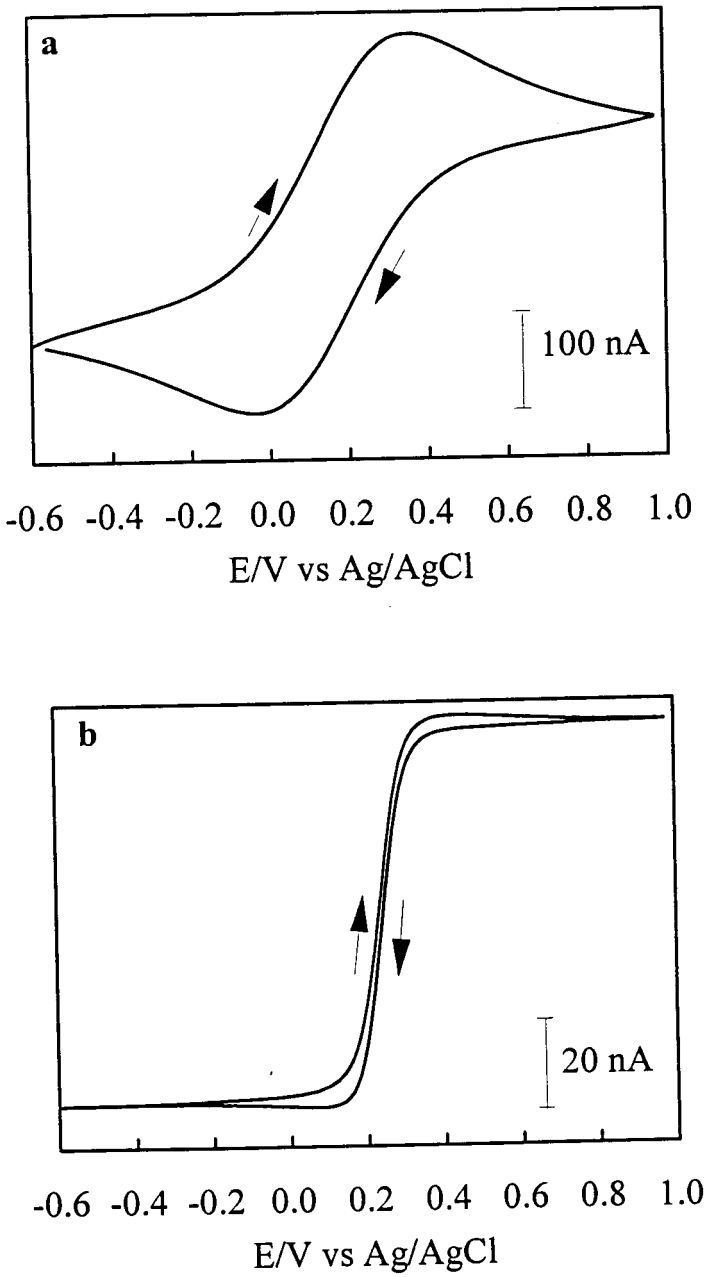

Figure 1.6. Cyclic voltammograms of a solution containing 5.0×10^{-3} mol/L of potassium ferrocyanide and potassium hexacyanoferrate in HBSS at a 25 μm gold microdisk electrode recorded at a) 2000 mV/s; b) 10 mV/s.

Thus, it is clear that equation (3) predicts the current to a microelectrode at very short and long times, but the intermediate time window leads to poor estimations since the experimental results are difficult to interpret.

Properties and advantages of microelectrodes

An important property of microelectrodes results from the mass transport regime described previously. The rapid steady-state diffusion currents attained by them permits the study of rapid electron transfer and fast coupled chemical reactions with determination of thermodynamic and kinetic parameters [124,125] that were impossible to achieve with conventional electrodes. Under these conditions the enhanced current is practically independent of convection because the resulting flux is very high when compared with the convective flux. Therefore, microelectrodes may be used in flow systems without concern about the flow rate effects [116]. This diffusion regime also offers a simple process to determine the diffusion coefficients of several species.

Another important consequence of using microelectrodes, is a much smaller contribution of capacitive charging currents, since it may exceed the value of the faradiac current at short times and with very low concentrations of electroactive species [126]. Its magnitude is dependent of the electrode area, it is additive to the

faradaic current and for short times distorts the chronoamperometric response. The great reduction of charging currents associated with the small area of microelectrodes allows to measure voltammetric experiments with very fast scan rates and hence to investigate the kinetics of very fast electron transfer and coupling chemical reactions [125,127].

Solution iR drop (ohmic drop) is a less serious problem when using microelectrodes. The iR drop is proportional to the solution resistance and the flow current between the working and reference electrodes. Because the current in microelectrodes is very small, larger solution resistances can be tolerated. The decreased ohmic distortions allow electrochemical studies to be made in new chemical environments which are not possible with conventional electrodes. Thus, the traditional systems can be restudied with little or in the absence of supporting electrolyte and only using a two electrode system [128,129,130,131]. In addition, microelectrodes experiments have been reported in highly resistive organic media [129,132] as well as at very low temperatures [133,134,135].

The dimensions and the small currents (few nanoamperes) that flows at microelectrodes make them a suitable tool for the determination of redox species *in vivo* [115,136,137], because they are relatively non evasive. A typical example of application is the determination of neurotransmitter concentrations in nerve tissues. O' Shea *et al.* [138] determined the levels of glutathione in the rat brain tissue

using a gold/mercury amalgam microelectrode as a thiol-specific detector for capillary electrophoresis. An obvious feature of microelectrodes is that can be used for analysis of very small volumes of samples [114,139,140,141] and also to study the nucleation processes, birth and growth, of single nucleus [142,143,144,145].

Owing to the inherent advantages focused by the microelectrodes, they are utilised in techniques such as anodic stripping voltammetry in the determination of heavy metal in wines, rain and sea waters [146,147,148,149].

Finally, other attractive and not less important advantage is that these type of microelectrodes are relatively inexpensive and are very easy to adapt to the electrochemical instrumentation needed, *i.e.* potentiostat/galvanostat, cell design, *etc.*

MERCURY FILM MICROELECTRODES

It is well known the favourable electrochemical properties of mercury such as high hydrogen overvoltage that extends the cathodic potential range, lower background current levels, lower detection limits and reproducibility [150,151]. Because of that, it has been in practical terms one of the most widely used electrode material. The hanging mercury drop electrode (HMDE) is the one more used in adsorptive stripping voltammetry [152,153,154].

Mercury film electrodes (MFE) permit shorter preconcentration times because of their larger area-to-volume ratio and yields superior sensitivity and selectivity than the traditional HMDE [83,155,156].

Development and characterisation of mercury film microelectrodes in different substrates, for microanalysis have been made by several authors. Wehmeyer and Wightman [157] deposited mercury(I) onto a platinum disk with a radius as small as 0.30 μm to form a film and used to demonstrate that anodic stripping voltammetry (ASV), with a quiescent solution during deposition, could be performed for lead in the concentration range of $7.0x10^{-7}$ to $1.0x10^{-10}$ mol/L. Baranski [140] prepared MFM (7-10 μm in diameter) by deposition of mercury(II) on carbon fibre and a thin platinum wire and used them for rapid voltammetric determinations of trace metals in very small samples. Peng *et al.*, [141] investigated the anodic stripping voltammetric characteristics of MFM on a gold base for trace lead in microsamples of digested human hair.

The selection of the substrate for MFM is crucial because many materials will amalgamate with mercury such as gold and platinum. Carbon fibres and iridium are totally "inert" substrates. However, it is difficult to grow stable and reproducible films on carbon since the mercury deposit is a finite number of small droplets [158,159,160] because inertness makes difficult for mercury to adhere to the surface, and as a result, the reproducibility and practical utility of such electrodes is

reduced [161]. It is very difficult to obtain commercially iridium wire with diameter less than 127 μm [162]. Recent studies with this substrate proved that mercury is well adhering and stable for long periods of time with very reproducible results [161,162,163].

Mercury films with platinum [157,146,164,165] are very irreproducible because its difficult to obtain a complete coverage of the platinum surface. Additionally, it is known that platinum-mercury intermetallic compounds crystallise progressively at the mercury, which decreases the hydrogen overpotential [166].

Mercury strongly adheres to gold and forms a homogeneous film very reproducible and with an extended lifetime [138,141,167]. The major problem of this substrate is its solubility in mercury that is rather large, 0.14% at 25 °C [168] and consequently, the surface of the gold microelectrode is deteriorated after several months of use.

Microelectrodes made of platinum, carbon and gold were tested with respect to mercury films onto their surfaces. After an exhaustive study, mercury films on gold microelectrodes gave a more reproducible response.

AIMS OF THE PRESENT THESIS

The objective of this thesis is to study the accumulation and the histological effects provoked individually by the major stainless steel corrosion products, *i.e.*, nickel, chromium and iron in the liver, kidney and spleen in an animal model used frequently in toxicology studies and to contribute to the development of an electrochemical technique: adsorptive stripping voltammetry using mercury film microelectrodes to quantify the metal levels found those mentioned organs of mice injected with metals ions (nickel, chromium and iron).

DESIGN OF THESIS

This thesis is organised in five chapters. The first one is the general introduction to the subjects developed along the dissertation as well as some theoretical aspects.

In chapter 2 is presented the quantitative and histological results in the liver, kidney and spleen attained after mice administration with a nickel solution prepared by dissolution of the pure metal. Simultaneously, an appropriate digestion procedure is mentioned for the mice organ samples. It is referred the optimal AdSV conditions that were developed to quantify the nickel content in the mice organs samples, using the dimetylglioxime as the complexing agent.

Chapter 3 presents the quantitative and histological results obtained after the mice administration with chromium. It is referred the optimisation of the experimental conditions for the adsorptive stripping measurements used to quantify the chromium content in the mice organs using the diethylenetriaminepentaacetic acid (DTPA) as the complexing agent.

In chapter 4 is presented the quantitative results obtained by AdSV using catechol as the complexing agent as well as the histological results, following mice injection with an iron solution. It is referred the influence of the optimisation parameters on the iron peak definition.

Chapter 5 deals with the main conclusions resulting from the envisaged studies. It reports to general aspects of the presented and discussed results, separately in the chapters 2, 3 and 4, together with same guidelines about interesting topics worthwhile of being investigated.

REFERENCES

[1] L. L. Hench and J. Wilson, "*Clinical Performance of Skeletal prostheses*", L. L. Hench and J. Wilson (eds.), Chapman & Hall, Great Britain (1996) 1.

[2] G. R. Mundy, *Nature*, **367** (1994) 216.

[3] B. D. Ratner, *J. Biomed. Mater. Res.*, **27** (1993) 837.

[4] E. M. Lenoe, *"Advances in Materials Science and Implant Orthopaedic Surgery"*, R. Kossowsky and N. Kossowsky (eds.), NATO-ASI series, **24** (1995) 103.

[5] J. Black, "*Orthopeadic Biomaterials in Research and Practice*", M. Otway (ed.), Churchil/Livingstone Press, (1988)163.

[6] S. D. Cook, E. A. Renz, R. L. Barrack, K. A. Thomas, A. F. Harding, R. J. Haddad, M. Milicic, *Clin. Orthop. Rel. Res.*, **194** (1985) 237.

[7] D. I. Bardos, "*Materials Sciences and Implant Orthopedic Surgery*", R. Kossowsky and N. Kossovsky (eds.), Nato ASI Series, (1986) 125.

[8] M. G. von Mallinckrodt, "*Handbook on metals in Clinical and Analytical Chemistry*", H. Sigel, A. Sigel and H. G. Seiler (eds.), Marcel Dekker, Inc., New York, (1994) 13.

[9] D. Williams, R. W. Cahn and M. B. Bever (eds.), "*Concise Encycopedia of Medical & Dental Materials*", Pergamon Press, Oxford, (1990) 232.

[10] K. H. W. Seah and X. Chen, *Corrosion Science*, **34** (1993) 1841.

[11] D. F. Williams, *The Journal of Metals and Materials*, **7** (1991) 24.

[12] J. B. Park, "*The Biomedical Engineering Handbook*", J. D. Bronzino (ed.), CRC Press, Florida, (1995) 538.

[13] J. Black, *J. Bone and Joint Surg.*, **70** (1988) 517.

[14] D. F. Williams and G. Meachim, *J. Biomed. Mater. Res. Symposium*, **5** (1974) 1.

[15] G. D. Winter, *J. Biomed. Mater. Res. Symposium*, **5** (1974) 11.

[16] H. S. Dobbs and M. J. Minski, *Biomaterials*, **1** (1980) 193.

[17] J. L. Woodman, J. Black and S. A. Jiminez, *J. Biomed. Mater. Res.*, **18** (1984) 99.

[18] H. Zitter and H. Plenk Jr., *J. Biomed. Mater. Res.*, **21** (1987) 881.

[19] M. A. Barbosa, "*Biomaterials Degradation*", M. A. Barbosa (ed.), Elsevier Science Publisher, The Netherlands, (1991) 227.

[20] F. Burny, Y. Andrianne, M. Donkerwolcke and J. Quintin, "*Biomaterials Degradation*", M. A. Barbosa (ed.), Elsevier Science Publisher, The Netherlands, (1991) 291.

[21] E. J. Sutow and S. R. Pollack, "*Biocompatibility of Clinical Implant Materials*", D. F. Williams (ed.), CRC Press, Boca Raton, Florida, **1** (1981) 45.

[22] R. Hazan, R. Brener and U. Oron, *Biomaterials*, **14** (1993) 570.

[23] O. E. M. Pohler, "*Biomaterials in Reconstructive Surgery*", L. R. Rubin (ed.), The C. V. Mosby Company, London, **15** (1983) 158.

[24] M. Trainsnel, D. le Maguer, H. F. Hildebrand and A. Iost, "*Clinical Materials*", **5** (1990) 309.

[25] K. E. Healy and P. Ducheyne, *J. Biomed. Mater. Res.*, **26** (1992) 319.

[26] G. L. Patrick, National Bureau of Standards Special Publication. Proceedings of a Symposium on Retrieval and Analysis of Orthopaedic Implants, (1977) 31.

[27] J. L. Woodman, J. Black and S. Jimenez, "*Biomaterials 1980*", G. D. Winter, D. F. Gibbons and H. Plenk Jr. (eds.), John Wiley and Sons Ltd., (1982) 245.

[28] D. F. Williams, "*Biocompatibility of Orthopedic Implants*", D. F. Williams (eds.), CRC Press, **1** (1982) 231.

[29] R. Kusec, V. Nikolic, S. Toric, J. Hanoevic, S. Davila and V. Alkovic, *Period Biol.*, **92** (1990) 325.

[30] E. Leitão, *Ph.D. Thesis*, Oporto Univ., (1996).

[31] J. Black, E. C. Maitin, H. Gelman and D. M. Morris, *Biomaterials*, **4** (1983) 160.

[32] K. Merritt, S. A. Brown and N. A. Sharkey, *J. Biomed. Mater. Res.*, **18** (1984) 1005.

[33] K. Merritt and S. A. Brown, *"Corrosion and Degradation of Implant Materials. Second symposium"*, A. C Fraker and .C. D. Griffin (eds.), American Society for Testing and Materials, Philadelphia, (1985) 195.

[34] K. Merritt, S. A. Brown and N. A. Sharkey, *J. Biomed. Mater. Res.*, **18** (1984) 991.

[35] S. A. Brown, L. J. Farnsworth, K. Merritt and T. D. Crowe, *J. Biomed. Mater. Res.*, **22** (1988) 321.

[36] K. Merritt, T. D. Crowe and S. A. Brown, *J. Biomed. Mater. Res.*, **23** (1989) 845.

[37] S. A. Brown, K. Zhang, K. Merritt and J. H. Payer, "*Biomaterial-Tissue Interfaces*", P. J. Doherty et al. (eds.), Advances in Biomaterials, **10** (1992) 13.

[38] S. A. Brown, K. Zhang, K. Merritt and J. H. Payer, *J. Biomed. Mater. Res.*, **27** (1993) 1007.

[39] K. Merritt, C. D. Fedele and S. A. Brown, "*Biomaterial-Tissue Interfaces*", P. J. Doherty et al. (eds.), Advances in Biomaterials, **10** (1992) 49.

[40] K. Merritt and S. A. Brown, *J. Biomed. Mater. Res.*, **29** (1995) 627.

[41] G. K. Smith and .J. Black, "*Corrosion and Degradation of Implant Materials: Second symposium*", A. C Fraker and .C. D. Griffin (eds.), American Society for Testing and Materials, Philadelphia, (1985) 223.

[42] M. L. Pereira, A. M. Abreu, J. P. Sousa and G. S. Carvalho, *J. Mater. Sci. Mater. Med.*, **6** (1995) 523.

[43] A. M. Abreu, R. B. Tracana, G. S. Carvalho and J. P. Sousa, *Biomedical Letters*, **52** (1995) 133.

[44] J. Black, *Biomaterials*, **5** (1984) 11.

[45] IARC, *"Monographs on the Evaluation of Carcinogenic risks to humans, chromium, nickel and welding*", International Agency for Research on Cancer, Lyons, **49** (1990) 213.

[46] R. G. Stevens, "*Iron and Human deseases*", R. B. Lauffer (ed.), CRC Press Inc., (1992) 333.

[47] R. S. Britton, G. A. Ramm, J. Olynyk, R. Singh, R. O'Neill and B. R. Bacon, "*Progress in Iron Research*", C. Hershko et. al., (eds.) Plenum Press, New York, 1994, 239.

[48] A. Martin, T. W. Bauer, M. T. Manley and K. E. Marks, *J. Bone Joint Surg.*, **70A** (1988) 1561.

[49] W. J. Gillespie, C. M. A. Frampton, R. J. Henderson and P. M. Ryan, *J. Bone Joint Surg.*, **70B** (1988) 539.

[50] W. W. Brien, E. A. Salvati, J. H. Healey, M. Bansal, B. Ghelman and F. Betts, *J. Bone Joint Surg.*, **72A** (1990) 1097.

[51] V. A. Memoli, J. R. Woodman, R. M. Urban and J. O. Galante, *Trans. Orthop. Res. Soc.*, 7 (1982) 164.

[52] J. L. Woodman, J. A. Memoli, R. M. Urban and J. O. Galante, *Trans. Soc. Biomater.*, **6** (1983) 43.

[53] E. D. Weinberg, "*Iron and Human deseases*", R. B. Lauffer (ed.), CRC Press Inc., (1992) 179.

[54] P. R. Wheater, H. G. Burkitt and V. G. Daniels, "*Functional histology*", Churchill Livingstone, London, (1979) 145.

[55] E. M. Evans, M. A. R. Freeman, A. J. Miller and B. Vernon-Roberts, *J. Bone Joint Surg.*, **56B** (1974) 626.

[56] M. Cramers and L. Lucht, *Acta orthop. Scand.*, **48** (1977) 245.

[57] K. Merritt and S. A. Brown, "*Systemic Aspects of Biocompatibility*", D. F. Williams (ed.), CRC Press Inc., Boca Raton, Florida, **2**, (1981) 33.

[58] K. Merritt and S. A. Brown, "*Clinical Aplications of Biomaterials*", A. J. C. Lee, T. Albrektsson and P. I. Branemark (eds.), John Wiley & Sons Ltd. (1982) 85.

[59] G. S. Carvalho, I. Bravo and M. Barbosa, "*Interfaces in Medicine and Mechanics-2*", K. R. Williams, A. Toni, J. Middleton and G. Palloti (eds.), Elsevier Applied Science, London, (1991) 19.

[60] I. Bravo, S. R. Sousa, G. S. Carvalho and M. Barbosa, "*Advances in Biomaterials*" P. J. Doherty et al. (eds.), **10** (1992) 7.

[61] J. H. Brock, "*Iron and Human Deseases*", R. B. Lauffer (ed.), CRC Press Inc., (1992) 161.

[62] M. C. Pereira, M. L. Pereira and J. P. Sousa, in press at *J. Biomed. Mater. Res.* (1997).

[63] M. H. Ross and L. J. Rowrell, (eds.), "*Histology a Text and Atlas*", Williams & Wilkins, (1985) 471.

[64] P. R. Wheater, H. G. Burkitt and V. G. Daniels, (eds.), "*Functional Histology*", Churchill Livingstone, New York (1979), 200.

[65] P. R. Wheater, H. G. Burkitt and V. G. Daniels, (eds.), "*Functional Histology*", Churchill livingstone, New York (1979), 208.

[66] M. H. Ross and L. J. Rowrell, (eds.), "*Histology a Text and Atlas*", Williams & Wilkins, (1985) 527.

[67] P. R. Wheater, H. G. Burkitt and V. G. Daniels, (eds.), "*Functional Histology*", Churchill livingstone, New York (1979) 145.

[68] J. Han, J. M. van Krieken and J. te Velde, "*Histology for Pathologists*", S. S. Sternberg, Raven Press, New York (1992) 253.

[69] M. H. Ross and L. J. Rowrell, "*Histology a Text and Atlas*", Williams & Wilkins, (1985) 324.

[70] R. Kalvoda, *Anal. Chem. Acta*, **162** (1984) 197.

[71] C. A. Johnson, *Anal. Chim. Acta*, **238** (1990) 273

[72] R. E. Cranston and J. W. Murray, *Anal. Chim. Acta*, **99** (1978) 275.

[73] F. Vydra, K. Stulik and E. Julaková, "*Electrochemical Stripping Analysis*", John Wiley & Sons Inc., New York, (1976) 20.

[74] P. Ostapczuk, P. Valenta, M. Stoeppler and H. W. Nurnberg, "*Chemical Toxicology and Clinical Chemistry of Metals*" S. S. Brown and J. Savory (eds.), Academic press, (1983) 61.

[75] P. Ostapczuk, *Clin. Chem.*, **38** (1992) 1995.

[76] J. A. del Pozo, A. Costa-García, P. Tunõn-Blanco, *Anal. Chim. Acta*, **273** (1993) 101.

[77] M. C. Pereira, J. L. Faria, M. L. Reis and J. P. Sousa, *Electroanalysis*, **9** (1997) 150.

[78] M. C. Pereira and J. P. Sousa, *Portugaliae Electrochem. Acta*, **13** (1995) 477.

[79] M. C. Pereira, M. L. Pereira and J. P. Sousa, *Electroanalysis* **9** (1997) 941.

[80] R. Kalvoda and M. Kopanica, *Pure & Appl. Chem.*, **61** (1989) 97.

[81] K. Brainina and E. Neyman, "*Electroanalytical Stripping Methods*", J. D. Winefordner (eds.), John Wiley & Sons, New York, **126** (1993) 71.

[82] M. Lambrechts and W. Sansen, "*Microelectrochemical Sensors*", John Wiley &Sons, Chichester, London (1992) 79.

[83] A. M. Bond, "*Modern Polarographic Methods in Analytical Chemistry*", Marcel Dekker, Inc., New York, (1980) 435.

[84] J. Wang, "*Electroanalytical techniques in Clinical Chemistry and laboratory Medicine*", VCH Publishers, Inc., New York, (1988) 1.

[85] J. M. Séquaris and P. Valenta, *J. Electroanal. Chem.*, **227** (1987) 11.

[86] H. Sawamoto, *J. Electroanal. Chem.*, **186** (1985) 257.

[87] S. Altinoz, D. Ozer, A. Temizer and N. Yuksel, *Analyst*, **119** (1994) 1575.

[88] L. Hernández, P. Hernández and O. Nieto, *Analyst*, **119** (1994) 1579.

[89] B. Pihlar, P. Valenta and H. W. Nurnberg, *J. Electroanal. Chem.*, **214** (1986) 157.

[90] C. M. G. van den Berg and Z. Q. Huang, *J. Electroanal. Chem.*, **177** (1984) 269.

[91] J. Golimowski, P. Valenta and H. W. Nurnberg, *Fresenius Z. Anal. Chem.* **322** (1985) 315.

[92] J. Wang and J. Lu, *Analyst*, **117** (1992) 1913.

[93] M. Paneli, A. V. Voulgaropoulos and K. Kalcher, *Mikrochim. Acta*, **110** (1993) 205.

[94] H. Li and C. M. G. van den Berg, *Anal. Chim. Acta*, **221** (1989) 269.

[95] K. Yokoi and C. M. G. van den Berg, *Anal. Chim. Acta*, **245** (1991) 167.

[96] J. Wang, "*Analytical Electrochemistry*", VCH Publishers, Inc., New York, (1994) 51.

[97] J. Wang, "*Electroanalytical Chemistry*", A. J. Bard (ed.), Marcel Dekker, Inc, New York, **16** (1989) 5.

[98] M. C. Pereira, M. L. Pereira and J. P. Sousa, in press *J. Trace Elem. Med. Biol.*, (1997).

[99] M. C. Pereira and J. P. Sousa, *Portugalie Electrochima Acta*, **14** (1996) 273.

[100] S. Morais, G. S. Carvalho and J. P. Sousa, in press *Electroanalysis* (1997).

[101] G. C. Barker, *Anal. Chim. Acta*, **18** (1958) 118.

[102] J. G. Osteryoung and R. A. Osteryoung, *Anal. Chem.*, **57** (1985) 101A.

[103] C. M. G. van den Berg, *Anal. Chim. Acta*, **250** (1991) 265.

[104] A. M. Bond, *Talanta*, **20** (1973) 1139.

[105] M. Wojciechowski, W. Go and J. Osteryoung, *Anal. Chem.*, **57** (1985) 155.

[106] C. Amatore, "*Physical Electrochemistry. Principles, Methods and Applications*", I. Rubinstein (ed.), Marcel Dekker, Inc., New York, (1995) 131.

[107] D. Pletcher, "*Microelectrodes: Theory and Applications*", M. I. Montenegro, M. A. Queirós, J. L. Daschbach (eds.), NATO ASI Series, **E197** (1991) 3.

[108] P. W. Davies and F. Brink, *Rev. Sci. Instrum.*, 13 (1942) 524.

[109] R. M. Wightman, *Anal. Chem.*, **53** (1981) 1125A.

[110] D. P. Whelan, J. J. O'Dea, J. Osteryoung and K. Aoki, *J. Electroanal. Chem.*, **202** (1986) 23.

[111] S. Pons and M. Fleischmann, A*nal. Chem.*, **59** (1987) 1391A.

[112] R. M. Wightman, D. O. Wipf, "*Electroanalytical Chemistry*", A. J. Bard (ed.), **15** (1989) 267.

[113] S. P. Kounaves, *Anal. Chem.*, **64** (1992) 2998.

[114] W. J. Bowyer, M. E. Clark and J. L. Ingram, *Anal. Chem.*, **64** (1992) 459.

[115] R.M. Wightman, S. Hochstetler, D. Michael and E. Travis, *Interface*, (1996) 22.

[116] J. Wang and B. A. Freiha, *Anal. Chem.*, **57** (1985) 1776.

[117] T. Malinski, F. Bailey and J. R. Fish, *Anal. Chim. Acta*, **249** (1991) 35.

[118] C.G. Zoski, *J. Electroanal. Chem.*, **296** (1990) 317.

[119] R. M. Penner, M. J. Heben and N. S. Lewis, *Anal. Chem.*, **61** (1989) 1630.

[120] G. Zhao, D. M. Giolando and J. R. Kirchhoff, *Anal. Chem.*, **67** (1995) 1491.

[121] J. Wang, "*Analytical Eletrochemistry*", VCH Publishers, Inc. New York, (1994) 95.

[122] A. J. Bard, L. R. Faulkner, *"Electrochemical Methods, Fundamentals and Applications"*, Wiley, New York (1980) 27.

[123] A. J. Bard, L. R. Faulkner, *"Electrochemical Methods, Fundamentals and Applications"*, Wiley, New York (1980) 143.

[124] S. Daniele, M. A. Baldo, P. Ugo and G. A. Mazzocchin, *J. Electroanal. Chem.*, **295** (1990) 95.

[125] A. Szulborska and A. Baranski, *J. Electroanal. Chem.*, **377** (1994) 269.

[126] A. J. Bard, L. R. Faulkner, *"Electrochemical Methods, Fundamentals and Applications"*, Wiley, New York (1980) 9.

[127] C. P. Andrieux, P. Haprot and J. M. Saveant, *Electroanalysis*, **2** (1990) 183.

[128] J. B. Cooper and A. M. Bond, *J. Electroanal. Chem.*, **315** (1991) 143.

[129] A. M. Bond, S. W. Feldberg, H. B. Greenhill, P. J. Mahon, R. Colton and T. Whyte, *Anal. Chem.*, **64** (1992) 1014.

[130] M. Ciszkowska and J. G. Osteryoung, *Anal. Chem.* **67** (1995) 1125.

[131] J. Wang and J. M. Zadeii, *J. Electroanal. Chem.*, **246** (1988) 297.

[132] J. Wang and P. Tuzhi, *Anal. Chim. Acta*, **197** (1987) 367.

[133] A. M. Bond and M. Svestka, *J. Electroanal. Chem.*, **301** (1991) 139.

[134] L. K. Safford and M. J. Weaver, *J. Electroanal. Chem.*, **331** (1992) 857.

[135] A. M. Bond and V. B. Pfund, *J. Electroanal. Chem.*, **335** (1992) 281.

[136] A. G. Ewing, M. A. Dayton and R. M. Wightman, *Anal. Chem.*, **53** (1981) 1842.

[137] J. Wang, *Anal. Chem.*, **54** (1982) 221.

[138] T. J. O'Shea and S. M. Lunte, *Anal. Chem.*, **65** (1993) 247.

[139] A.S. Baranski and H. Quon, *Anal. Chem.*, **58** (1986) 407.

[140] A.S. Baranski, *Anal. Chem.*, **59** (1987) 662.

[141] J. Peng and W. Jin, *Anal. Chim. Acta*, **264** (1992) 213.

[142] B. Scharifker and G. Hills, *J. Electroanal. Chem.*, **130** (1981) 81.

[143] J. D. Genders and D. Pletcher, *J. Electroanal. Chem.*, **199** (1986) 93.

[144] M. Fleischmann, L. J. Li and L. M. Peter, *Electrochim. Acta*, **34** (1989) 459.

[145] J. P. Sousa, *Ph. D. Thesis*, University of Utah (1991).

[146] S. Daniele, M. A. Baldo, P. Ugo and G. A. Mazzocchin, *Anal. Chim. Acta*, **219** (1989) 9.

[147] S. Daniele, M. A. Baldo, P. Ugo and G. A. Mazzocchin, *Anal. Chim. Acta*, **219** (1989) 19.

[148] D. K. Y. Wong and A. G. Ewing, *Anal. Chem.*, **62** (1990) 2697.

[149] A. R. Harman and A. S. Baranski, *Anal. Chim. Acta*, **239** (1990) 35.

[150] A. M. Bond, *"Modern Polarographic Methods in Analytical Chemistry"*, Marcel Dekker, Inc., New York, (1980).

[151] A. J. Bard, L. R. Faulkner, *"Electrochemical Methods, Fundamentals and Applications"*, Wiley, New York (1980) 5.

[152] C. Elleouet, F. Quentel and C. Madec, *Anal. Chim. Acta*, **257** (1992) 301.

[153] J. Golimowski, B. Krasnodebska and E. Najdeker, *Fresenius J. Anal. Chem.*, **352** (1995) 544.

[154] J. Wang and J. Mahmoud, *Fresenius Z. Anal. Chem.*, **327** (1987) 789.

[155] B. H. Vassos and G. W. Ewing *"Electroanalytical Chemstry"*, A Wiley-Interscience Publication, John Wiley and Sons, (1983) 90.

[156] J. Wang, P. Tuzhi and J. Zadeii, *Anal. Chem.*, **59** (1987) 2119.

[157] K. R. Wehmeyer and R. M. Wightman, *Anal. Chem.*, **57** (1985) 1989.

[158] J. P. Sottery and C. W. Anderson, *Anal. Chem.*, **59** (1987) 140.

[159] M. Ciszkowska and Z. Stojek, *J. Electroanal. Chem.*, **191** (1985) 101.

[160] M. Ciszkowska, M. Donten and Z. Stojek, *Anal. Chem.*, **66** (1994) 4112.

[161] S. P. Kounaves and W. Deng, *Anal. Chem.*, **65** (1993) 375.

[162] S. P. Kounaves and W. Deng, *J. Electroanal. Chem.*, **301** (1991) 77.

[163] R. R. De Vitre, M. L. Tercier, M. Tsacopoulos and J. Buffle, *Anal. Chim. Acta*, **249** (1991) 419.

[164] J. S. Feinberg and W. J. Bowyer, *Microchemical J.*, **47** (1993) 72.

[165] Z. Stojek and J. Osteryoung, *Anal. Chem.*, **60** (1988) 131.

[166] M. Donten and Z. Kublik, *Chem. Anal. (Warsaw)*, **61** (1989) 1305.

[167] W. Lu, A. S. Baranski, *J. Electroanal. Chem. Interfacial Electrochem.*, **335** (1992) 105.

[168] C. Guminski and Z. Galus, "*Solubility Data Series*", A. S. Kertes (ed.) Pergamon Press, Oxford, (1986) 25.

Chapter 2

EVALUATION OF NICKEL EFFECTS IN MICE ORGANS

2

INTRODUCTION

The toxicity of nickel species has been outlined in the literature since they account for lung tissue diseases [1] and allergic sensitisation of living systems [2,3]. Adverse effects induced by nickel have been tackled and embrace questions of mutagenicity, carcinogenic activity, immunotoxicity and allergic reactions in patients [3,4]. Biochemical analysis of some tumour tissues in rats suggest that high concentrations of nickel are present in the tumours supporting its potential role as a carcinogen [5] and current *in vitro* and *in vivo* studies suggest that the

mechanism of nickel carcinogenesis is mediated by binding of this metal to nuclear DNA [6].

Stainless steel manufactured implants are widely used for biomedical applications, especially for replacing or supporting broken bones with plates or screws, replacing joints at the hip or knee and fixation of hard tissues in dentistry [7,8]. These metallic implants contain 4-17% nickel [9]. Also nickel-chromium dental casting alloys (which contain 61-77% nickel) have been used in dentistry since the early 1930's [8]. Despite their highly generalised corrosion resistance due to the formation of oxide passivation films upon implantation [10,11] and good mechanical properties [12], surface corrosion (*e.g.* crevice corrosion and pitting corrosion) occurs, promoting release of small amounts of metal ions into the surrounding biological tissues [13,14] as well as in extracellular body fluids or in distant organs such as the liver, kidney and spleen [15,16,17]. Despite efforts to answer the question "How safe is a biomaterial?" questions still remain regarding understanding of the side effects caused by nickel ions released from metallic implanted biomaterials during the biodegradation process.

In a previous study [18] a nickel salt, $NiCl_2.6H_2O$, was used to evaluate the role of nickel and toxicity in mice organs such as the liver, kidney and spleen. Results obtained clearly indicate that nickel accumulates in the mentioned organs. In

addition, histological studies have demonstrated that hepatic parenchyma vacuolation and periportal changes occur after 10 days of solution administration.

Adsorptive stripping voltammetry with mercury electrodes have been widely used to determine trace nickel in aqueous solutions [19,20,21,22,23,24,25], biological [19,26] and environmental samples [19] because it is recognised as one of the most sensitive methods in electroanalytical chemistry [27]. The organic ligand that seems more effective for nickel (II) species is dimethylglioxime (DMG) [19-26]. This ligand is very selective, has a high adsorption rate and greatly enhances the charge transfer process [23]. The mechanism involved in the Ni(II)-DMG reduction have been the subject of many investigations [20,23]. In broad terms they encompass three different stages, namely homogeneous equilibrium between species in solution, adsorption process and, finally, reduction of adsorbed complex through an irreversible charge transfer process.

The development of mercury film electrodes (MFE) opens up new opportunities in the electroanalytical field [28,29]. Economou *et al.* [25] has claimed that they are more advantageous than HMDE because it is possible to control the mass transfer of species to the electrode surface, are easy to construct, less wasteful of mercury, higher stability is achieved, lower susceptibility to noise and they have renewable surfaces. Furthermore, the use of mercury film microelectrodes (MFM)

greatly improves the quality of experimental data as well as the sensitivity owing to the properties and advantages of microelectrodes [30].

In the present study a series of experiments was designed to evaluate the alterations occurring in the liver, kidney and spleen of mice administered with a physiological solution containing nickel ions *per si* for 30 days. Nickel accumulation was assessed by adsorptive stripping voltammetry with mercury film microelectrodes, as an alternative technique to atomic absorption spectrometry (AAS). Histological changes were investigated in an attempt to explain the toxicity of nickel ions when released from metallic implantable biomaterials.

MATERIALS AND METHODS

Nickel dissolution

Metallic nickel (99.99% purity from Mathews) was anodically dissolved in Hank´s Balanced Salt Solution (HBSS) by imposition of a constant current. The nickel content was determined by flame atomic absorption spectrometry (AAS) and a solution of 115 mg/L was prepared. The solution pH was 7.72.

Animals and experimental design

Charles River mice nearly 60 days old and weighing 23-34 g supplied from "Instituto Gulbenkian de Ciências", Portugal were used in this study. They were housed in groups of four per cage and food and water were given *ad libitum* . A volume of 0.50 mL of the solution of nickel was subcutaneously injected in the back dorsal surface at days: 0- group I; 0, 7- group II; 0, 7, 14- group III and 0, 7, 14, 21- group IV. Each group was composed of eight animals. Control mice were similarly injected with HBSS. One week after the last injection, animals were anaesthetised with ether vapours and immobilised by cervical dislocation. Small fragments of liver, kidney and spleen were used for histological studies and the remaining organs were stored in PTFE bottles and kept in a freeze chamber at -20 °C for quantitative analysis.

Chemicals

Nitric acid (HNO_3), 65%, Suprapur and perchloric acid ($HClO_4$), 70%, were used for oxidation of organic material. In the voltammetric method a buffer solution, NH_3/NH_4Cl 2.0 mol/L, was prepared by mixing appropriate amounts of NH_4Cl and NH_3 25%. Dimethylglyoxime (DMG) and absolute ethanol were used to prepare a solution of 0.1 mol/L. The required standards were prepared daily

from a stock solution of Ni(II) 1000 mg/L (BDH). The solution of 1.0 mol/L KNO_3 containing 6.0 mmol/L of mercury (II) chloride ($HgCl_2$) and 0.5% HNO_3 was used for mercury-coated film deposition. Ultra pure water was used in sample and solution preparations. All glassware and polyethylene bottles were soaked in solutions of HNO_3 20% for several hours and then rinsed with an excess of water, and then dried.

Instrumentation

A microwave oven Model, CEM MDS 2000, with a maximum power of 630 W and pressure control, was used to remove the water content present in the organs and subsequently proceed to digestion. The voltammograms were obtained using a potentiostat/galvanostat Model Autolab from Eco Chemie equipped with a module ECD specific for microelectrodes, which was connected to a PC Model 1120 SX, used in conjunction with an electrochemical microcell placed in a polarographic Stand 663 VA from Metrohm. Voltammetric measurements were performed using a three electrode configuration system; a mercury film grown on a gold microelectrode of 25 μm diameter as the working electrode; a silver/silver chloride in 3.0 mol/L KCl as the reference electrode and a carbon bar auxiliary electrode. The graphite furnace atomic absorption determinations were made using a Perkin

Elmer Model 4100ZL spectrometer, using pyrolytic THGA (transverse heated graphite atomiser) tubes.

FTIR spectra using diffuse reflectance (DRIFT) [31] were recorded on a Nicolet FT-510P spectrometer. Samples were analysed in a Collector device (Spectra-Tech). The spectrometer chamber was purged with CO_2-free air, -70 °C (pressure) dew point and measurements were made at room temperature. Spectra were obtained from powdered samples approximately 4 mg sample/ 200 mg KBr (Uvasol, Merck), over the 400-4800 cm^{-1} wave number range, with a resolution of 2 cm^{-1}. Each sample and background (typically pure KBr) interferogram was Fourier transformed to its equivalent frequency component spectrum. DRIFT spectrum of pure *p*-nitrobenzoic acid (BDH, 99% GC) was run for comparison purposes.

The XRD spectra were made in a Philips semiautomatic X-ray diffractometer for polycrystalline substances, equipped with a graphite monochromator and an anticathode of copper.

Sample digestion procedure

Approximately 1.0 g of these organs were placed into each previously weighed vessel and then dried in the microwave. The most suitable dryness microwave

program was composed of four stages of fifteen minutes each one, at a power percentage of 10, 15, 20 and 25.The temperature was monitored until samples reached a constant weight to control the state of dryness of the samples. After this procedure, 1.50 mL of HNO_3 was added per 100 mg of dry weight. After digestion, the resulting solutions were evaporated with the addition of 1.0 mL of $HClO_4$ per 0.50 g dry mass on a hot plate in the hood until perchloric acid fumes were no longer observed. The residue was then diluted with ultra pure water to an appropriate volume. Solutions prepared in this way were partially used to analyse the nickel contents by AAS using the standard addition method.

Mercury film microelectrodes preparation

Mercury-coated gold microelectrodes were prepared by application of a constant potential of 0.0 V during 60 s, onto their surface from a deoxygenated mercury solution. This amount of time was chosen since it was observed experimentally that it leads to the formation of a very adherent mercury film at the gold surface. For shorter times, the microelectrode does not present a reproductive response.

Voltammetric determination of nickel

A 5.0 mL of each sample solution was pipetted into the electrochemical cell. A 5.0 μL of DMG solution (ideal concentration in solution $1.0x10^{-4}$ mol/L) was added to complex the nickel present in solution. The determination of nickel by adsorptive stripping voltammetry (AdSV) using the square wave mode was carried out under the following conditions: deposition potential -0.70 V; the deposition time was a function of the nickel concentration present in the sample; cleaning potential -1.20 V; the cleaning time was the same as the deposition time; step 5 mV; amplitude 20 mV and frequency 100 Hz. Quantification of the nickel in the samples was done by the standard addition method. All measurements were performed three or more times to guarantee data reproducibility and the voltammograms were switched in the cathodic direction for each measurement four times or more.

Histological studies

Small fragments of each organ were fixed in Bouin´s solution, embedded in paraffin and sections with approximately 3-5 μm were made in a microtome. After staining with Hematoxylin-eosin, sections were then dehydrated in ethanol series

and mounted in Canada Balsam. Observations and photographs were made using a Nikon optical microscope.

Statistical analysis

Student's *t*-test was applied to determine the statistical significance ($P<0.01$) of the differences observed between means of the two analytical methods and the nickel values found for the four animal groups.

RESULTS

Sample treatment

The precise determination of trace levels of metals in biological materials is very important allowing to establish normal levels in tissues and fluids and, furthermore, to detect metabolic alterations by small changes in these reference values [32,33]. It is important to notice that there are physiological sources of variations such as age [34], sex, dietary habits, environmental conditions or occupational exposure which might explain some disparities found in normal levels [35]. The organs have to be digested and this is the most crucial step within the entire analytical procedure proposed [36,37]. Sample preparation is a long step because organic matter has to be completely destroyed [38] without the loss of the metallic elements to be analysed and it is very important to avoid any source of contamination.

The quantification of several elements in biological samples have to be expressed on a dry tissue basis which makes the drying stage an indispensable step in the analytical procedure and, the most suitable process for drying tissues, is using a microwave oven. The advantage of this process when compared with the traditional thermal ovens is the rapidity of the dryness [39]. In Figure 2.1 is shown the approximate time required for the drying stage for the three organs

investigated, *i.e.* liver, kidney and spleen. The larger loss of weight is verified in the first stage of dryness and the progressive increase of power is applied to avoid the spattering of the biological tissues in the vessels. The percentage of weight loss for these organic matter was 68.40 ± 0.25%. The differences of the values obtained for the three organs dried are not statistically significant.

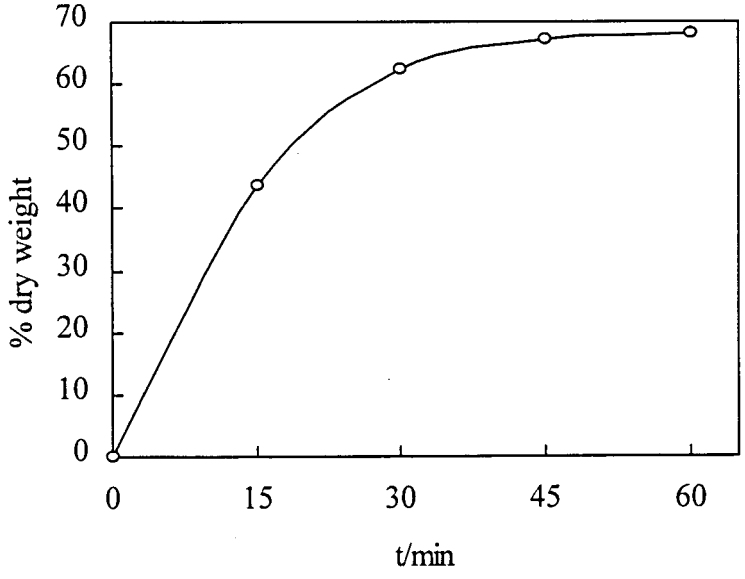

Figure 2.1. Typical drying microwave oven curve for mice organ samples.

Biological samples, namely liver, kidney and spleen are characterised by having a high protein content which makes it difficult to perform a complete decomposition with HNO_3, resulting in the obtainment of incomplete digestion products along with the inorganic species of interest in solution. Some of these products interfere with the electrochemical response by distorting the results. The

influence of these residues on the nickel signal during determinations by AdSV recorded at a MFM is shown in Figure 2.2a. All the voltammograms obtained with the solutions of the microwave-assisted digestion presented a large, reproducible and well defined peak at -0.615 V. The amplitude of this peak is dependent of the protein content in the samples analysed but is independent of the deposition time at the MFM. The absence of a nickel peak around -0.95 V is because the surface of the microelectrode is poisoned by the organic matter adsorbed, hindering the accumulation of the Ni(II)-DMG complex at the same surface. In Figure 2.2b is plotted a typical voltammogram of this solutions evaporated with $HClO_4$. No detectable peak of organic matter in the potential range considered is observed under the experimental circumstances. A comparison between the two figures shows the importance of eliminating the organic matter completely, otherwise nickel cannot be quantified by the electrochemical method developed in this work.

Evaporation of the microwave digested samples yielded a residue that contains incomplete digestion products. These formed a precipitate that is relatively insoluble in cold water but soluble at 100 °C and when these solutions are buffered with ammonium adjusting the pH to 9.2 for further nickel voltammetric analysis. It was through the analysis of these precipitates and the liquid part of these solutions that enabled to identify by FTIR and XRD the organic components that are adsorbed at the microelectrode surface, giving rise to the unpredictable peak.

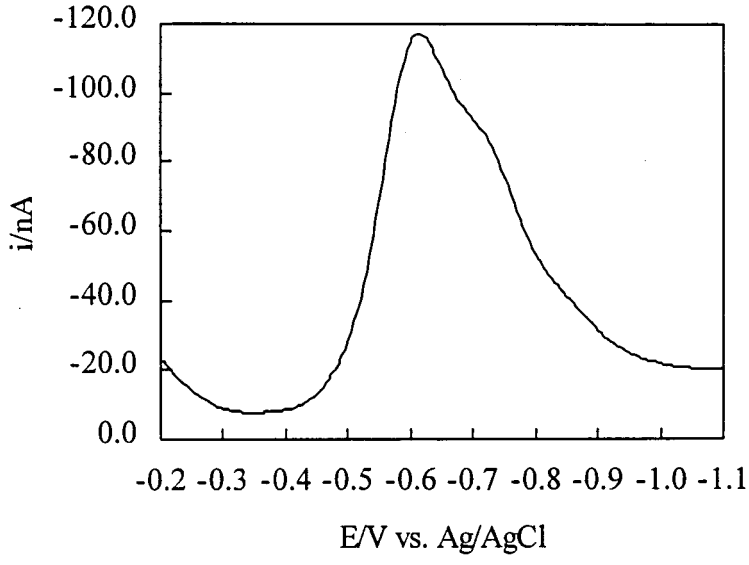

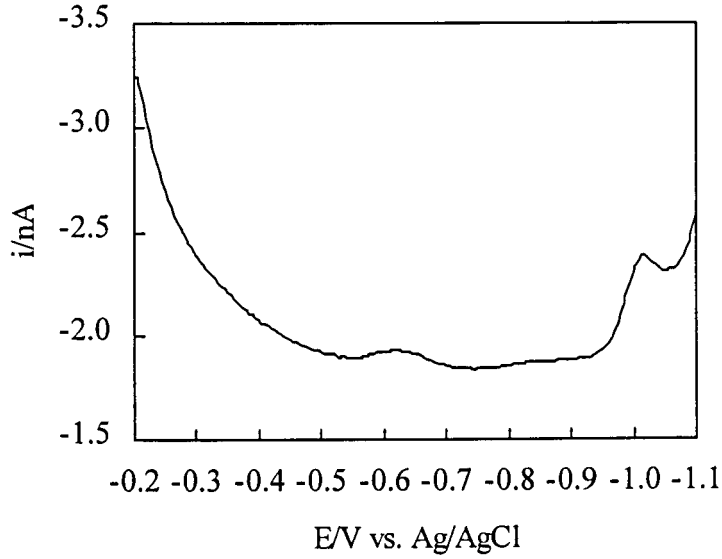

Figure 2.2. Square wave voltammograms of control mice liver samples using a mercury film microelectrode: a) after microwave digestion with HNO_3; b) after evaporation with $HClO_4$. Operating conditions: deposition time 30 s, deposition potential -0.70 V, step 5 mV, amplitude 20 mV and frequency 100 Hz.

DRIFT spectra of KBr solid solutions containing the digested samples (Figure 2.3a) were very consistent with the IR absorption spectrum of *p*-nitrobenzoic acid reported in literature [40]. Direct comparison with the DRIFT spectrum of *p*-nitrobenzoic acid in KBr (Figure 2.3b) gives a match of 95%. XRD spectrum of the precipitate compared to that of *p*-nitrobenzoic acid leads to the observation of similar patterns (Figure 2.4). Thus the conclusion is that the precipitate after digestion with HNO_3 is mainly composed of the isomer *p*-nitrobenzoic acid.

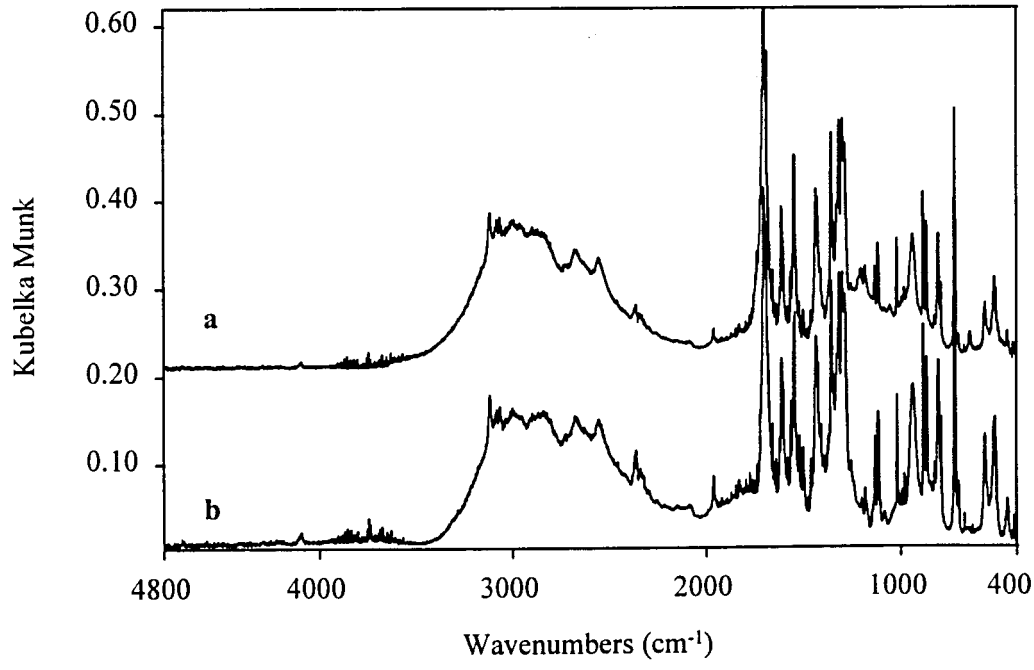

Figure 2.3. DRIFT spectra in Kubelka-Munk units of KBr solid solutions containing: a) the digested sample (offset scale); b) pure *p*-nitobenzoic acid.

It is important to draw attention to the fact that using HNO_3 to digest biological samples leads to the formation of the isomer *p*-nitrobenzoic acid. Even though this compound does no react with nickel, it accumulates at the mercury surface increasing the background current, masking the electrochemical response of nickel. When analysing this kind of biological samples, a further digestion stage using $HClO_4$ must be considered otherwise the electrochemical data will be distorted.

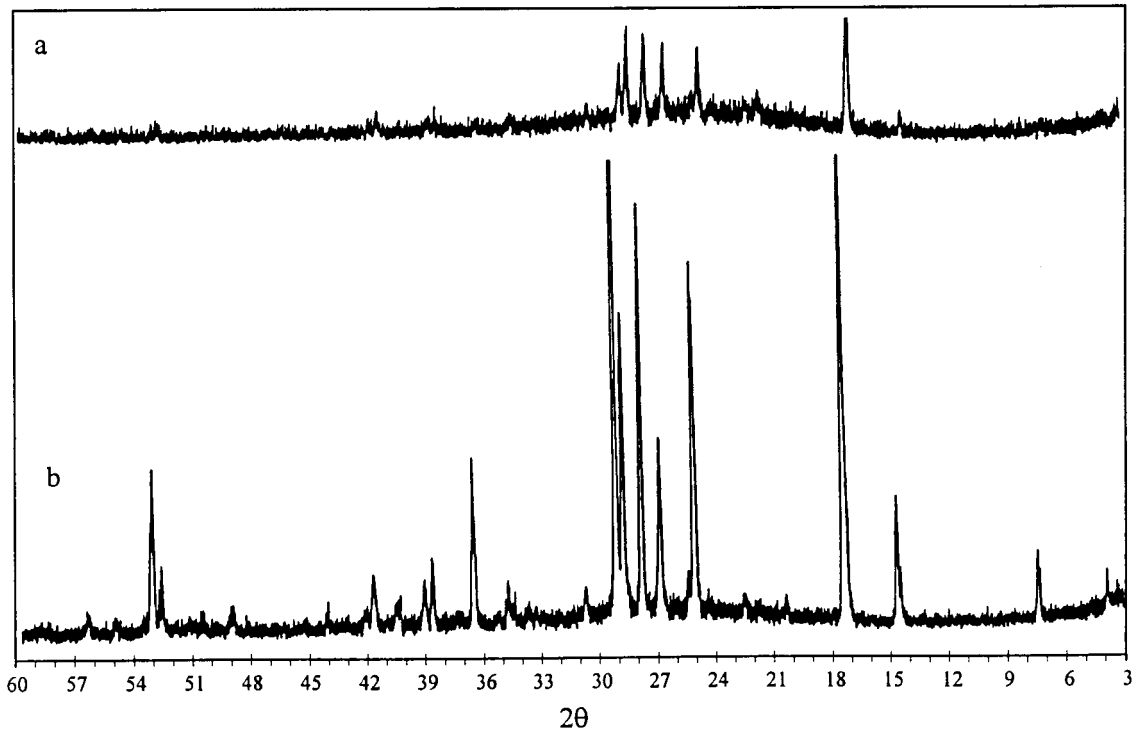

Figure 2.4. XRD spectra of solid solutions containing: a) the digested residues; b) pure *p*-nitrobenzoic acid.

Quantitative analysis of nickel

Adsorptive stripping voltammetry (AdSV) using the square wave technique (SWV) was the electrochemical process used to quantify nickel levels in these biological solutions and involves adsorption and accumulation of the complex, Ni(II)-DMG, at the mercury film microelectrode and subsequent reduction of the adsorbed nickel complex. A typical voltammogram obtained by this technique is presented in Figure 2.5 for a mouse liver sample at day 7.

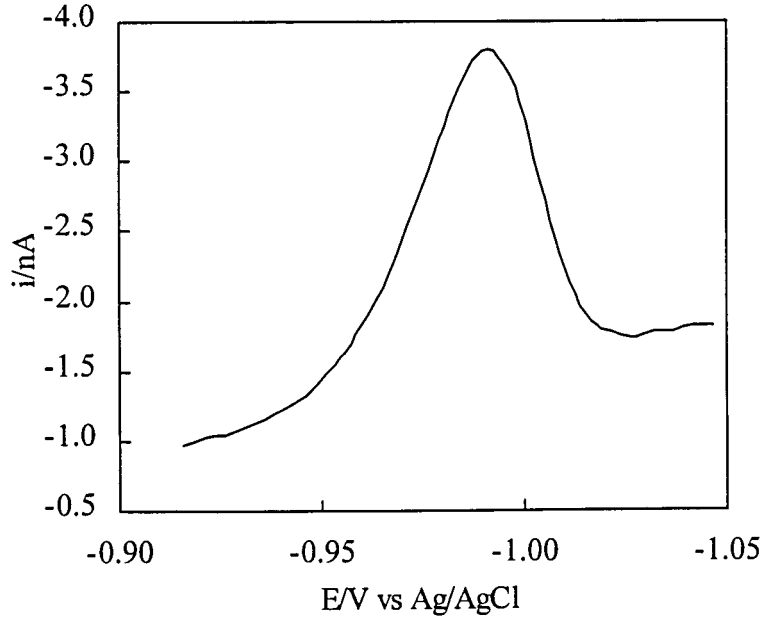

Figure 2.5. Nickel voltammogram of mouse liver sample at day 7, using a MFM. Operating conditions: deposition potential -0.70 V; deposition time 15 s; step 5 mV; amplitude 20 mV; frequency 100 Hz.

The behaviour of the DMG organic ligand for the range of nickel concentrations present in the biological samples (Figure 2.6), is very similar with the behaviour of this ligand to nickel in natural waters [20,41] suggesting that some residues of organic matter, destroyed by the digestion process seem not to be competitive with nickel ions. 0.10 mmol/L seems to be the ideal concentration of DMG because the resolution of the peaks observed decreases for higher concentrations of this complexing agent.

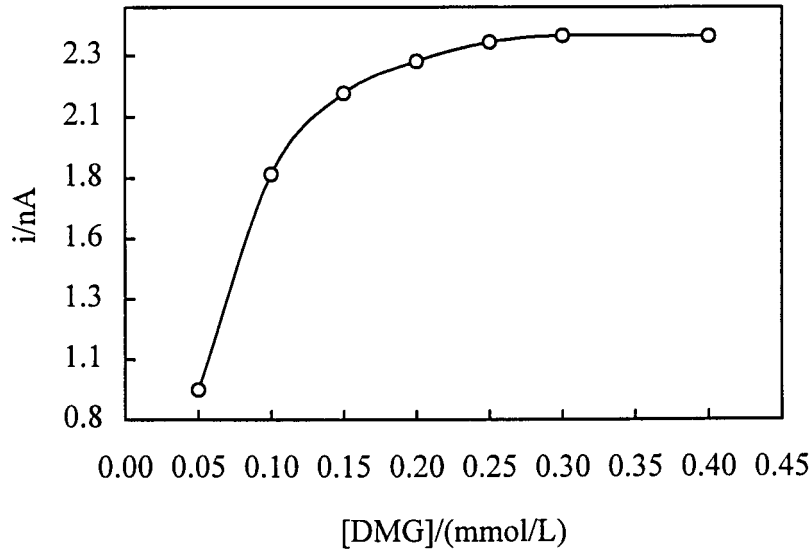

Figure 2.6. Effect of DMG concentration on the nickel peak current. Operating conditions: deposition potential -0.70 V; deposition time 15 s; step 5 mV; amplitude 20 mV; frequency 100 Hz.

The effect of the NH_3/NH_4Cl buffer concentration on the amplitude of the nickel peak current in these samples has been reported previously [24] and similar results (Figure 2.7) were obtained in the work presented herein. The concentration of the buffer solution used in all solutions was 0.10 mol/L. This concentration gives the largest peak current associated with the improvement in the background current, *i.e.*, more flat and reproducible. For higher NH_3/NH_4Cl buffer concentrations the sensitivity starts to decrease due to the competition between the buffer components and the DMG for the available nickel [19].

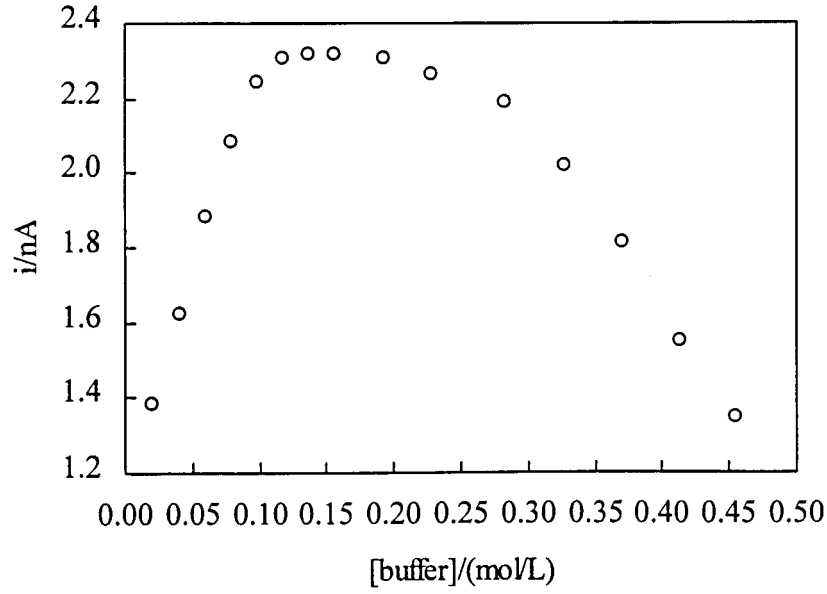

Figure 2.7. Effect of NH_3/NH_4Cl buffer concentration on the nickel peak current. Operating conditions: deposition potential -0.70 V; deposition time 10 s; step 5 mV; amplitude 20 mV; frequency 100 Hz.

The variation of the peak current of nickel with pH, was studied between 7.9 and 10.8 (Figure 2.8). The peaks are linearly shifted by about 39 mV in the negative direction per unit of pH increase. The present results are in agreement with similar studies in water performed by Flora *et al.* [20] and Pihlar *et al.* [23] using a DME and a HMDE, respectively.

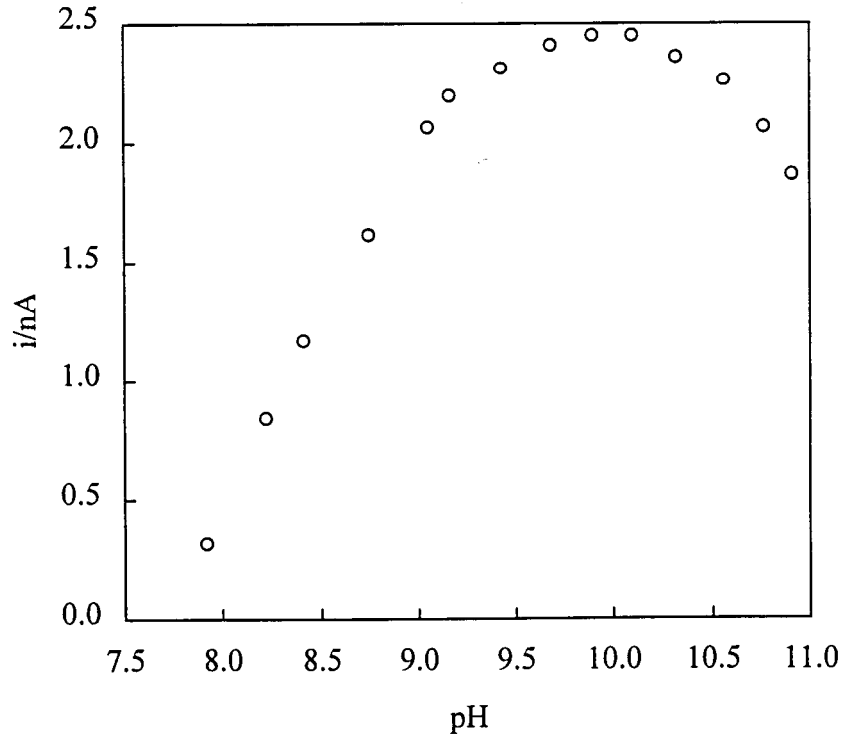

Figure 2.8. Variation of the nickel peak current with pH. Operating conditions: deposition potential -0.70 V; deposition time 15 s; step 5 mV; amplitude 20 mV; frequency 100 Hz.

Another parameter investigated was the amplitude and the step, which together affects the electron transfer process of the adsorbed complexes on the MFM surface. The best compromise between resolution and sensitivity for these square wave parameters investigated was obtained for 20 mV amplitude and a step of 5 mV. It seems that the constituents of the biological solutions analysed do not affect the electron transfer process because in the water system these two parameters behave in the same way [22].

Figure 2.9 illustrates the influence of the deposition time on the nickel peak current. The deposition time was changed between 5 and 120 s. The nickel peak current increases linearly until 30 s, and for deposition times higher than 80 s the surface of the mercury film microelectrode is saturated for a concentration of 14.8±0.3 μg/L present in the biological sample. The peak potential is not dependent of the deposition time. The maximum time used in these biological solutions was 30 s for the range of concentrations studied. Under such conditions, the full coverage of the microelectrode surface is avoided and the adsorbed amount of Ni(II)-DMG remains in the rising part of the adsorption isotherm (Langmuir type) [20] and, at the same time, when standard additions of nickel were made, the peak current was still directly proportional to nickel concentration in the samples studied.

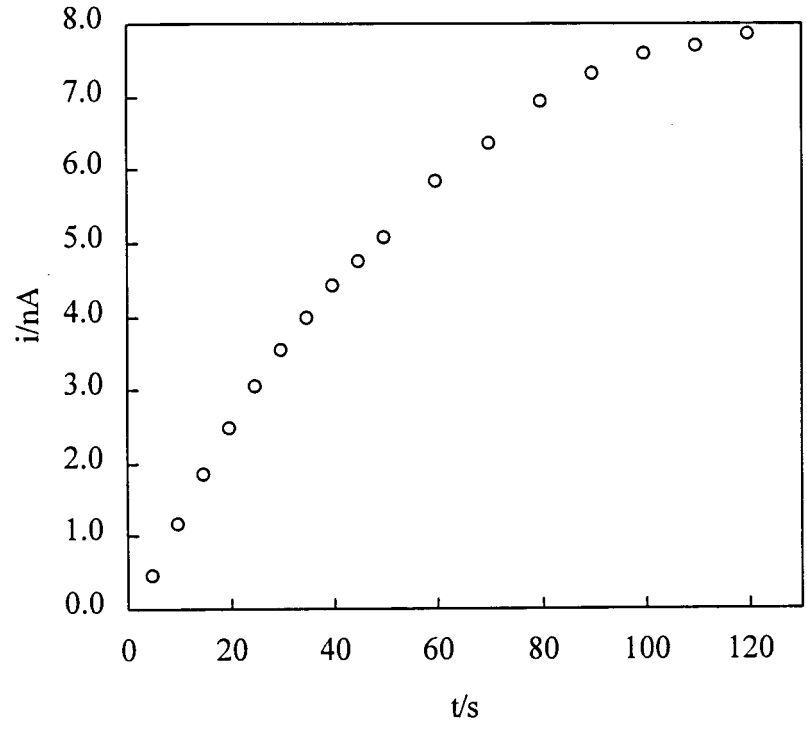

Figure 2.9. Effect of the deposition time in mice liver sample containing 14.8±0.3 µg/L of nickel.

Figure 2.10 shows several voltammograms obtained by the standard addition method from a solution of control kidney mice at day 7 which allows to quantify the amount of this metal ion in the biological samples. Thus the smallest peak is the one of the biological sample response and has a nickel content of 9.1±0.2 µg/L corresponding to 0.188±0.004 µg/g per dry weight. The other solutions were quantified by the same process.

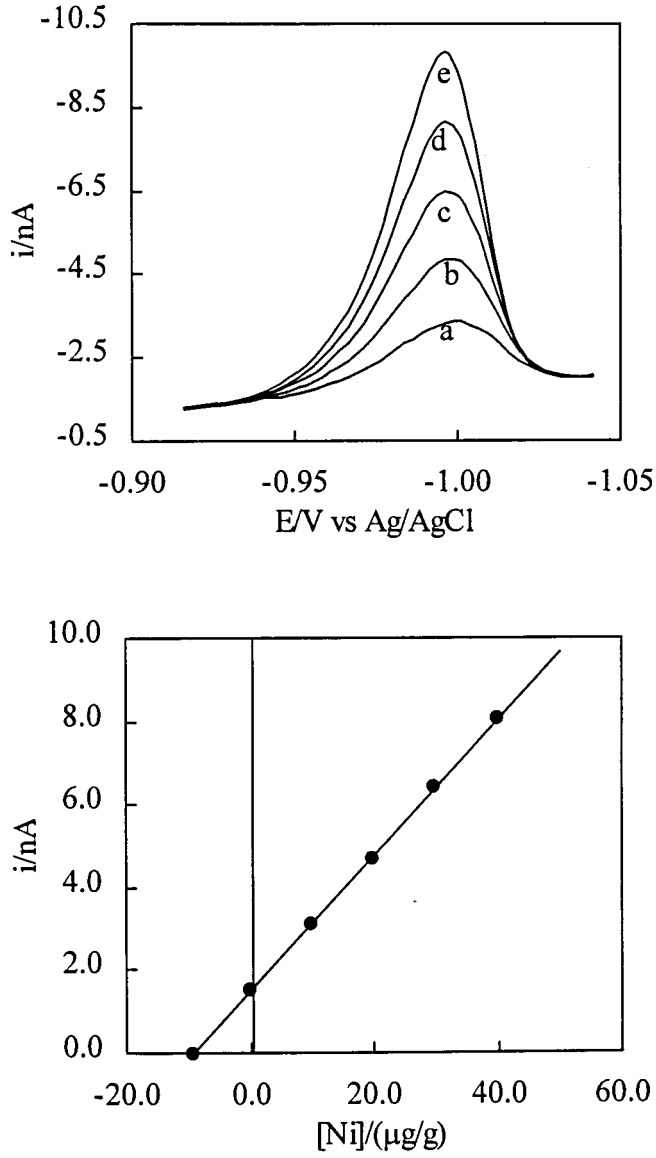

Figure 2.10. Determination of nickel level in a control mouse kidney sample at day 7, by AdSV onto mercury microelectrode using: a) the standard addition method, a, sample; b, c, d, and e, standard additions of 10 μg/L each one. Operating conditions: deposition time 15 s, deposition potential -0.70 V, step 5 mV, amplitude 20 mV and frequency 100 Hz. b) Plot of the resulting standard addition method used to quantify the nickel level in the sample. The sample contained 9.1±0.2 μg/L.

Reproducibility of SWV measurements on the same mercury film was assessed by carrying out fifty successive analyses for a mice liver sample at day 21 containing 12.3±0.3 μg/L of nickel, and the relative standard deviation was 2.4%.

To determine the accuracy of this method spike experiments were performed to test the recovery of nickel in these solutions which are characterised by a strong matrix effect. Table 2.1 contains recovery data for the three organs studied and the recovery is nearly 100%, indicating that matrix effects seem to be similar for all organs and do not interfere with nickel ions present in the samples.

Table 2. 1. Recovery of 10 μg/L of nickel added as a standard solution to liver, kidney and spleen sample solutions.

	Original value detected (μg/L)	*Detected value after spike (μg/L)*	*Recovery (%)*
Liver	12.84±0.32	22.92±0.41	99.7±0.4
Kidney	9.81±0.27	19.85±0.26	99.3±0.5
Spleen	7.64±0.15	17.73±0.19	99.8±0.2

Comparisons between data acquired by AdSV using microelectrodes and the classical technique, AAS are presented in Table 2.2. A student's *t* test comparing the values obtained by both methods was done and the differences were not statistically significant ($P>0.05$). Furthermore, from these data it is clear that a significant increase of nickel content ($P<0.01$) with administration time in the

organs herein investigated is observed when compared with the corresponding controls.

Detection limits for nickel by both methods (calculated from 3 times the standard deviation) were attained with three determinations in a diluted control liver sample at day 7 and were 1.58 nmol/L for a deposition time of 15 s and 5.48 nmol/L by AAS. The detection limit by AdSV may be improved by more than one order of magnitude if longer deposition times are used.

Liver

A progressive increase of nickel accumulation in liver with time is presented in Figure 2.11. The nickel content was significantly higher ($P<0.01$) at all time intervals when compared with the control animals. Major accumulation of this metal can be seen at day 28, after 4 weekly injections, and corresponds to a nickel increase of approximately sevenfold compared with the control group. At day 7, the nickel level in this organ was already twofold compared with the control group. Nickel concentrations in the control mice remained essentially unchanged during the different injections.

Table 2.2. Comparative Results Obtained in Mice Organs by AdSV and AAS Following injections of metallic nickel

The values are expressed in μg/g of dry weight

	Liver		*Kidney*		*Spleen*	
	AdSV	*AAS*	*AdSV*	*AAS*	*AdSV*	*AAS*
7 days						
Control	0.199±0.003	0.193±0.004	0.188±0.004	0.198±0.006	1.52±0.03	1.57±0.05
Injection	0.413±0.012	0.424±0.008	1.19±0.04	1.27±0.03	5.20±0.11	5.33±0.14
14 days						
Control	0.200±0.004	0.192±0.004	0.170±0.004	0.167±0.006	1.48±0.03	1.34±0.06
Injection	0.643±0.008	0.639±0.017	0.717±0.009	0.703±0.019	2.65±0.10	2.70±0.12
21days						
Control	0.184±0.003	0.188±0.005	0.216±0.005	0.208±0.004	1.64±0.05	1.59±0.07
Injection	0.815±0.017	0.805±0.016	1.03±0.02	1.03±0.04	4.16±0.06	4.09±0.21
28 days						
Control	0.187±0.004	0.182±0.004	0.201±0.006	0.214±0.008	1.30±0.03	1.36±0.04
Injection	1.23±0.03	1.27±0.04	0.950±0.03	0.960±0.015	4.98±0.16	4.96±0.18

[a]Mean for at least three separate determinations and their standard deviation.
Each control and injected group was composed of 8 animals.
The differences in results with both methods are not significant at $P>0.01$.

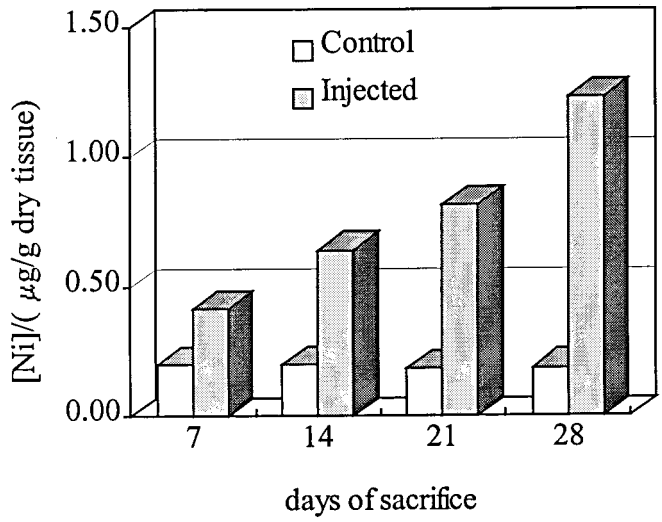

Figure 2.11. Comparison of nickel concentration in mouse liver injected with metallic nickel and the control animals. The animals were sacrificed at days 7, 14, 21 and 28. Values attained by AdSV.

Kidney

Figure 2.12 demonstrates that there was a significant accumulation ($P<0.01$) of nickel in the kidney of animals submitted to nickel injections. The maximum peak value occurred at day 7 while the accumulation ratio between injected mice and the control was approximately 5. At day 14 the nickel level decreased and rose again at day 21. The levels of nickel in the control groups were very similar throughout the experiment.

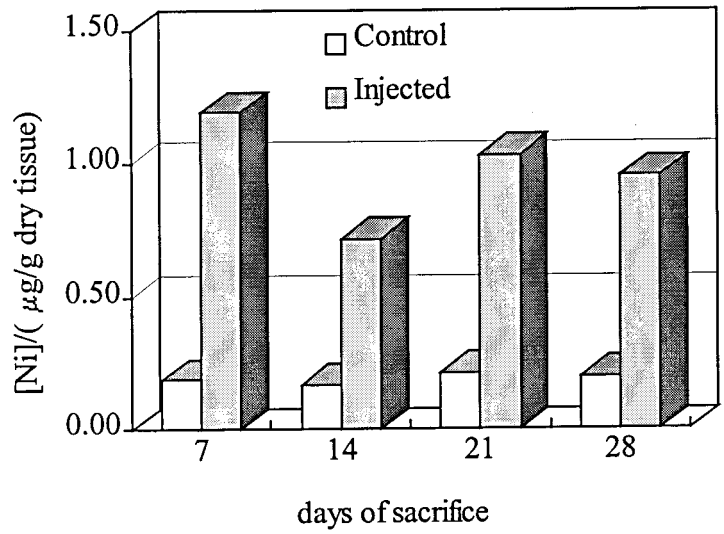

Figure 2.12. Comparison of nickel concentration in mouse kidney injected with metallic nickel and the control animals. The animals were sacrificed at days 7, 14, 21 and 28. Values attained by AdSV.

Spleen

Figure 2.13 shows a pronounced rise in nickel concentration from the control animals, demonstrating a significant accumulation in the spleen ($P<0.01$). At day 7 the nickel concentration appeared elevated, having an accumulation ratio of 3.4. However, the amount of nickel decreased at day 14. This behaviour is very similar to that of nickel accumulation in the kidney at the same sacrifice times. After day 14, a progressive increase in the nickel concentration in the analysed organ with an accumulation ratio of 3.3 can be seen.

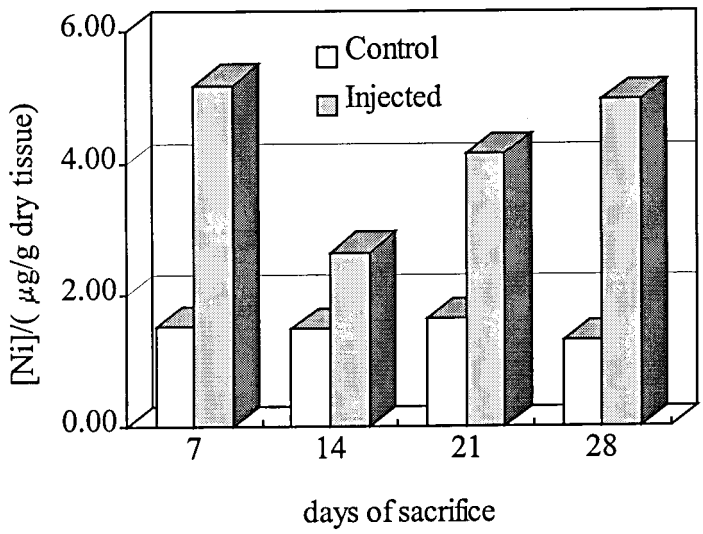

Figure 2.13. Comparison of nickel concentration in mouse spleen injected with metallic nickel and the control animals. The animals were sacrificed at days 7, 14, 21 and 28. Values attained by AdSV.

Morphological observations

The body weight of animals expressed in g was controlled at the day of the first injection and at the day of sacrifice and mean values with the standard deviations were, respectively: Group I- 28.10±3.45 and 29.18±1.82; Group II- 29.26 ±1.84 and 27.41±2.33; Group III- 29.42±1.94 and 29.7±2.74; Group IV- 29.13±2.77 and 27.36±3.32. The same procedure was used with the control groups. Differences between body weights at sacrifice and the initial weights were not statistically significant (P>0.01) and were the same for both test and control animals.

No animal mortality was observed during this study, nor apparent signs of toxicity, and no macroscopic changes were detected in the three organs. In addition, no differences were observed in the liver, kidney and spleen between control and mice of Groups I and II.

Hepatic changes were observed in group III and IV within the last two weeks of treatment when compared to the control liver, although histological alterations were quite similar. Such changes were confined to the parenchyma, as the portal track presented normal features (Figure 2.14). No enlargement between the hepatic cords was observed. Hepatocytes exhibited a typical oval and round shape, but a swollen and clear cytoplasm was noted. Nuclei of hepatocytes exhibited very strong staining, but normal morphological features were observed.

In the spleen, some changes were observed within the group IV when compared to the control group (Figure 2.15). Splenic sections demonstrated a capsular fibrosis at the periphery. The most relevant finding is concerned with the increase in number and size of giant cells, spreading not only in the periphery but in the bulk as well. The remaining groups of animals demonstrated regular features for this lymphoid organ, similar to the control group.

As illustrated in Figure 2.16, the kidney of group IV showed an altered histology which included an accentuated alteration of renal tubule epithelium compared to the control group. A disrupted epithelium was denoted throughout the renal

tubules. This aspect included the spreading of some cells, or even nuclei.

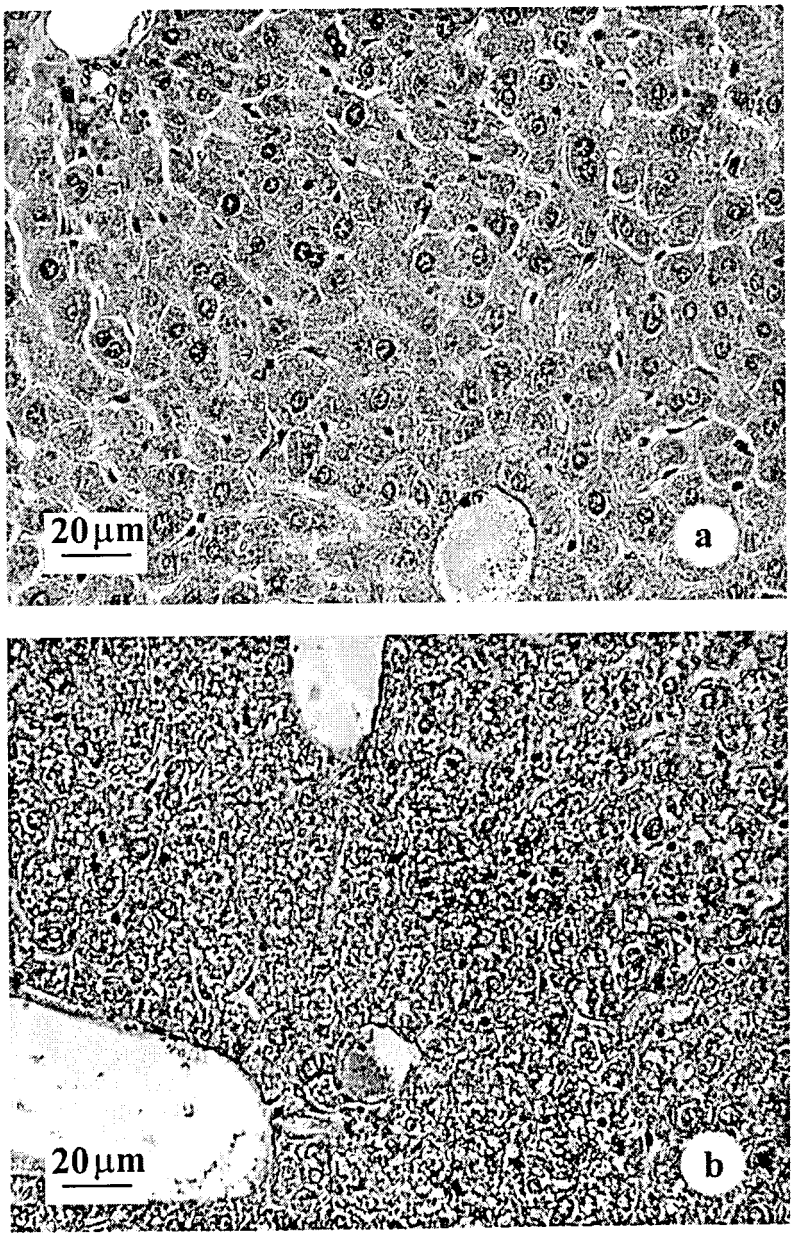

Figure 2.14. a) Light micrograph of liver from a control mouse showing regular histologic features and representative hepatocellular morphology; b) Light micrograph from liver of group II administered animals showing several alterations where swollen hepatocytes are clearly seen in the parenchyma but nuclei show apparently normal morphology.

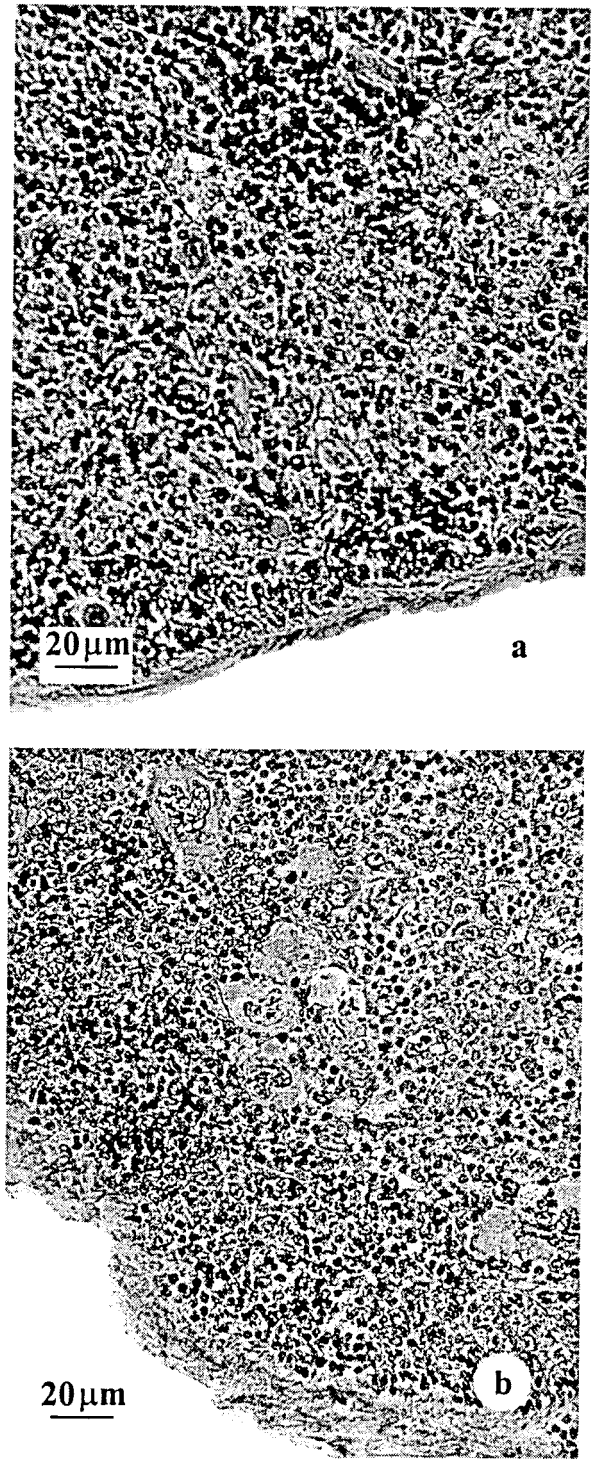

Figure 2.15. a) Control spleen in which clusters of lymphoid tissue are clearly visible through the organ; b) Splenic tissue from group IV animals where giant cells dominate the picture.

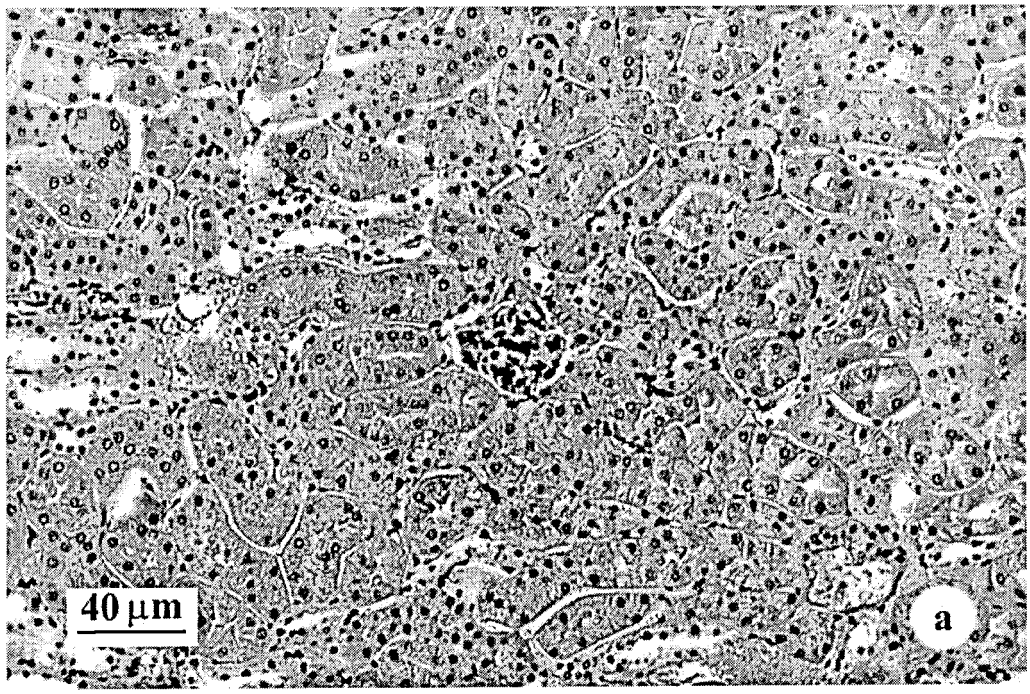

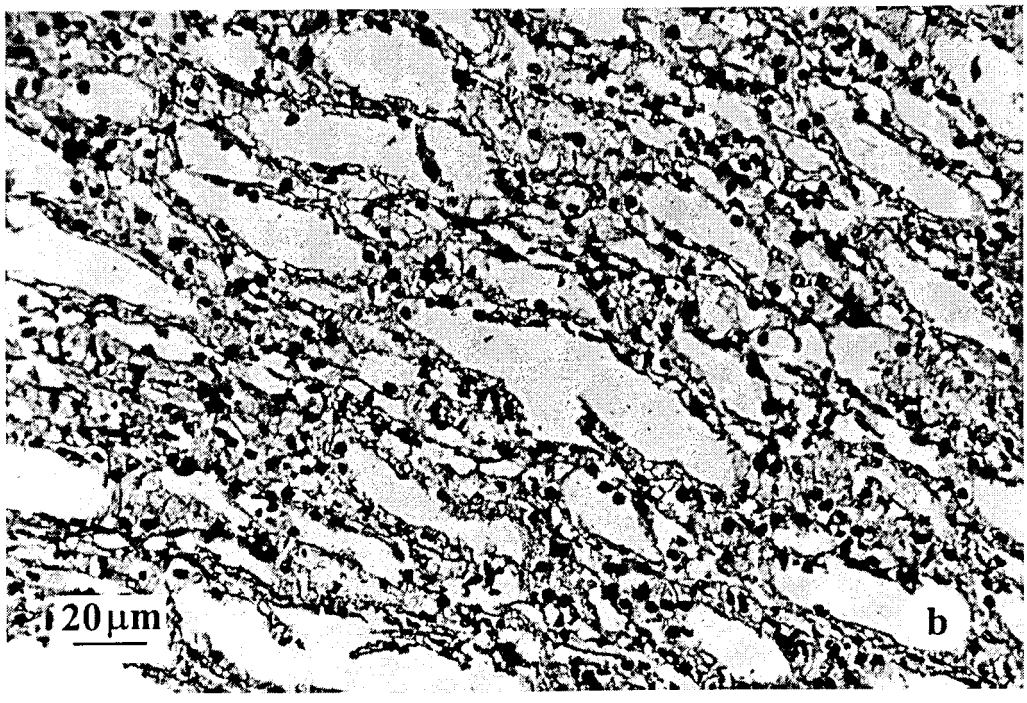

Figure 2.16. a) Renal tissue of the control group showing normal epithelium; b) a very disrupted epithelium is observed in the renal tubules of group IV where irregularities and degenerated cell line the renal tubules.

DISCUSSION

It has been demonstrated that AdSV in conjunction with mercury film microelectrodes provides a simple and suitable technique for determination of trace levels of nickel in biological tissues. This technique possesses very good sensitivity and the detection limit established above is adequate for most biological tissues. Additionally, it presents good reproducibility and is a faster analytical technique compared to AAS. Other main advantages associated with nickel determinations by AdSV using MFM are: i) there is no need for oxygen removal, which usually is time consuming, and ii) its surface remains stable and reproducible for long periods (four to six hours) in contrast to conventional mercury electrodes.

Special care has to be taken at the digestion step required, namely the $HCLO_4$ chemical attack because of the possible contamination of samples.

The results obtained for nickel concentration in the kidney and liver mice control are comparable in magnitude to previous values reported by Merritt *et al.* [42] in Syrian hamsters. For the spleen the values found are greater than those attained by the same authors.

The results obtained by both analytical methods indicate that, indeed, there is an accumulation of nickel in the treated organs when compared to the control ones. While in liver the accumulation gradually increases in time, in kidney and spleen a

higher accumulation is observed in group I, decreasing for group II and increasing for the two remaining groups. The pattern of behaviour observed for the kidney and the spleen is in agreement with previous results obtained for mice treated intraperitoneally with a stainless steel AISI 316L slurry [16].

From what is known about nickel corrosion in patients who had implants made of nickel alloys, the maximum rate of nickel release is 20 μg/Kg/day [43]. In this study we simulate a corrosion rate of 300 μg/Kg/day (15 times more than the normal corrosion rate) to guarantee a rapid distribution of this metal, bearing in mind that in tissues adjacent to stainless steel 316L plates and screws the nickel concentration ranges between 116 to 1200 mg/L [44].

After a week from the first injection (group I), the quantity of nickel that was accumulated in the three organs was approximately 0.35 μg per animal in contrast with the quantity initially injected 57.5 μg. Globally, this means that nickel is rapidly and mostly eliminated from the body by urine [42,45] and the quantity that accumulates in the studied organs is vestigial. But this very small quantity of nickel accumulated in the organs suggests that the tolerance of these organs to store this metal has been exceeded and caused pathological changes.

In this work some histological alterations were observed in the liver, kidney and spleen of animals injected with nickel ions, even though these alterations are most relevant within groups III and IV. These results confirm previous data obtained at

our laboratory, showing that under these experimental conditions, nickel promotes some deleterious effects in the liver, kidney and spleen [16]. Similar effects on hepatic tissue were described for an injected slurry of stainless steel, although splenic effects were also noted in the same group of animals [46,47]. The most conspicuous alterations in liver were observed at weeks 3 and 4 of treatment. Such alterations are in agreement with the chemical analysis data which illustrate a significant accumulation of nickel with treatment time (Figure 2.11). The observed alterations may suggest an altered function of this organ, namely the detoxification function. Chemical analysis of the kidney indicates that a higher nickel content was attained in group I, whereas in the remaining groups it fluctuates but is always much higher than in the control groups. This pattern of behaviour may be explained by the fact that nickel was eliminated in urine. However, this is in disagreement with the histological observations, in which normal features were clearly seen in group I. Such discrepancies point to the fact that after short periods of treatment, nickel is accumulated in the organ but the time is not enough to induce histological changes.

Very conspicuous alterations were observed in the spleen for group IV (Figure 2.15), which is the organ involved in the removal of aged or damaged erythrocytes [48]. It is assumed that the capsule is mainly composed of myofibroblasts which may contract inducing a discharge of red cells into the blood vessels, as the spleen

has the ability to hold large volumes of red blood cells in reserve. In this way, the great width of the capsule observed in nickel injected animals may be involved in the release of a higher amount of blood.

The increased number and volume of giant cells in the spleen have already been observed in mice injected with strontium 90 and stainless steel corrosion products [45]. As liver and spleen are blood filtering organs, the observed histological changes may be attributed to their physiological role in blood clearance, pointing to the fact that after the injection of a high-dose metal ions the organs are able to faster the elimination process.

CONCLUSIONS

The AdSV technique associated with a gold disc microelectrode modified with a MFM is suitable for determining low nickel concentrations in these biological samples.

The analysis time in AdSV with the MFM are much lower, compared with conventional mercury electrodes and AAS making this technique very attractive for its decrease in time associated with the excellent reproducibility of the method.

It was verified a significant increase in the nickel level with time in the liver, kidney and spleen compared with the control animals indicating that there are an accumulation of this specie in the studied organs.

At the different periods of the treatment time the total nickel levels that remained in the studied organs were less than 1% compared with the quantity of nickel initially injected.

This vestigial nickel quantity that remained in the organs caused morphological alterations at four weeks of treatment.

Apparently, the morphology of the liver, kidney and the spleen are seriously affected by the presence of this metal.

REFERENCES

[1] EPA, "*Health Assessment Document for Nickel and Nickel Compound*", EPA/600/8-83/012FF, U.S. Environment Protection Agency, Research Triangle Park, NC, (1986).

[2] J. Black, "*Orthopeadic Biomaterials in Research and Practice*", Churchill Livingstone, New York, (1988).

[3] R. P. Hausinger, "*Biochemistry of Nickel*", Plenum Press, New York, (1993) 221.

[4] E. Nieboer, F. E. Rossetto, and C. R. Menon, "*Nickel Toxicology*", S. S. Brown and F. W. Sunderman Jr (eds.), Academic Press, (1980), 359.

[5] J. C. Heath, "*Biocompatibility of Implant Materials*", D. Williams (ed.), Sector Publishing Limited (1976) 49.

[6] V. A. Memoli, R. M. Urban, J. Alroy and J. O. Galante, *J. Orthop. Res.*, **4** (1986) 346.

[7] J. B. Park and R. S. Lakes, "*Biomaterials an Introduction*", Plenum Press, New York, (1992) 1.

[8] J. D. Bumgarder and L. C. Lucas, "*Compatibility of Biomedical Implants*", P. Kovacs and N. S. Istephanous, (eds.), The Electrochemical Society, Inc., Pennington, New Jersey, (1994) 241.

[9] A. Cigada, G. Rondelli, B. Vicentini, F. Brunella, and G. Dallaspezia, "*Compatibility of Biomedical Implants*" (eds.), P.Kovacs and N. S. Istephanous, The Electrochemical society, Inc., Pennington, New Jersey, (1994) 185.

[10] D. F. Williams, "*Encyclopedia of Medical and Dental Materials*", Pergamon Press, Oxford, (1990).

[11] A. W. J. Muller, F. J. M. J. Maessen, and C. L. Davidson, *Dent. Mater.*, **6**, (1990) 63.

[12] J. D. Bumgardner and L. C. Lucas, *Dent. Mater.*, **9** (1993) 252.

[13] D. F. Williams, *"Systemic Aspects of Biocompatibility"*, C. R. C. Press, Boca Raton, Florida, Vol. I and II, (1981).

[14] B. N. Stulberg, K. Merrit, and T. W. Bawer, *J. Appl. Biomater.*, **5** (1994) 9.

[15] M. A. Panigutti, K. Merrit, R. J. Bruner, M. J. Kraay, and S. A. Brown, *Tra. Soc. for Biomaterials*, **15** (1992) 7.

[16] A. M. Abreu, R. B. Tracana, G. S. Carvalho, and J. P. Sousa, *Biomedical Letters*, **52** (1995) 133.

[17] G. K. Smith and J. Black, *"Corrosion and Degradation of Implant Materials"*, Second Symposium, A. C. Fraker and C. D. Griffin (eds.), American Society for testing and materials, Philadelphia, (1985) 223.

[18] M. L. Pereira, M. C. Pereira, and J. P. Sousa, *Biomedical Letters*, **52** (1995) 235.

[19] B. Pihlar, P. Valenta and H. W. Nurnberg, *Fresenius Z. Anal. Chem.*, **307** (1981) 337.

[20] C. J. Flora and E. Nieboer, *Anal. Chem.* **52** (1980) 1013.

[21] A. M. Bond and D. L. Luscombe, *J. Electroanal. Chem.*, **214** (1986) 21.

[22] P. Ostapczuk, P. Valenta and H. W. Nurnberg, *J. Electroanal. Chem.*, **214** (1986) 51.

[23] B. Pihlar, P. Valenta and H. W. Nurnberg, *J. Electroanal. Chem.*, **214** (1986) 157.

[24] H. Zhang, R. Wollast, J. C. Vire and G. J. Patriarche, *Analyst*, **114** (1989) 1597.

[25] A. Economou and P. R. Fielden, *Analyst*, **118** (1993) 47.

[26] S. B. Adeloju, A. M. Bond and M. H. Briggs, *Anal. Chim. Acta*, **164** (1984) 181.

[27] J. Wang, *American Laboratory*, (1985) 41.

[28] J. Wang, "*Stripping Analysis. Principles, Instrumentation and Applications*", VCH, Deerfield Beach, Florida, (1985) 65.

[29] M. C. Pereira and J. P. Sousa, *Portugaliae Electrochim. Acta*, **13** (1995) 477.

[30] R. M. Wightman and D. O. Wipf, "*Electroanalitycal Chemistry*", A. J. Bard (ed.), **15** (1989) 267.

[31] P. R. Griffiths, S. A. de Haseth, "*Fourier Transform Infrared Spectrometry*", Chemical Analysis, P. J. Elving, S. D. Winefordner, (eds.), John Wiley & Sons, **83** (1986).

[32] C. Veillon, *Anal. Chem.*, **58** (1986) 851A.

[33] K. S. Subramanian, *Atomic Spectroscopy*, **9** (1988) 169.

[34] F. Takeshita, K. Murai, Y. Ayukawa and T. Suetsugu, *J. Biomed. Mater. Res.*, **34** (1997) 1.

[35] J. Versieck and L. Vanballenberghe, "*Handbook on Metals in Clinical and Analytical Chemistry*", H. G. Seiler, A. Sigel and H. Sigel eds., Marcel Dekker, Inc., New York, (19 4)

[36] S. Lugowki, D. C. Smith and J. C. Vanloon, *Clinical Materials*, **6** (1990) 91.

[37] W. C. Purdy, "*Chemical Toxicology and Clinical Chemistry of Metals*", S. S. Brown and J. Savory, (eds.), Academic Press, (1983) 17.

[38] M. C. Pereira, J. L. Faria, M. L. Reis and J. P. Sousa, *Electroanalysis*, **9** (1997) 150.

[39] T. S. Koh, *Anal. Chem.*, **52** (1980) 1978.

[40] D. Lin-Vien, N. B. Colthup, W. G. Fateley, J. G. Grasselli, "*The Handbook of Infrared and Raman Characteristic Frequencies of Organic Molecules*", Academic Press, Inc. (1991).

[41] B. J. Basu and S. R. Rajagopalan, *Analyst*, **117** (1992) 1623.

[42] K. Merritt, T. D. Crowe and S. A. Brown, *J. Biomed. Mater. Res.*, **23** (1989) 845.

[43] J. Black, "*Biomedical Engineering and Instrumentation*", R. Plonsey and J. L. Katz (eds.), Marcel Dekker, New York, (1981) 180.

[44] O. E. M. Pohler, "*Biomaterials in Reconstructive Surgery*", L. R. Rubin (ed.), The C.V. Mosby Company, (1983), 197.

45 S. A. Brown, L. J. Farnsworth, K. Merritt and T. D. Crowe , *J. Biomed. Mater. Res.*, **22** (1988) 321.

[46] R. B. Tracana, J. P. Sousa and G. S. Carvalho, *J. Mater. Sci. Mater. Med.*, **5** (1994) 596.

[47] R. B. Tracana, M. L. Pereira, A. M. Abreu, J. P. Sousa and G. S. Carvalho, *J. Mater. Sci. Mater. Med.*, **6** (1995) 56.

[48] M.H. Ross and L.J. Romrell, (eds.), "*Histology - A Text and Atlas*", Williams and Wilkins, 2nd edition, New York, (1989) 326.

Chapter 3

EVALUATION OF CHROMIUM EFFECTS IN MICE ORGANS

3

INTRODUCTION

Chromium was considered one of the essential metals to the human organism due to a complex of trivalent chromium that has been found to participate in the glucose metabolism [1]. However it is well known that hexavalent chromium causes dermal irritancy and allergy [2] and it is suspected to be a chemical carcinogen [3,4,5]. Apparently, the trivalent form is not so toxic as it is hexavalent chromium [6].

Chromium may be absorbed into the human body from surgically implanted orthopedic prostheses fabricated from chromium-containing alloys such as AISI 316L stainless steel [7]. This alloying element (16-18% Cr) imparts to stainless steel their

resistance to corrosion by formation of a transparent protective film of Cr_2O_3 at the metal surface. Even so, it is now confirmed that surface corrosion of metallic implants does take place [8] and considerable amounts of chromium can be released into the tissues and transported to the organs [9] by the blood stream.

It has been reported in the literature that chromium is released from the implants in the hexavalent form [10,11,12,13] and elevated chromium concentrations and other elements were found in the blood, urine and also in tissues of patients carrying cobalt-chromium alloys and stainless steel implanted devices [14,15,16,17]. It attaches to albumin [18,19] and easily permutes with body fluids entering in the circulation. There is evidence that hexavalent chromium is rapidly reduced to the trivalent form before or during binding to haemoglobin and after uptake by cells, *i.e.* is reduced intracellularly [16].

Pereira *et al.* [20] have reported acute studies in Charles River mice. In that work animals were injected with a single dose of a solution containing 30 mg of K_2CrO_4 and were sacrificed after 15 and 30 days. The spleen evidenced major changes, namely enlargement of the capsule and decrease in the red pulp cell, accompanied by an increase of the megakaryocyte number. Chronic studies were also performed during 9 weeks but no alterations were observed in the splenic compartments.

Therefore, the determination of trace amounts of chromium in biological tissues is important and much work has been carried out for chromium determinations in

biological samples by atomic absorption spectrometry (AAS) due to its high sensitivity [21,22,23,24].

Electrochemical techniques, particularly adsorptive stripping voltammetry at a hanging mercury drop electrode (HMDE) have been reported in literature to determine chromium in natural waters [25], sea water [26], ground water [27] and in soils and sediments [27,28] in the presence of diethylenetriaminepentaacetic acid (DTPA) [25,26,28] and cupferron [27], down to the nanomolar levels. The advantage of this method is that total chromium can be determined in a single measurement and furthermore it is possible to perform the distinction between oxidation states, *i.e.*, hexavalent and trivalent chromium. Mercury film microelectrodes (MFM) present several advantages over the HMDE namely short deposition times (few seconds), deposition under non-stirring conditions, no need for a quiescent period, less interferences by the presence of oxygen and small sample volumes [29,30,31] making the analysis time very rapid.

Most of the metallic materials used in implantology contain significant quantities of at least three elements and each one have distinct biological properties. When stainless steel or other alloys are used, it is extremely difficult to correlate the specific histological features with the characteristics of each specific metal ion. With this in mind, one of the objectives of this work is to investigate the histological alterations with time in mice liver, kidney and spleen induced by chromium after several injections of a physiological solution of hexavalent chromium that was prepared by

anodic dissolution of the pure metal. Simultaneously, the content of this metal in the involved organs was determined by performing adsorptive stripping voltammetry (AdSV) measurements of Cr^{3+}-DTPA complex at a MFM using the square-wave technique. Several parameters were optimised in order to improve the detection limit of the method. The results were also assessed by AAS and were compared with those obtained by AdSV for the same set of samples.

These three organs were chosen because of their excretory functions [32]. Similar studies were done for nickel and iron with similar purposes [33,34]. Both metals induced with time several morphological alterations in the mentioned organs. Pure metals were used with the intention to differentiate between the individual effects of chromium, nickel and iron in the stainless steel alloy.

MATERIALS AND METHODS

Chromium dissolution

Discs of chromium Patinal (Merck) were anodically dissolved in Hank's Balanced Salt Solution (HBSS) by imposition of a constant current. The chromium content was determined by flame atomic absorption spectrometry (AAS) and a solution of 140 mg/L was prepared. The colour of the solution was yellow/orange indicating that the valence state of chromium in the physiological solution is hexavalent.

Animals

Male Charles River mice nearly 60 days old and weighing 27-34 g supplied from "Instituto Gulbenkian de Ciências", Portugal were selected as the laboratory animal model to administer the chromium solution. They were housed in groups of four per cage and food and water were given *ad libitum*. During one week the animals were allowed to equilibrate relative to their new environment and diet.

Chromium injections and mice sacrifice

A volume of 0.50 mL of the solution of chromium was subcutaneously injected in the back dorsal surface at days: 0- group I; 0, 7- group II; 0, 7, 14- group III and 0, 7, 14, 21- group IV. Each group was composed of eight animals. Control mice received HBSS only. The body weight of animals was registered at the day of the first injection with the chromium solution and at the day of sacrifice. The animals were sacrificed after a week of the last injection, under ether anaesthesia. By surgical incision in the abdominal cavity the liver, kidney and spleen were removed. Small fragments of the organs were used for histological studies and the remaining part was stored in PTFE bottles and kept in a freeze chamber at -20 °C for quantitative analysis.

During the dissection and in posterior treatment, the organs were not touched with any metallic instrument to insure no chromium contamination. All glassware and

polyethylene bottles used were soaked in solutions of HNO_3 20% for several hours and then rinsed with an excess of water and leave to dry.

Mineralisation procedure

Approximately 1.0 g of each organ studied was placed into previously weighed vessels and then dried in a microwave oven model MDS 2000 CEM. Inside the vessels 1.50 mL of HNO_3 Suprapur from Merck was added per 100 mg of dry weight. The microwave digestion proceeds during 30 minutes. After that, the resulting solutions were evaporated with the addition of 1.0 mL of $HClO_4$ (Merck) per 0.50 g dry mass until perchloric acid fumes were no longer observed. The residue was then diluted with ultrapure water to an appropriate volume. More details of the digestion procedure were previously described elsewhere [31].

Solutions prepared in this way were directly analysed by graphite furnace atomic absorption spectrometry.

Analytical procedure

The voltammograms were obtained using a potentiostat/galvanostat Model Autolab from ECO Chemie equipped with a module ECD specific for microelectrodes, which

was connected to a PC Model 1120 SX, used in conjunction with an electrochemical microcell. Voltammetric measurements were performed using a three electrode configuration system; a mercury film microelectrode as the working electrode, a silver/silver chloride in 3.0 mol/L KCl as the reference electrode and a cylindrical carbon auxiliary electrode.

Mercury film microelectrodes (MFM) were prepared by application of a constant potential of 0.0 V versus Ag/AgCl during 60 s, onto a gold surface of 25 μm diameter, from a deoxygenated solution of 6.0×10^{-3} mol/L mercury (II) chloride, 1.0×10^{-3} mol/L potassium nitrate and 0.50% of nitric acid.

The chemicals used for chromium determinations were DTPA purified two times by crystallisation from Sigma. Sodium nitrate, sodium acetate and sodium hydroxide (99.99%) from Aldrich were used as purchased. A 1.93×10^{-2} mol/L of hexavalent chromium atomic absorption standard solution (Aldrich) was used daily to prepare the standard solutions.

For the adsorptive stripping voltammetry measurements in square-wave mode the supporting electrolyte added to the mice organ digested solutions was 2.0×10^{-2} mol/L of DTPA, sodium acetate 4.0×10^{-2} mol/L and sodium nitrate 0.40 mol/L. The pH was adjusted to 6.1 with sodium hydroxide. Total chromium concentration was obtained by addition of $KMnO_4$ 1.0×10^{-3} mol/L to convert all trivalent chromium to hexavalent [28]. These solutions were purged with nitrogen for 10 minutes prior to the

electrochemical determinations to remove oxygen. The deposition potential was carried out at -1.15 V during 20 s for the levels of chromium presented in the samples (during this step the solution does not need to be stirred to enhance the chromium adsorption). After the adsorption period, the potential scan was initiated in the cathodic direction from -0.80 V to -1.45 V. The square wave parameters used were a frequency of 100 Hz, a step of 2.5 mV and an amplitude of 20 mV. To remove residual adsorbed chromium complex from the mercury film a potential of -1.30 V was applied during 10 s.

These biological solutions were also quantified by graphite atomic absorption spectrometry using a Perkin Elmer Model 4100ZL spectrometer in conjunction with pyrolytic THGA (transverse heated graphite atomiser) tubes and autosampler. $Mg(NO_3)_2$ was used as the matrix modifier.

The chromium levels in the samples were quantified by both techniques using the standard addition method and all measurements for the same sample were repeated at least three times.

Histological analysis

Small fragments of each organ were fixed in Bouin's solution, embedded in paraffin and sections with approximately 3-5 μm were made in a microtome. After

staining with Hematoxylin-eosin, sections were then dehydrated in an ethanol series and mounted in Canada Balsam. Observations and photographs were made using a Nikon optical microscope.

Statistical analysis

Statistical analysis of the significance of the differences between all groups injected by chromium and the control ones were carried out by the Student's *t* method. The acceptable level of significance was at $P<0.01$.

The statistical significance of the differences observed between means of the two analytical methods were done by the same method.

RESULTS

Chromium analysis

The precise determinations of very low concentrations of chromium in biological materials is very important to establish normal levels of this metal in the tissues and detect metabolic alterations by small changes in these reference values. The organs have to be digested and this is the most crucial step within the entire analytical procedure proposed. Sample preparation is a long process because organic matter must be completely destroyed [31] without any loss of chromium avoiding all sources of contamination. During this treatment, the oxidation state of chromium changes and is no longer possible to know if the chromium present in the organs is trivalent or hexavalent. Therefore only the total quantification of this element is achievable.

Several chelating agents, namely DTPA, TTHA [35] and cupferron appear in literature to determine levels of trivalent, hexavalent and total chromium down to the nanomolar range existing in various types of natural waters. The first chelating agent tested with mice organ samples was cupferron who is very selective to chromium and absorbs spontaneously in the mercury electrode surface giving a sensitive and very well-defined peak. Cupferron has been found to precipitate iron and this element exists in high concentrations in the digested mice organs suppressing completely the chromium signal. DTPA was found to be more adequate to complex with chromium in these biological samples.

Adsorptive stripping voltammetry measurements of chromium using a mercury film microelectrode (MFM) in digested mice organ samples were based on the procedure developed by Golimowski *et al.* [25] and Boussemart *et al.* [26]. The procedure involves complexion of trivalent chromium with DTPA and adsorption onto the mercury microelectrode. During the adsorption step, at a potential sufficiently negative, the dissolved hexavalent chromium is reduced to trivalent chromium and instantaneously complexed by DTPA. In the stripping step the Cr^{3+}-DTPA complex is reduced in a one electron step producing a peak around -1.25 V. This reduction current in augmented in the presence of nitrate ions owing to the chemical reoxidation of Cr^{2+} to Cr^{3+} (catalytic effect) which is again reduced at the MFM.

To determine the optimum conditions for the adsorption of Cr^{3+}-DTPA complex on the MFM, the effects of varying the concentration of $NaNO_3$, DTPA, CH_3COONa, pH, deposition potential, deposition time, square-wave parameters, as well as the effects of other elements on the peak current were investigated.

The influence of pH, the concentration of DTPA and $NaNO_3$ has a pronounced effect on the AdSV peak current. The individual response of these parameters were very similar to those reported in the literature [25,26]. At pH 6.1, $2.0x10^{-2}$ mol/L DTPA and $NaNO_3$ 0.40 mol/L a stable and well defined peak is obtained (Figure 3.1).

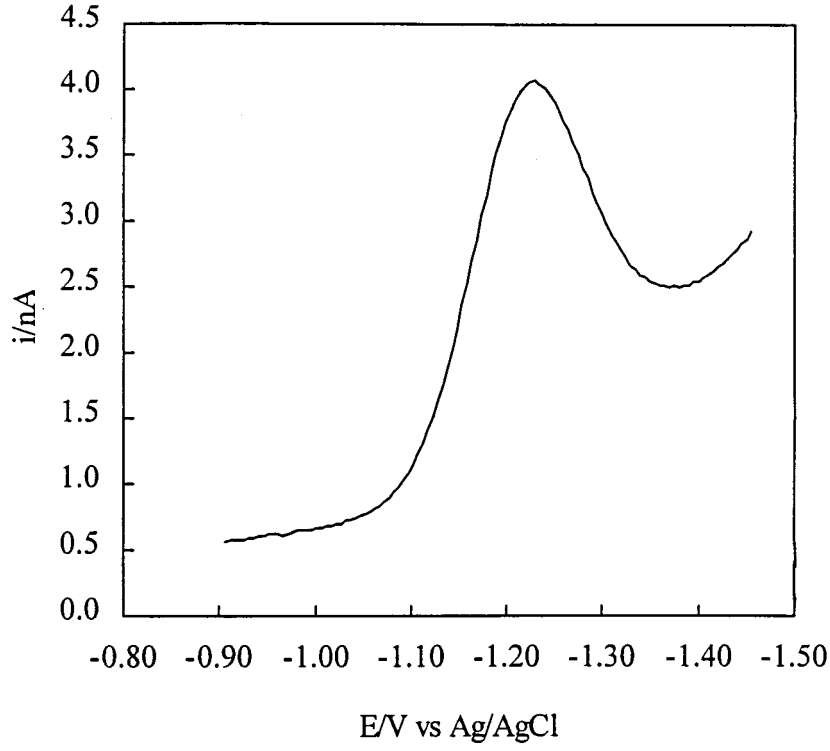

Figure 3.1. Typical voltammogram of chromium obtained in the digested mice samples using a MFM by square wave voltammetry. Operating conditions: deposition time 20 s; step 5 mV; amplitude 20 mV; frequency 100 Hz.

The influence of the peak current with pH was examined between pH 5 and 7 (Figure 3.2) in a digested liver sample solution containing 9.76×10^{-8} mol/L of chromium. Experimental observations indicates a peak increase until pH 6 which starts to level off at pH 6.5. At pH near 6 it is achieved the stability region of the Cr^{3+}-DTPA complex.

DTPA dependence with peak height was studied between 5.0×10^{-3} and 3.0×10^{-2} mol/L. Maximum peak height is attained at 2.0×10^{-2} mol/L (Figure 3.3). For

higher concentrations, the peak height starts to decrease maybe due to the formation of higher order complexes with chromium [26].

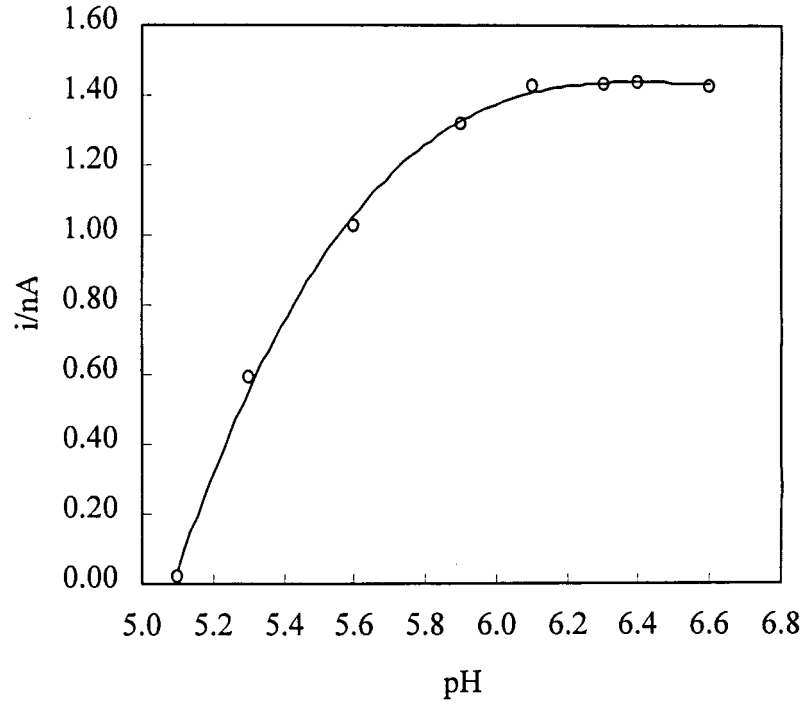

Figure 3.2. Dependence of the peak current as a function of the pH. Operating conditions: deposition time 20 s; step 5 mV; amplitude 20 mV; frequency 100 Hz.

The influence of nitrate concentration was investigated within the range of $5.0x10^{-2}$ to 0.60 mol/L. It was observed that the peak height increases linearly until 0.20 mol/L whereas for higher concentrations a slight increase occurs (Figure 3.4). This linear relationship between the peak height and nitrate concentration was expected since the reduction current is a function of the diffusion rate of nitrate

species to the electrode surface during the scan. To minimise the chromium concentration in the blank, the nitrate concentration chosen was 0.40 mol/L.

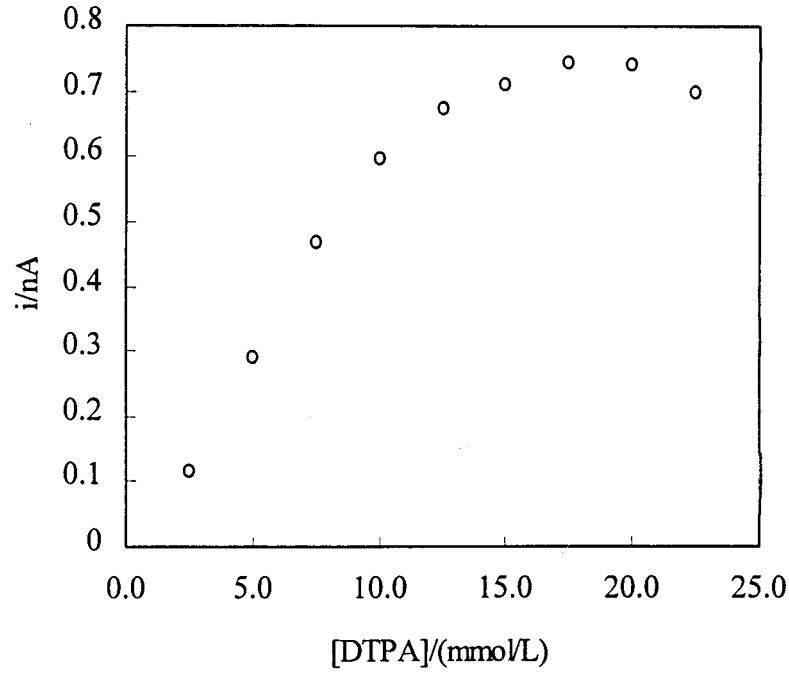

Figure 3.3. Effect of the DTPA concentration on the chromium peak current. Operating conditions: deposition time 20 s; step 5 mV; amplitude 20 mV; frequency 100 Hz.

The CH_3COONa concentration also has a considerable effect on the peak current. Increasing the concentration, the peak current increased almost linearly in the range $1.0x10^{-2}$ mol/L to $5.0x10^{-2}$ mol/L. For higher values of CH_3COONa, the peaks still increased but become broaden. As a result, the concentration chosen was $4.0x10^{-2}$ mol/L.

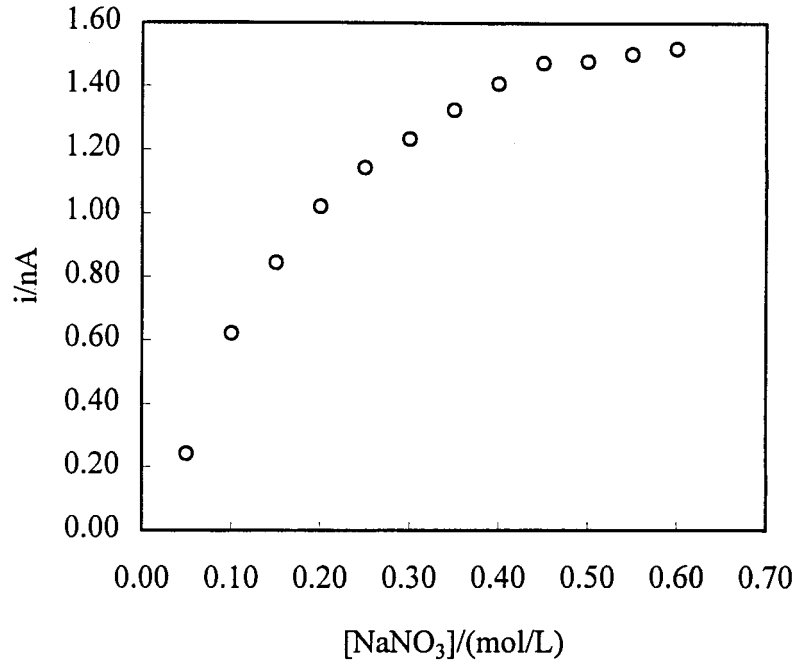

Figure 3.4. Effect of the nitrate concentration on the chromium peak current. Operating conditions: deposition time 20 s; step 5 mV; amplitude 20 mV; frequency 100 Hz.

The influence of the square wave parameters were studied. The peak rises almost linearly with the increase of frequency between 10 and 110 Hz (Figure 3.5). For higher values of frequency the background current provoked by the capacitive current increases more rapidly than the faradaic current due probably to poor electrochemical reversibility of the reduction step [26,36] and the peak current gradually starts to diminish. For a relative short experimental time without loss of the sensitivity and good definition of the peak, a frequency of 100 Hz and a step of 2.5 mV (scan rate of 250 mV) were chosen with an amplitude of 20 mV.

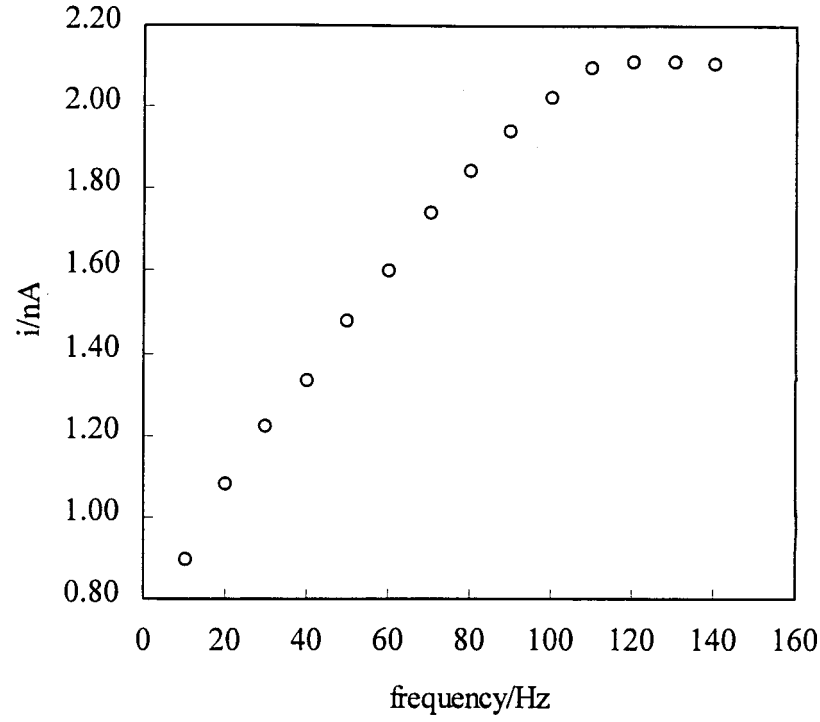

Figure 3.5. Effect of the frequency on the chromium peak current in a digested kidney sample with a concentration of 1.13×10^{-7} mol/L. Operating conditions: deposition time 20 s; step 5 mV; amplitude 20 mV; frequency 100 Hz.

Figure 3.6 shows the effect of the deposition potential on the peak current evaluated over the range between -0.50 and -1.30 V. Maximum response was attained following a deposition potential of -1.10 V. Nevertheless the best stability and reproducibility of the peak was achieved at -1.15 V. The adsorption of Cr^{3+}-DTPA complex is favoured at potentials more negative than the potential of zero charge for the mercury electrode (about -0.50 V) suggesting that the adsorbing complex has a positive charge. At potentials more negatives than -0.80 V the strong increase in peak current may be

explained by the chemical oxidation of Cr^{2+}-DTPA complex in the presence of nitrate ions. At potentials more negatives than -1.0 V the peak current starts to decrease perhaps because the catalytic reduction of Cr^{3+}-DTPA complex which is followed by desorption of the Cr^{2+}-DTPA complex from the electrode surface [25].

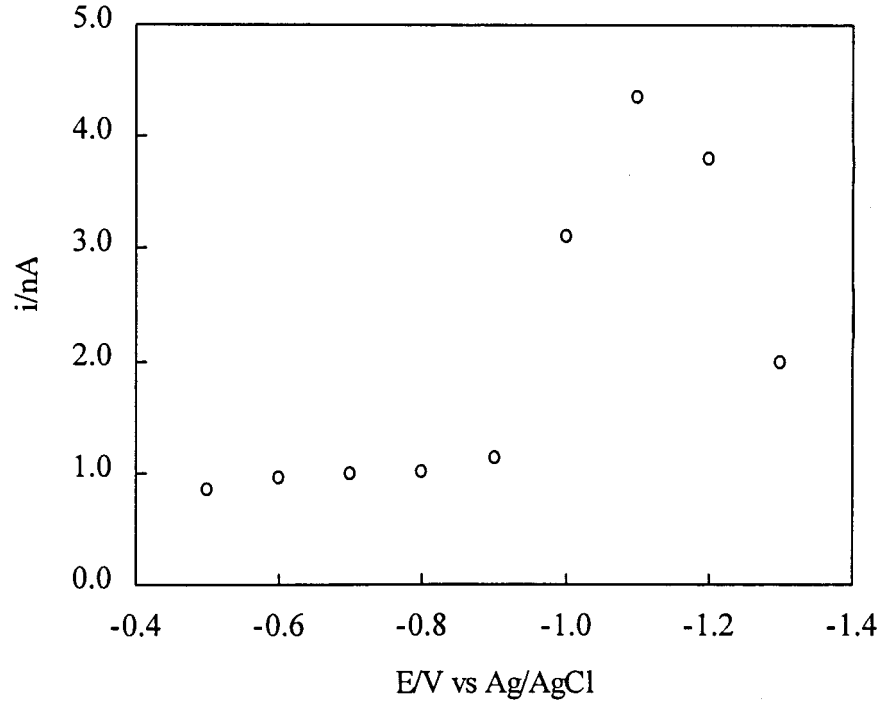

Figure 3.6. Effect of the deposition potential on the Cr-DTPA complex response in a treated mice liver sample at day 7 which has a chromium concentration of $2.00x10^{-7}$ mol/L. Operating conditions: deposition time 20 s; step 5 mV; amplitude 20 mV; frequency 100 Hz.

To avoid memory effects on the MFM a potential of -1.30 V was applied after each scan to remove any residual chromium complexes that may remain onto the mercury surface.

The linear range was established by successive additions of chromium until nonlinearity was observed due to saturation of the MFM surface for a deposition time of 20 and 40 s. It was found that for a deposition time of 20 s the peak height increased linearly until 1.25×10^{-6} mol/L (r=0.9991) whereas for longer deposition times, 40 s, the linear range was diminished to 7.69×10^{-7} mol/L (Figure 3.7).

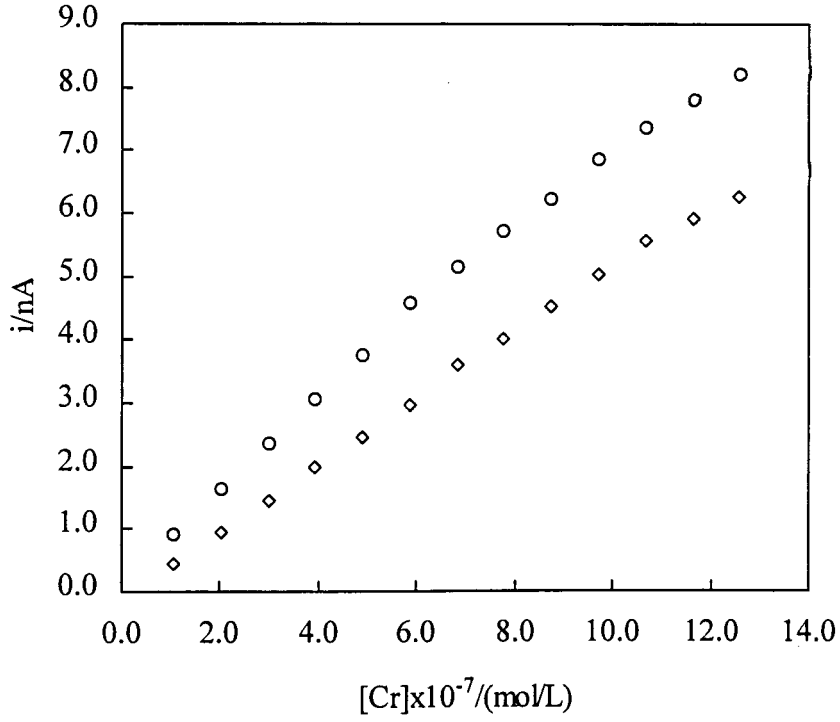

Figure 3.7. Resulting plots illustrating the dependence of peak current as a function of the chromium concentration following a deposition of a) 20 s; b) 40 s. Operating conditions: deposition potential -1.15 V; step 2.5 mV; amplitude 20 mV; frequency 100 Hz.

The reproducibility of the method was estimated during a long run of fifteen successive measurements of a digested mice kidney at day 7 sample containing $(1.87\pm0.01)x10^{-7}$ mol/L of chromium. The peak and the baseline practically remained unchanged during the scans. The relative standard deviation was found to be 2.17 %.

The detection limit of this electrochemical method was limited by the chromium content in the blank solution and was found to be $1.54x10^{-8}$ mol/L, calculated from 3 times the standard deviation of the blank [37]. The detection limit calculated by AAS was $3.30x10^{-9}$ mol/L.

After digestion, the main inorganic elements in these organs are potassium, sodium, magnesium, calcium and iron which are present in quite high concentrations. However, concentrations of iron in the order of $9.0x10^{-5}$ mol/L did not suppress the chromium peak and for calcium concentrations near to $5.0x10^{-5}$ mol/L a peak decrease of 10 % was observed. This may be justified by the formation of complexes with calcium which can be adsorbed onto the electrode interfering with the adsorption of the chromium complex [26]. In the experiments carried out in this study, this problem was eliminated due to the fact that in order to work in the linear range established by the method, the samples have to be very diluted. After dilution, the chromium content in samples ranged from $5.70x10^{-8}$ to $31.2x10^{-8}$ mol/L.

To observe if this type of matrix suppresses the chromium signal, some samples were spiked with $9.62x10^{-8}$ mol/L of this metal. The recovery was nearly 100% (Table 3.1) indicating that the matrix constituents do not interfere with chromium

determinations, including calcium and iron at concentrations below $5.0x10^{-5}$ and $9.0x10^{-5}$ mol/L, respectively.

Table 3.1. Recovery of $9.62x10^{-8}$ mol/L of chromium added as a standard solution to the mice organ samples.

	Cr present in sample (10^{-7} mol/L)	*Cr found after spike (10^{-7} mol/L)*	*Recovery (%)*
Liver	1.95±0.05	2.89±0.02	97.6±0.4
Kidney	3.13±0.08	4.08±0.02	98.8±0.4
Spleen	1.59±0.03	2.55±0.02	99.6±0.5

Figure 3.8 shows several voltammograms obtained for a treated mice liver sample at day 7 by the standard addition method. The deposition time was 20 s and a chromium concentration of $(2.00\pm0.09)x10^{-7}$ mol/L was found corresponding to 2.78 μg/g per dry weight. The slope of the baseline is enhanced due to the reduction of hydrogen ions and changes the peak shape of chromium as it is located at the bottom of the hydrogen wave. After several measurements, the slope of the baseline augment so much that the peaks are distorted and the standard additions of chromium shift from linearity. Consequently, the stability of the mercury film is affected and the durability of the mercury is limited to more or less fifty scans.

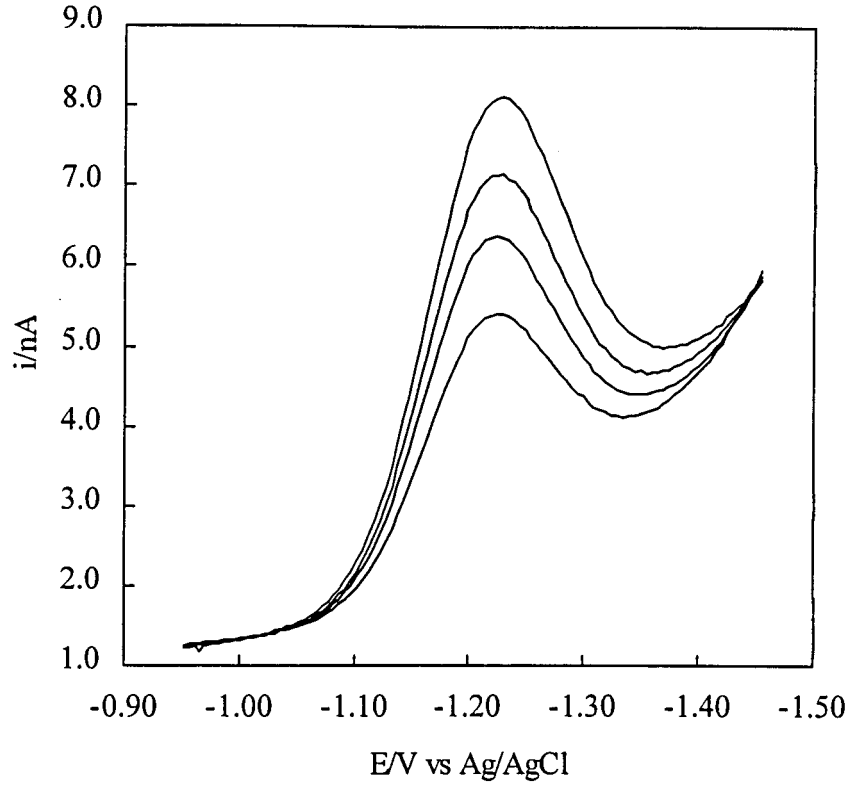

Figure 3.8. Standard additions for a treated mice liver at day 7. Voltammogram a, sample containing 10.4 μg/L of chromium, b, c, d, standard additions of 5.0 μg/L each one. Operating conditions: deposition potential -1.15 V; deposition time 20 s; step 2.5 mV; amplitude 20 mV; frequency 100 Hz.

The control organs were analysed by AAS after the digestion process and were stored during four months in PTFE bottles at -20 °C. When the solutions were again analysed by AdSV and AAS the concentration of chromium decreased considerably in almost all the samples. This is why the values of the control organs are not determined by AdSV.

The results of the chromium concentrations in treated mice organs at the days of sacrifice, obtained by AdSV and AAS are present in Table 3.2. Data acquired by both methods were compared, using the Student's *t*-test analysis, and the differences encountered were not statistically significant ($P>0.01$), the values differed only by 1.2-6.1% indicating a good accuracy of the proposed method.

From the analysis of the values presented in the Table 3.2 comparing the means of the levels in the control organs versus the treated animals, there is a significant elevation ($P<0.01$) of chromium concentration in the three organs studied during the experimental assay. The levels of chromium in the control mice organs remained essentially unchanged.

Morphological observations

The mean values of body weight for each group expressed in grams plus the standard deviation were respectively: Group I- 23.99±3.6 and 24.94±3.72; Group II- 30.98±2.96 and 33.11±2.57; Group III- 33.03±2.6 and 30.90±1.73; Group IV- 33.86±4.22 and 33.45±0.37. The differences between the body weights at the day of sacrifice and the initial weight were not statistically significant ($P>0.01$) and they are very similar with the control animals.

Table 3.2. Results obtained by AdSV and AAS analysis in treated mice organ samples after injections of HBSS containing $2.70x10^{-3}$ mol/L of chromium. The values are expressed in μg/g of dry weight.

	Liver		*Kidney*		*Spleen*	
	AdSV	*AAS*	*AdSV*	*AAS*	*AdSV*	*AAS*
7 days						
Control	-	0.119±0.003	-	0.127±0.004	-	0.357±0.007
Injection	2.78±0.12	2.67±0.10	1.83±0.06	1.95±0.08	4.89±0.13	5.07±0.15
14 days						
Control	-	0.106±0.003	-	0.153±0.006	-	0.444±0.009
Injection	3.18±0.08	3.33±0.10	1.64±0.08	1.52±0.05	6.01±0.12	5.94±0.12
21days						
Control	-	0.159±0.005	-	0.107±0.004	-	0.423±0.006
Injection	4.12±0.12	4.20±0.08	1.96±0.05	2.05±0.04	6.74±0.23	6.70±0.19
28 days						
Control	-	0.125±0.004	-	0.124±0.003	-	0.401±0.005
Injection	5.46±0.16	5.37±0.13	2.15±0.05	2.08±0.04	8.62±0.22	8.75±0.25

[a]Mean for at least three separate determinations and their standard deviation.
Each control and injected group was composed of 8 animals.
The differences in results with both methods are not significant at $P>0.01$.

During the animal treatment no mortality was observed neither signs of toxicity associated with chromium administration. The macroscopic appearance of the removed organs in all groups seems to be apparently similar to the control ones.

The histological sections of liver, spleen and kidney from all groups that were injected with chromium were similar to the control groups (see figures 14a, 15a and 16a with normal morphology for liver, spleen and kidney from the chapter 2 and figures 8a, 9a and 10a from the chapter 4). In all tissues analysed the morphological aspects do not present degenerative features.

Chromium accumulation in the liver, kidney and spleen

In Figure 3.9a is shown a progressive and significant increase ($P<0.01$) of chromium concentration with time when compared to the normal values found in control animals. At day 7 the chromium level was already approximately twenty times more elevated than the control group. At day 28 the chromium accumulation was approximately forty times compared to the control group, *i.e.* twofold compared with day 7.

It is possible to see a significant increase ($P<0.01$) of chromium concentration in kidney of animals injected with chromium and the control ones with time (Figure

3.9b). The rise is about fifteen times the normal values found in this organ, but it seems that accumulation is independent of time.

Figure 3.9c shows a progressive augment in spleen chromium concentration from the control animals, demonstrating a significant accumulation in this organ ($P<0.01$). At day 7 the chromium concentration is fourteen times more elevated than the control organs. At day 28 the accumulation rises for approximately twenty times from the control organs.

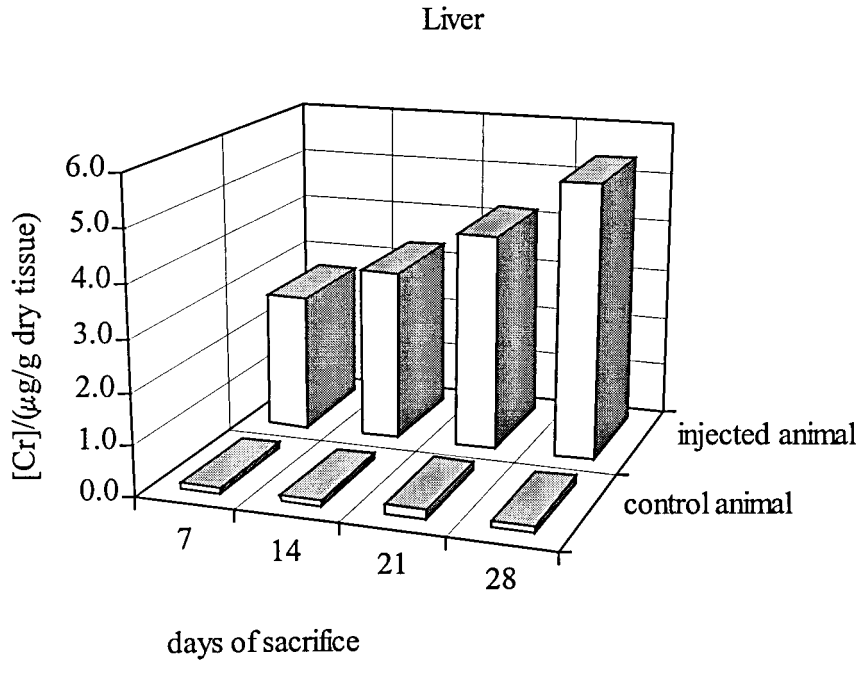

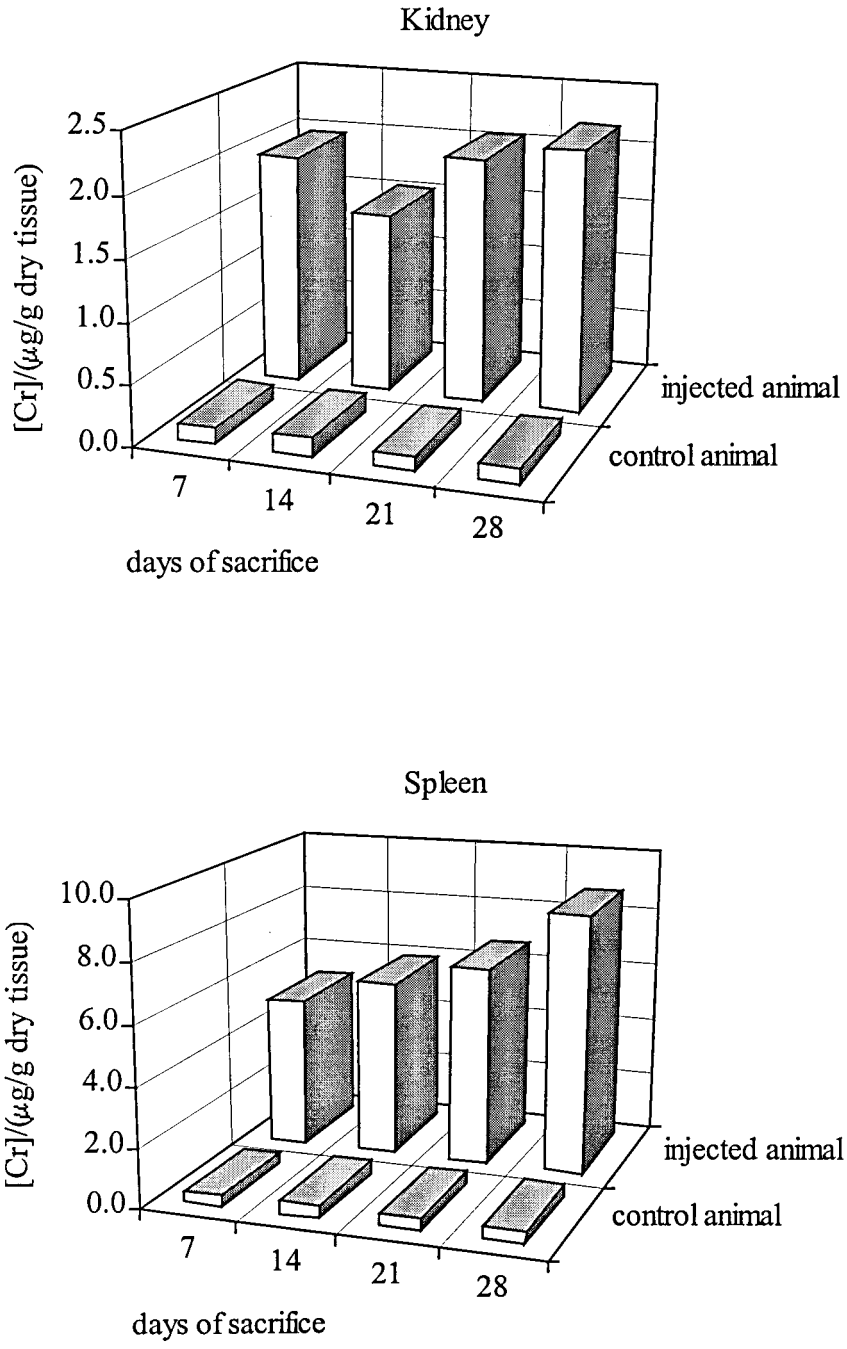

Figure 3.9. Concentration of chromium found in mice at the days of sacrifice after injection of a chromium solution: a) liver; b) kidney; c) spleen. The animals were sacrificed at days 7, 14, 21 and 28. Values attained by AAS.

DISCUSSION

The ligand DTPA shows to be suitable to determine the total concentration of chromium by AdSV. The analysis time with mercury film microelectrodes is much lower compared with conventional mercury electrodes making this technique very attractive since it has an excellent reproducibility and sensitivity.

The quantity of chromium initially administered to the mice was based in previous published results of analyses of human tissues adjacent to stainless steel implants [1,38]. From these studies, in a tissue close to the alloy with a medium discoloration the chromium concentration may ranges between 1100 to 2700 mg/L. In this study the corrosion rate simulated was 330 μg/kg/day.

The normal values found for chromium concentration in the investigated mice organs were comparable in magnitude to previous values reported by Merritt *et al.* [39] in hamsters.

It is evident from this study that chromium appears in the tissues far from the place of the injection indicating a distribution of this element in the body system. Consequently, chromium partially accumulates to a greater extent in the studied organs during the treatment time. These results are in agreement with an identical study in Syrian hamsters [39] who received four doses of 117 μg of Cr, 90 μg Ni and 94 μg Co at monthly intervals. The final conclusions were that the chromium levels were elevated in all the organs (liver, lung, spleen, kidney) compared to control, it was

found associated to the red blood cells and was eliminated in the urine very slowly [40].

After one week from the first injection, the quantity of chromium accumulated in the liver, spleen and kidney organs was approximately 1.4 μg per animal and the quantity initially injected was 70 μg. The Group IV was submitted to four injections corresponding to 280 μg of chromium and retained approximately 2.5 μg. Only nearly 1% of the total injected chromium was accumulated in these organs. From the literature, it seems that one part of this metal tends to remain at the impregnation site once chromium is cell binding [41]. However, the major part of the injected chromium appears to be excreted mainly by the kidneys: approximately 80% of an injected dose has been recovered in urine [42]. Brown *et al.* [43] have reported in a previous study that 67.3% of the injected chromium was recovered in urine and 8.7% in organs.

The chromium quantity accumulated by the kidneys during the first week, practically remained unchanged during the posterior treatment time. This suggests an impregnation of the kidney cells with chromium producing a slow, long term release and that this organ was incapable to a rapid elimination by urine. From a study of Bartolozzi *et al.* [16] in patients who received conventional polymethilmethacrylate cement cobalt-chromium alloy, a post-operative increase excretion of chromium by urine was observed in conjunction with a serum rise suggesting that there is a saturation of the urinary excretory pathway.

A progressive accumulation of this metal was observed in the spleen and the liver indicating the storage capacity of these organs and this ability is confirmed by the inexistence of histological alterations in these organs. Smith and Black [44] implanted 316L stainless steel in male New Zealand white rabbits and found that at the end of the seven months of implantation the chromium concentration in liver was 85% more elevated compared to the control animals.

The higher accumulation of chromium observed in this study may be associated with a greater binding of chromium by the blood cells as confirmed by several studies [41,46].

It is accepted that the corrosion implants lead to release of biologically active hexavalent chromium [45,46] and this work suggests that the chromium administered in mice was rapidly reduced to the trivalent form in cells once the higher accumulation of chromium observed in this study apparently did not induce morphological alterations in the cells of the liver, kidney and spleen.

Apparently, it is possible to deduce that chromium is not the metal of concern for short term stainless steel implants once did not induced morphological alterations in the mice organs mentioned. However, further studies must be carried out for longer periods of treatment, to observe whether or not it causes histological alterations.

CONCLUSIONS

The electrochemical stripping procedure to quantify chromium in biological solutions using MFM was successfully demonstrated as an alternative and reliable method to AAS.

There are two main advantages to use AdSV instead of AAS, firstly, the analysis time by AdSV with MFM is faster than with the AAS technique because in this type of matrix it is necessary to resort the standard additions method and by AAS is a extremely slow procedure, and secondly it is cheaper to use this electrochemical method than AAS once the matrix effects rapidly decrease the lifetime of the graphite tube.

For the different periods of the treatment time the total amount of chromium accumulated in the liver, kidney and spleen was only approximately 1% compared with the quantity of chromium initially injected. However, this remained quantity provoked a significant rise in the chromium levels compared to the control animals in the mentioned organs.

An intense and progressive accumulation of chromium was detected in the liver and the spleen with time compared with the values found in these organs in the control animals. In kidney it is possible to see a significant increase in the chromium

concentration (fifteen times more elevated than the normal values found in this organ) but it seems that accumulation in independent of time.

The histological analysis of these organs did not evidence any relevant morphological alterations induced by the chromium accumulations during the time of treatment considered.

REFERENCES

[1] S. A. Katz and H. Salem (eds), "*The Biological and Environmental Chemistry of Chromium*", VCH Publishers, Inc., 1994.

[2] E. Young and R. H. Houwing, *Contact Dermatitis*, **17** (1987) 104.

[3] S. A. Katz and H. Salem, *J. Appl. Toxicol.*, **13** (1993) 217.

[4] A. Martin, T. W. Bauer, M. T. Manley and K. E. Marks, *J. Bone Joint Surg.*, **70-A** (1988) 1561.

[5] W. W. Brien, E. A. Salvati, J. H. Healey, M. Bansal, B. Ghelman and F. Betts, *J. Bone Joint Surg.*, **72-A** (1990) 1097.

[6] R. A. Anderson, *Sci. Total Environ.*, 86 (1989) 75.

[7] S. Langard and A. Hensten-pettersen, "*Systemic Aspects of Biocompatibility*", D. F. Williams (ed.), CRC Press, Boca Raton, Florida, (1981) 143.

[8] J. Black, *J. Bone Joint Surg.*, **70-B** (1988) 517.

[9] M. J. Minski, H. S. Dobbs, "*Trace Element Analytical Chemistry in Medicine and Biology*", P. Bratter and P. Schramel (eds.), Walter de Gruyter, Berlim, (1980) 339.

[10] K. Merritt, S. A. Brown and N. A. Sharkey, *J. Biomed. Mater. Res.*, **18** (1984) 991.

[11] K. Merritt, C. D. Fedele and S. A. Brown, "*Biomaterial- Tissue Interfaces*", P. J. Doherty et al. (eds.), Advances in Biomaterials, **10** (1992) 49.

[12] K. Merritt and S. A. Brown, *J. Biomed. Mater. Res.*, **29** (1995) 627.

[13] M. L. Pereira, A. M. Abreu, J. P. Sousa and G. S. Carvalho, *J. Mater. Sci: Mater. Med.*, **6** (1995) 523.

[14] H. S. Dobbs and M. J. Minski, *Biomaterials*, **1** (1980) 193.

[15] J. Black, E. C. Maitin, H. Gelman and D. M. Morris, *Biomaterials*, **4** (1983) 160.

[16] A. Bartolozzi and J. Black, *Biomaterias*, **6** (1985) 2.

[17] F. W. Sunderman Jr, S. M. Hopfer and T. Swift, *J. Orthop. Res.*, **7** (1989) 307.

[18] K. Merritt, S. A. Brown and N. A. Sharkey, *J. Biomed. Mater. Res.*, **18** (1984) 1005.

[19] K. Merritt and S. A. Brown, "*Corrosion and Degradation of Implant Materials: Second Symposium*", A. C. Fraker and C. D. Griffin (eds)., American Society for Testing and Materials, Philadelphia, (1985) 195.

[20] M. L. Pereira, F. C. Correia, T. M. Santos and J. Pedrosa de Jesus, "*Proceedings Book of The Congress of The Institute of Biomedical Science*", Birmingham, (1995).

[21] C. Veillon, K. Y. Patterson and N. A. Bryden, *Clin. Chem.*, **28** (1982) 2309.

[22] S. Lugowski, D. C. Smith and J. C. van Loon, *J. Biomed. Mater. Res.*, **21** (1987) 657.

[23] K. S. Subramanian, "*Metabolism of Minerals and Trace Elements in Human Disease*", M. Abdulla *et al.* (eds.), Smith-Gordon Ltd., (1989).

[24] H. Minami, Q. Zhang, H. Itoh and I. Atsuya, *Microchem. J.*, **49** (1994) 126.

[25] J. Golimowski, P. Valenta and H. W. Nurnberg, *Fresenius Z. Anal. Chem.*, **322** (1985) 315.

[26] M. Boussemart, C. M. G. van den Berg, M. Ghaddaf, *Anal. Chim. Acta.*, **262** (1992) 103.

[27] J. Wang, J. Lu and K. Olsen, *Analyst*, 117 (1992) 1913.

[28] K. B. Olsen, J. Wang, R. Setiadji and J. Lu, *Environ. Sci. Technol.*, **28** (1994) 2074.

[29] M. C. Pereira and J. P. Sousa, *Portugaliae Electrochemica Acta*, **13** (1995) 477.

[30] M. C. Pereira and J. P. Sousa, *Portugaliae Electrochemica Acta,* **14** (1996) 273.

[31] M. C. Pereira, J. L. Faria, M. L. Reis and J. P. Sousa, *Electroanalysis*, **9** (1997) 150.

[32] M. H. Ross and L. J. Rowrell, (eds.), "*Histology a Text and Atlas*", Williams & Wilkins, (1985).

[33] M. C. Pereira, M. L. Pereira and J. P. Sousa, in press *J. Biomed. Mater. Res.*, (1997).

[34] M. C. Pereira, M. L. Pereira and J. P. Sousa, , submitted to *J. Biomed. Mater. Res.*, (1997).

[35] M. Paneli, A. V. Voulgaropoulos and K. Kalcher, *Mikrochim. Acta*, **110** (1993) 205.

[36] C. M. G. van den Berg, *Anal. Chim. Acta*, **250** (1991) 265.

[37] J. N. Miller, *Analyst*, 117 (1992) 1913.

[38] O. E. M. Pohler, "*Biomaterials in Reconstructive Surgery*", L. R. Rubin (ed.), The C. V. Mosby Company, chap.15, (1983) 158.

[39] Merritt, T. D. Crowe and S. A. Brown, *J. Biomed. Mater. Res.*, **23** (1989) 845.

[40] S. A. Brown, L. J. Farnsworth, K. Merritt and T. D. Crowe, *J. Biomed. Mater. Res.*, **22** (1988) 321.

[41] Brown, K. Zhang, K. Merritt and J. H. Payer, *J. Biomed. Mater. Res.*, **27** (1993) 1007.

[42] D. Burrows (ed.), "*Chromium: Metabolism and Toxicity*", CRC Press, Inc., Boca Raton, Florida, (1983).

[43] S. A. Brown, K. Zhang, K. Merritt and J. H. Payer, "*Biomaterial- Tissue Interfaces*", P. J. Doherty et al. (eds.), Advances in Biomaterials, **10** (1992) 13.

[44] G. K. Smith and J. Black, "*Corrosion and Degradation of Implant Materials: Second Symposium*", A. C. Fraker and C. D. Griffin, (eds)., American Society for Testing and Materials, Philadelphia, (1985) 223.

[45] J. Yang and J. Black, *Biomaterials*, **23** (1989) 845.

[46] B. Kargacin, K. S. Squibb, S. Cosentino, A. Zhitkovich and M. Costa, *Biol. Trace Element Res.*, **36** (1993) 307.

Chapter 4

EVALUATION OF IRON EFFECTS IN MICE ORGANS

4

INTRODUCTION

Iron is an essential metal to life [1] and is the most abundant heavy metal in tissues and body fluids. This metal is involved in many biological functions by varying the ligands to which it is coordinated and participates in a wide range of electron transfer reactions, namely in the transport of oxygen. The iron metabolism in humans is essentially conservative, absorbing iron from the dietary and excrete roughly the same amount under normal conditions. A small shortfall in iron absorption over excretion may result in iron deficiency while a small excedent in absorption over excretion can result in iron overload [2]. Metabolically active iron

is mostly contained in circulating haemoglobin and less than 1% is presented in enzymes or is attached to transferrin in transit throughout the plasma [3]. Iron in excess of metabolic needs is stored intracellularly as either ferritin which is found in greater quantities in the liver, spleen and bone or hemosiderin (intracellular granules) if larger accumulations of iron occur in various tissues of the body. However, the liver reticuloendothelial system and intestinal mucosa are the most significant metabolic storage sites [4,5].

Extra iron may enter the body tissues by the presence of metallic orthopaedic implants made of stainless steel AISI 316L. This alloy is the biomaterial most commonly used for implants and it is mainly composed by iron *c.a.* 67%. It was deduced from several studies [5,6,7,8,9,10,11] that the iron released by corrosion from this alloy is present in tissues near the implants in high concentrations and is locally processed by macrophages and a mixture of hydrated ferric oxides similar to hemosiderin is formed.

Several studies were performed to evaluate the effects of chromium and nickel in systemic organs [12,13,14,15,16] and they ignore the possibility that iron could be a risk factor for human disease if present in high concentrations [4,17]. This can be justified because during this century the developing picture of the importance of iron was associated with iron deficiency [18] which implemented only a positive image of this element.

From the biological and clinical point of view, knowledge about the magnitude of the debris release in the biological environment is necessary to evaluate tissue responses, followed by retention of the various elements or their compounds in the various human tissues. There is evidence that in some specimens the tissue tolerance for stored iron has been exceed locally with consequent pathological changes [4,6] and most of the iron excess is deposited in the reticuloendothelial system and in parenchymal cells. Only when there is a significant parenchymal cell involvement the organ damage may occur resulting in arthritis, liver disease, cardiac failure and diabetes [6,19].

Other consequences of the iron overload is the enhancement of infections at the site of the implant or in other parts of the body, once a high iron concentration is available for the bacteria metabolism [20].

The most recognised technique for quantification of metals in biological tissues and fluids is atomic absorption spectrometry (AAS) [21,22,23,24,25,26]. However, during the last years interest has been devoted to the development of electroanalytical methods to determine organic and metallic species in solution [27]. A variety of these electroanalytical methods including square wave voltammetry have been improved together with the optimisation of the instrumental devices and electrodes [28,29]. Taking advantages of the properties of microelectrodes [30,31] associated with these electroanalytical techniques in trace

analysis [32,33,34] being these procedures characterised by high sensitivity, good selectivity and improvements in detection limits.

Bearing this in mind, the aim of the present work is to investigate the histological features of organs that are directly related with the iron metabolism, namely liver, kidney and spleen, after several injections of a metallic iron solution in mice. For a better understanding of the histopathological alterations, the iron present in the organs was quantified by an electrochemical technique, adsorptive stripping voltammetry (AdSV), using mercury film microelectrodes (MFM). The accuracy of the new method proposed for these biological samples was confirmed by the atomic absorption spectrometry (AAS) which is normally accepted for routine analysis of biological samples.

MATERIALS AND METHODS

Iron dissolution

Metallic iron was anodically dissolved in Hank´s Balanced Salt Solution (HBSS) by imposition of a constant current. After dissolution, the iron content was determined by atomic absorption spectrometry (AAS) finding a value of 538 mg/L and the pH was adjusted to 7.4.

Animals and experimental design

Male Charles River mice, nearly two months old and weighing 25-35 g were supplied from "Instituto Gulbenkian de Ciências", Portugal. They were kept under standard laboratory lighting conditions, housed in groups of four per cage and food and water were given *ad libitum.*

In order to simulate the *in vivo* degradation process, a volume of 0.50 mL of the iron solution was subcutaneously injected in the back dorsal surface at days: 0- group I; 0, 7- group II; 0, 7, 14- group III and 0, 7, 14, 21- group IV. Each group was composed of four animals. Control animals were similarly injected with HBSS only.

After a week of the last injection, animals were sacrificed under ether anaesthesia. Small fragments of freshly removed organs (liver, kidney and spleen) were routinely processed for histological studies. The remaining tissues were frozen at -20 °C in PTFE bottles until appropriate use for chemical analysis.

During the dissection and in posterior treatment, no metallic instruments were used in order to avoid iron contamination.

Samples Preparation

The removed organs were placed in appropriate vessels previously weighed and then dried in a microwave oven (CEM MDS 2000). The temperature was monitored until samples reached a constant weight to control the state of dryness of the samples. After this procedure, 1.50 mL of HNO_3 (Suprapur, Merck) was added per 100 mg of dry weight. After the microwave digestion, the resulting solutions were evaporated to dryness with the addition of 1.0 mL of $HClO_4$ (Merck) per 0.50 g dry mass. Finally, the resulting residues were diluted with ultra pure water to an appropriate volume. This digestion process was described with more detail elsewhere [35]. These digested solutions were directly used to quantify the iron levels by both AdSV and AAS techniques.

Iron quantitative analysis

The voltammograms were obtained using a potentiostat/galvanostat Model Autolab from ECO Chemie equipped with a module ECD specific for microelectrodes, which was connected to a PC Model 1120 SX, used in conjunction with an electrochemical microcell. Voltammetric measurements were performed using a three electrode configuration system; a mercury gold microelectrode of 25 μm diameter (purchased from Department of Chemistry,

University of Southampton) as the working electrode, a silver/silver chloride in 3.0 mol/L KCl as the reference electrode and a vitreous carbon auxiliary electrode.

Mercury gold microelectrodes were prepared by application of a constant potential of 0.0 V versus Ag/AgCl during 60 s, onto their surface from a deoxygenated mercury solution composed by 6.0 mmol/L of $HgCl_2$, 1.0 mol/L KNO_3 and 0.50% HNO_3. To clean the mercury microelectrode surface a potential of +1.0 V was applied. After several films it was found necessary to polish the microelectrode surface with a polishing cloth witch contains a suspension of highly pure aluminium oxide 0.015 μm (BDH reagents) for 5-10 minutes.

The digested samples were pipetted into the cell. The pH was adjusted to *c.a.* 7.2 by addition of PIPES buffer to a final concentration of $8.0x10^{-3}$ mol/L and the samples were purged with nitrogen during 12 minutes to remove oxygen. The complexing agent, catechol was added giving a final concentration of $3.0x10^{-4}$ mol/L. The catechol solution was prepared every day and oxygen was removed by purging with nitrogen during 12 minutes. The preconcentration step was carried out at -1.80 V during 25 s for the levels of iron presented in the samples. After this period the scans were performed from -0.15 V to -0.65 V (cathodic direction). AdSV was made in square wave mode and the parameters used were a frequency of 50 Hz, an amplitude of 20 mV and a step of 4 mV.

To remove the adsorbed iron complex from the mercury film a potential of -0.80 V was applied during 10 s.

The atomic absorption determinations were done using a spectrometer model GBC 904AA.

The quantification procedure used by both techniques was the standard addition method, since the main inorganic elements present in this biological solutions are sodium, potassium, calcium, magnesium and their concentration vary considerably depending of the organ and the amount of mass digested. All measurements for the same sample were repeated at least three times.

A 1000 mg/L of iron (III) nitrate stock standard solution from BDH reagents was used daily to prepare iron standard solutions.

Histological studies

Small fragments of each organ were fixed by immersion in Bouin's solution, dehydrated by successive passages in ethanol baths of crescent grade, embedded in paraffin and sections with approximately 3-5 μm were made in a microtome. After staining with Hematoxylin-eosin, sections were then routinely processed for

histological studies. Observations and photographs were made using a Nikon optical microscope.

Statistical analysis

Student´s *t*-test was applied to determine the statistical significance ($P<0.01$) of the differences observed between means of the two analytical methods and the iron values found for the four animal groups, including the control groups.

RESULTS

Iron analysis

The electrochemical process used, adsorptive stripping voltammetry (AdSV), for iron determinations in the digested organ samples involves the preliminary adsorptive concentration of the complex iron-catechol on the surface of a mercury film microelectrode (MFM) at a fixed potential, and subsequent measurement of the reduction peak current of the adsorbed complex during the cathodic scan. The peak current corresponding to this reduction appeared at -0.345 V. The amplitude of the reduction peak current is proportional to the concentration of iron in the sample. Some analytical applications of this method were described by van den Berg *et al.* [36] in sea water and by Morais *et al.* [37] who determined iron in digested osteoblast-like cell culture medium. Wang *et al.* [38] also proposed this complexing agent for the determination of the total iron content in wines and used Solochrome Violet Red to determine iron (III).

Figure 4.1 shows the effect of various operational parameters on the iron-catechol adsorptive stripping response in the digested organ samples. The solution analysed was a control liver sample at day 28 with a concentration in iron of 97.2±2.4 μg/L. The pH dependence of the peak was studied over the 6.0-7.4 pH range (Figure 4.1a). The peak gradually increases and the maximum peak height is

reached at pH 7.2, reflecting an increased stability of the iron-catechol complexes. A similar pH effect was observed by van den Berg *et al.* [36] in a HMDE. A negative shift in the peak potential, from -0.28 to -0.39 V was observed as the pH increases.

The pH solution was adjusted with PIPES buffer. Figure 4.1b shows the influence of PIPES concentration on the iron peak. The peak current increases linearly from $2.0x10^{-3}$ to $8.0x10^{-3}$ mol/L and decreases slightly for higher concentrations.

The catechol concentration also has a pronounced effect on the adsorptive response (Figure 4.1c). The peak current increases rapidly with the catechol concentration and the maximum value was attained at *c.a.* $3.0x10^{-4}$ mol/L. For higher concentrations the peak enlarges and the resolution decreases.

The effect of the preconcentration step on the peak current was evaluated over the -0.10 to -1.90 V range (Figure 4.1d). Maximum response is attained following a deposition potential of -1.80 V. This behaviour may be due to the fact that at this potential iron amalgamates with mercury and at the beginning of the stripping step where the potential is set to -0.15 V, the amalgamated iron becomes re-oxidised forming iron(III)-catechol complexes [39]. At this potential, it is possible sometimes to observe some adsorption of copper with catechol [40] once the adsorption of this competing metal is greater than iron. This peak is very small and

well separated from the iron peak (Figure 4.2). Copper concentration in these biological solutions is 100-300 times less than iron and for this concentration range, copper does not interfere in the iron determinations.

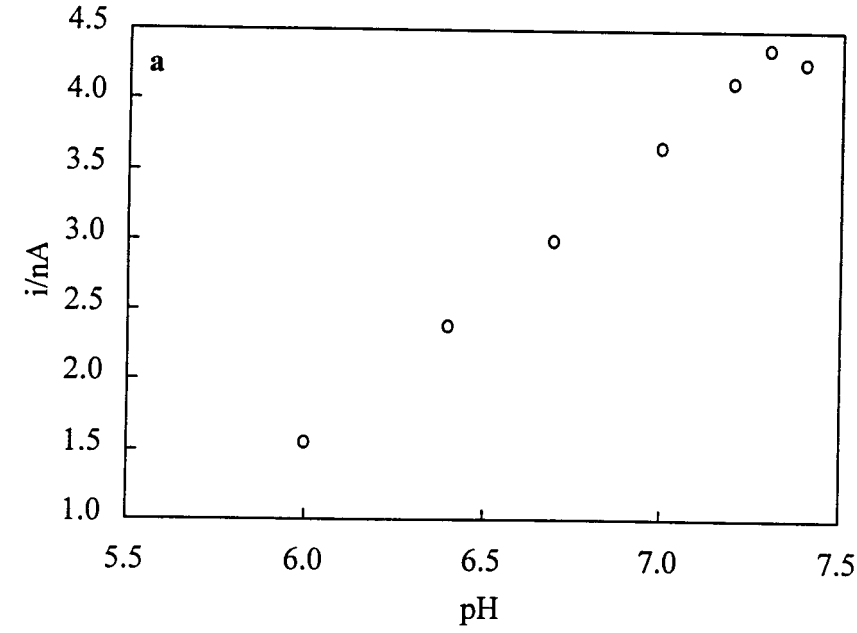

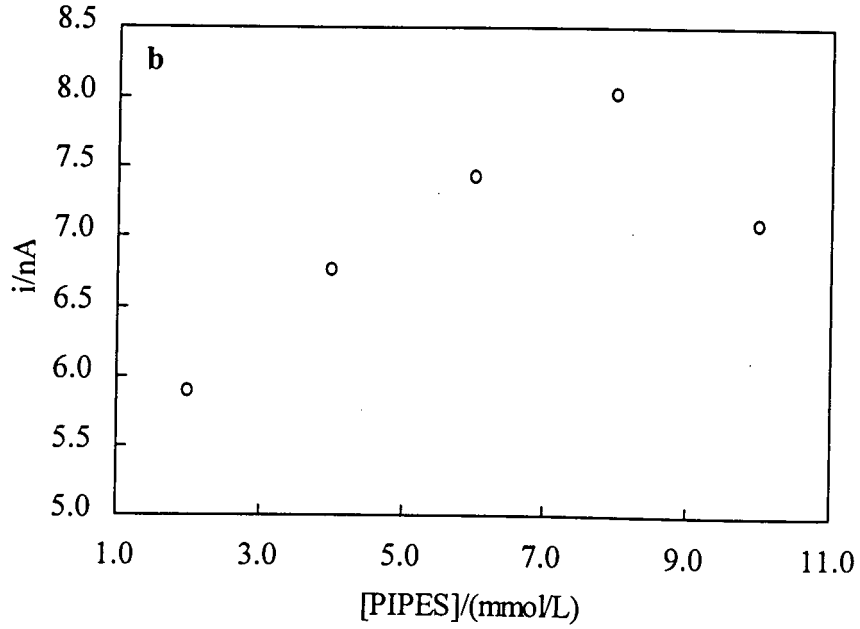

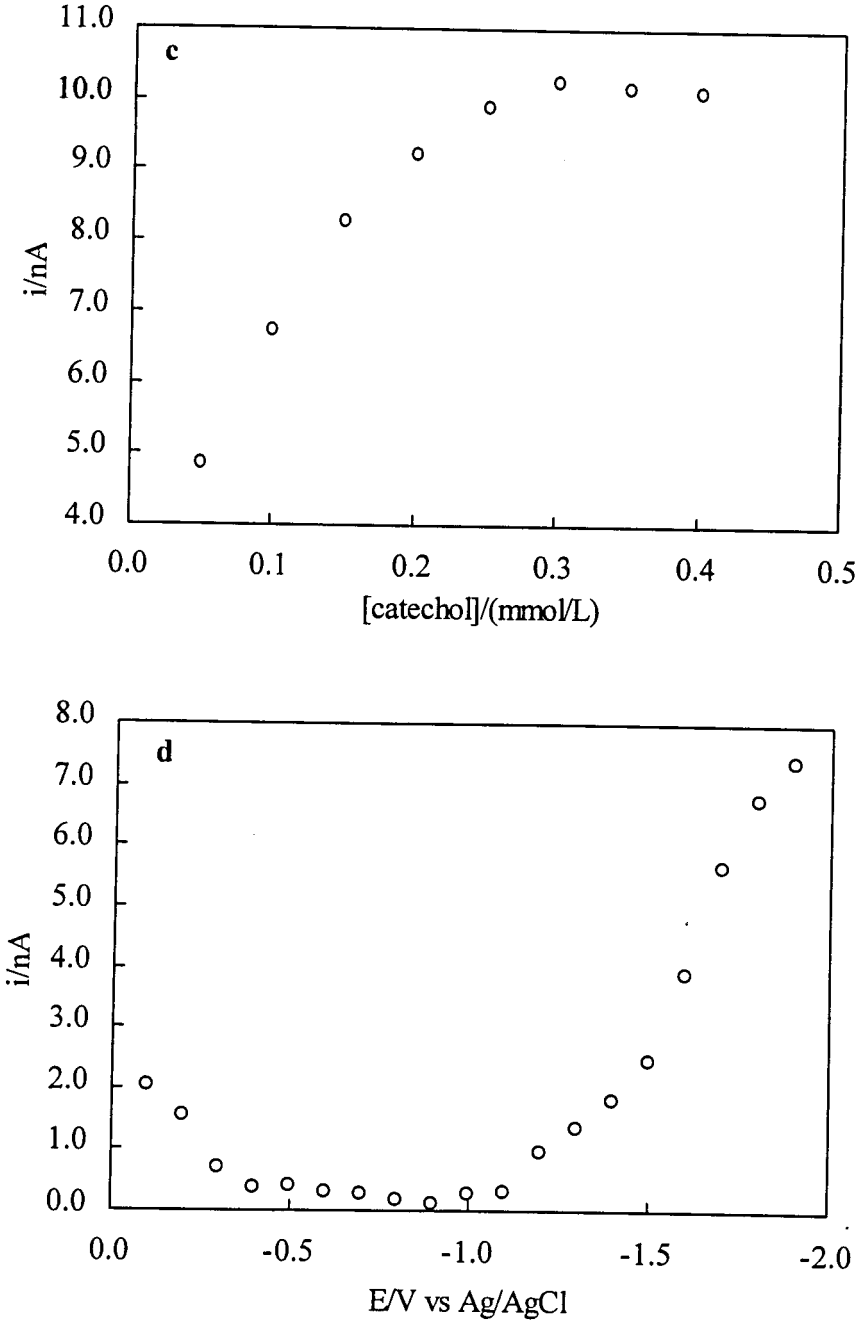

Figure 4.1. Optimisation of AdSV working parameters: a) effect of pH; b) PIPES concentration; c) catechol concentration and d) deposition potential on the complex iron-catechol AdSV response in a digested control liver sample at day 28 which has a iron concentration of 97.2±2.4 μg/L.

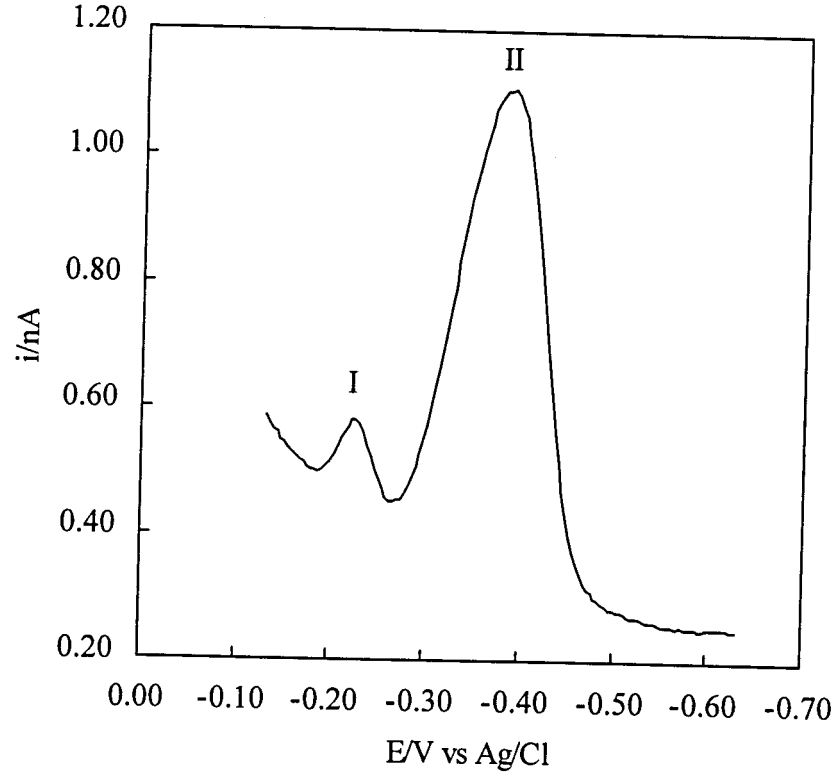

Figure 4.2. Square wave voltammogram of a spleen sample at day 21 containing 89.4 μg/L of iron and 0.56 μg/L of copper. I) copper peak; II) iron peak. Operating conditions: deposition potential -1.80 V; deposition time 25 s; step 4 mV; amplitude 20 mV; frequency 50 Hz.

The SWV parameters that gave the best compromise between resolution and sensitivity were achieved with a frequency of 50 Hz, an amplitude of 20 mV and a step of 4 mV.

The deposition time was changed between 5 and 70 s. The iron peak current increases linearly until 45 s (r=0.999). For deposition times higher than 60 s the MFM was saturated for a iron concentration of 93.6±2.5 μg/L in a control liver

mice at day 7. The small decrease in the iron peak after longer deposition times is probably caused by dissociation and desorption of the iron-catechol complexes.

The optimal working conditions for the digested mice organ samples were found to be pH 7.2 provided by 8.0×10^{-3} mol/L PIPES buffer, catechol concentration of 3.0×10^{-4} mol/L, deposition potential -1.80 V. This value of potential gives the maximum peak current enhancement with a very good balance between sensitivity and reproducibility.

The linear range was established by successive additions of iron to a control kidney sample at day 7 until nonlinearity was observed due to saturation of the MFM surface. It was found that for a deposition time of 40 s the peak height increased linearly until 200 μg/L (r=0.999) (Figure 4.3). For the levels of iron presented in the samples the linear range was extended by using shorter deposition times (20-30 s).

The reproducibility of AdSV measurements was assessed by carrying out fifteen successive voltammograms, for a kidney sample at day 28 containing 85.4±2.4 μg/L of iron after a stabilisation period of the peak (10-15 min) and the relative standard deviation was 1.25%.

The detection limit for iron by AdSV in kidney digested solutions was 13.7 nmol/L (calculated from 3 times the standard deviation of the blank [41]) for a

deposition time of 25 s. This result was attained with three determinations in a diluted control kidney sample at day 7.

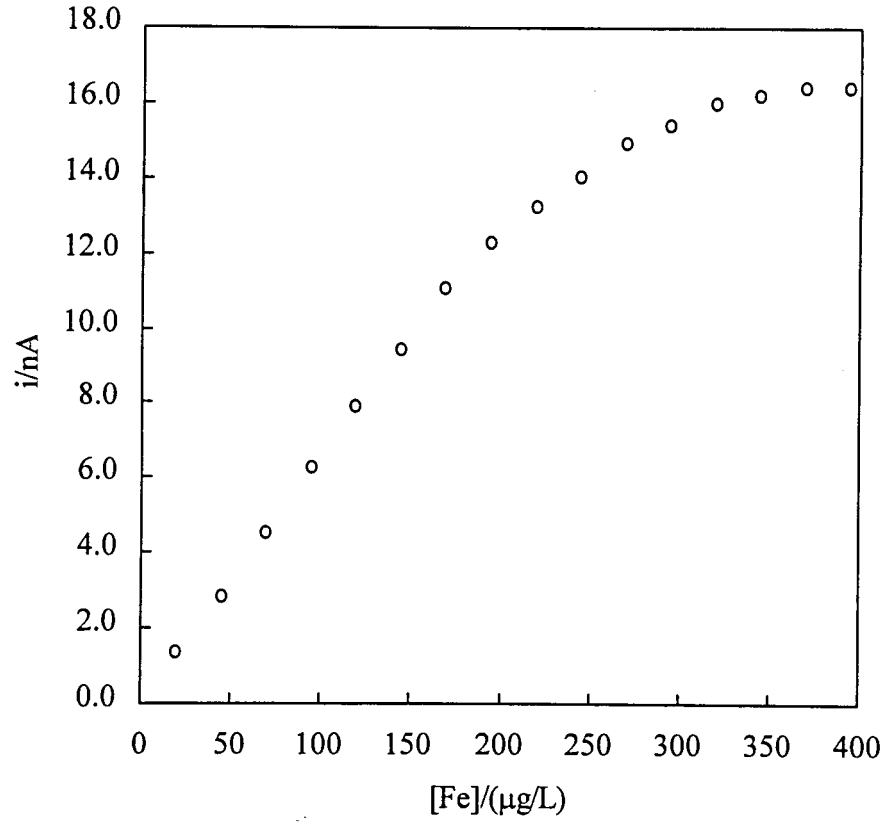

Figure 4.3. Dependence of peak current as a function of the iron concentration. Operating conditions: deposition potential -1.80 V; deposition time 40 s; step 4 mV; amplitude 20 mV; frequency 50 Hz.

To guarantee that the digestion process used was adequate and sufficient to eliminate all organic residues which might compete with catechol causing a suppression of the iron signal, spike experiments were performed to test the

recovery of the metal in biological samples. The recovery was calculated with a kidney sample at day 28 with a concentration of 85.4±2.4 μg/L and the value obtained was 99.4±0.7 %.

Figure 4.4a shows several voltammograms obtained by AdSV for a liver sample at day 21 by the standard addition method which indicates that the current amplitude is proportional to the concentration of iron in the mice organ samples (Figure 4.4b). The deposition time was 25 s and a concentration of 61.2±1.7 μg/L was found.

Iron concentrations in the liver, kidney and spleen obtained by AdSV using MFM and AAS are reported in Table 4.1 for the control and injected animals. The values are expressed in mg/g per dry tissue and corresponds to the arithmetical mean of at least three determinations for each group of animals. The obtained results are the iron levels for each group of animals at the day of sacrifice. By comparison of the results obtained by both techniques it was possible to confirm the high accuracy of the electrochemical method since the differences found comparing the values obtained by both methods are not statistically significant (P>0.01).

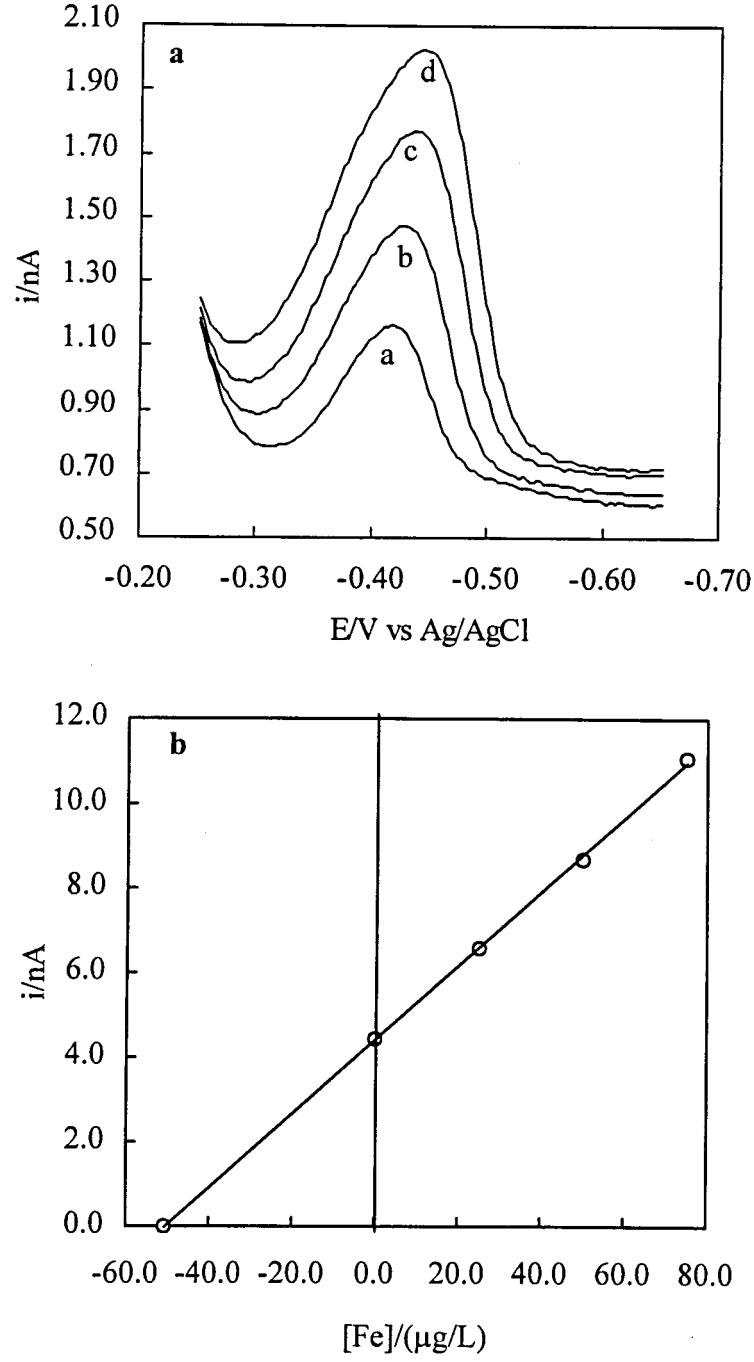

Figure 4.4. a) Standard additions for a mice liver at day 21. Sample containing 61.2±1.7 µg/L Fe. Voltammogram a, sample, b, c, d, standard additions of 20 µg/L each one. Deposition time 25 s. b) Plot of the resulting standard addition method.

Table 4.1. Results Obtained in Mice Organs by AdSV and AAS Following injections of metallic iron
The values are expressed in mg/g of dry weight

	Liver		*Kidney*		*Spleen*	
	AdSV	*AAS*	*AdSV*	*AAS*	*AdSV*	*AAS*
7 days						
Control	0.736±0.020	0.754±0.021	0.332±0.008	0.335±0.006	0.863±0.022	0.857±0.030
Injection	0.938±0.018	0.927±0.028	0.436±0.011	0.429±0.012	1.55±0.04	1.51±0.04
14 days						
Control	0.719±0.019	0.712±0.018	0.409±0.010	0.418±0.005	0.790±0.024	0.796±0.031
Injection	1.74±0.05	1.80±0.07	0.543±0.015	0.531±0.009	1.62±0.03	1.58±0.05
21days						
Control	0.858±0.023	0.886±0.023	0.347±0.007	0.362±0.010	0.896±0.025	0.905±0.040
Injection	1.67±0.06	1.63±0.06	0.667±0.018	0.661±0.015	1.20±0.03	1.24±0.03
28 days						
Control	0.826±0.020	0.835±0.030	0.432±0.009	0.437±0.008	0.801±0.019	0.823±0.028
Injection	1.29±0.03	1.24±0.05	0.528±0.012	0.539±0.015	1.68±0.05	1.74±0.05

[a]Mean for at least three separate determinations and their standard deviation.
Each control and injected group was composed of 4 animals.
The differences in results with both methods are not significant at $P>0.01$.

Iron accumulation

The normal concentration of iron in the liver and spleen is very similar and is two times higher than in kidney (Table 4.1). However, only a negligible difference was found in the iron concentrations of the control groups at the different days of sacrifice for the three organs.

Treated animals with the prepared solution, present an iron content in the liver, kidney and spleen significantly higher at all time intervals when compared with the control organs. Student's *t* test comparing the iron levels in the control and the injected animals was done within 99% confidence interval and the differences between the obtained values are no significant for both organs.

A progressive increase of iron concentration in the liver can be seen until day 14 (Figure 4.5). At that day this organ presents the major accumulation for this metal, twofold compared with the control group. At days 21 and 28 a decrease of the iron concentration was observed.

Figure 4.6 shows a pronounced accumulation of iron in the spleen, approximately twofold the values found in the control groups. At day 7 and 14 no significant changes ($P>0.01$) were seen.

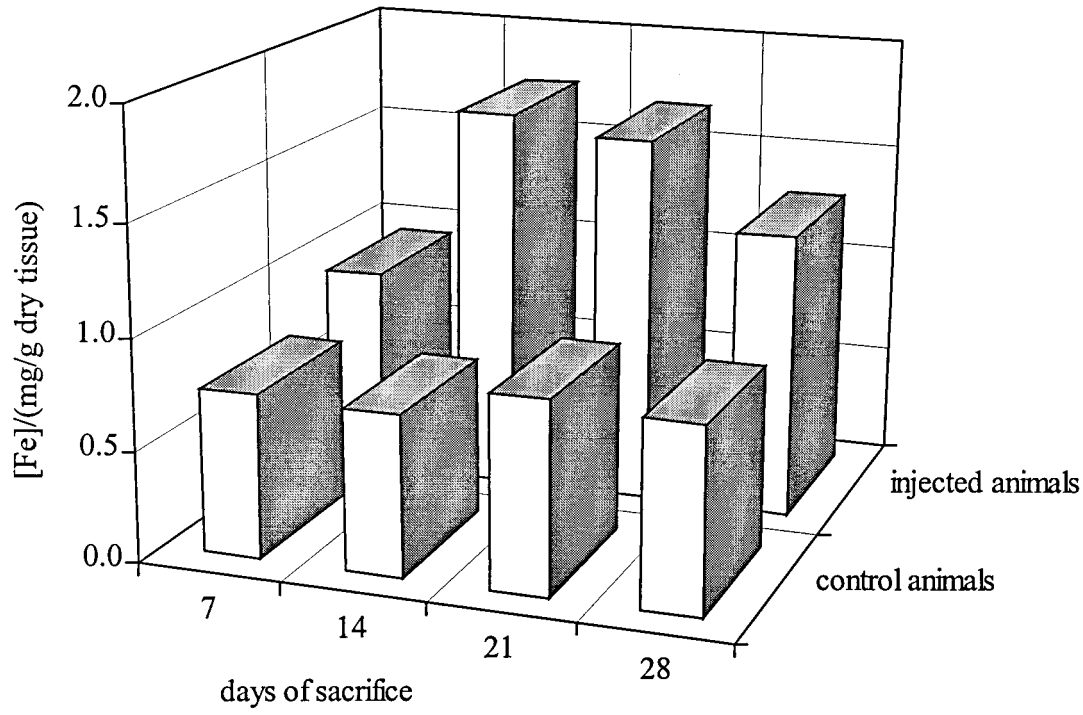

Figure 4.5. Comparison of iron concentration in mice liver groups after several injections with a solution of metallic iron and the respective control animals. The animals were sacrificed at days 7, 14, 21 and 28. Values attained by AdSV.

A small decrease in iron concentration was observed at day 21 and rose again at day 28. Once again, no significant changes (P>0.01) were seen in the accumulation values at day 14 and 28. The spleen had tendency to maintain and increase the iron concentration as the time went on.

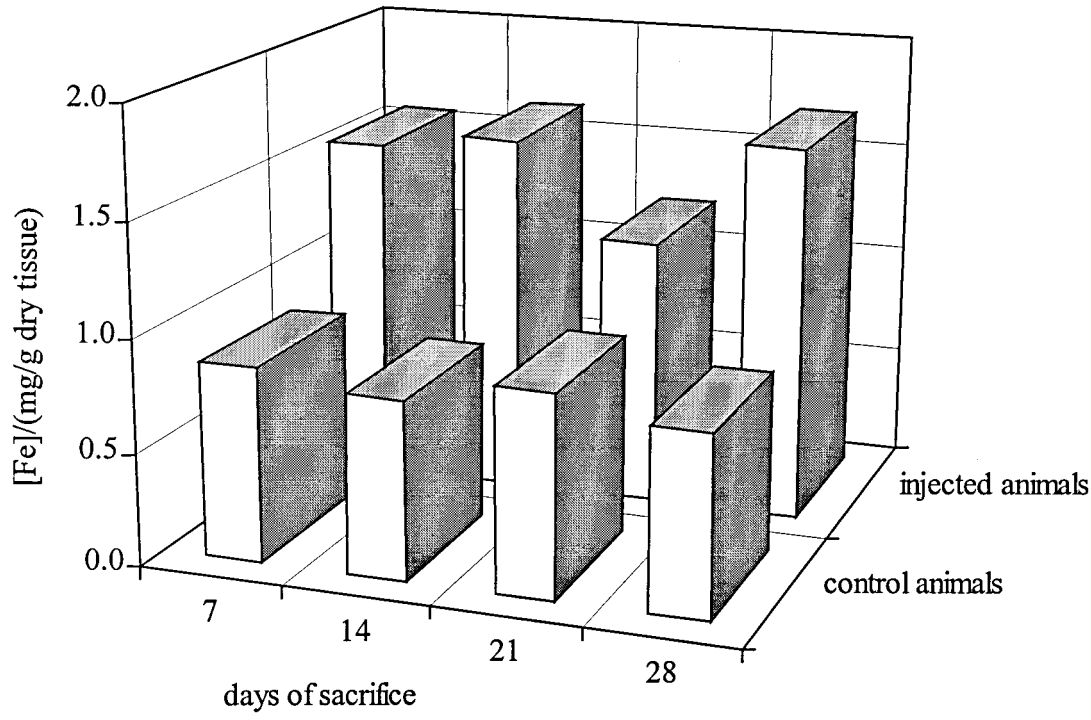

Figure 4.6. Comparison of iron concentration in mice spleen groups after several injections with a solution of metallic iron and the respective control animals. The animals were sacrificed at days 7, 14, 21 and 28. Values attained by AdSV.

Comparison between the means of each group at day of sacrifice and the control animals showed a significant increase ($P<0.01$) of iron in the kidneys through this study, namely till day 21 (Figure 4.7). At day 7 the iron increase is about 24% whereas at day 21 rises to 48%. However, a reduction in the amount of iron was

denoted at the last group of experimental animals, *i.e.* an iron increase of only 18%. This result may explain the severe alterations in the renal tubules, suggesting that it was partially released by them inducing in this way those remarkable changes.

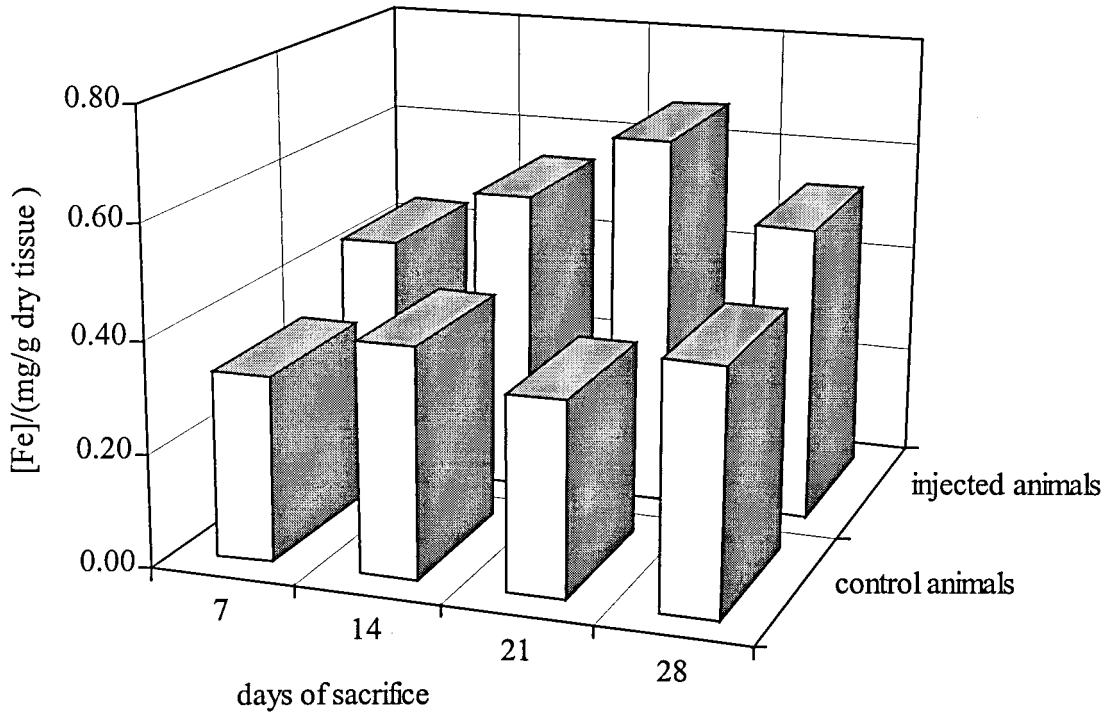

Figure 4.7. Comparison of iron concentration in mice kidney after several injections with a solution of metallic iron and the respective control animals. The animals were sacrificed at days 7, 14, 21 and 28. Values attained by AdSV.

Morphological observations

No animal mortality or signs of illness were observed during this study nor apparent signs of toxicity associated with the iron injections. The removed organs did not present macroscopic changes, even during the last week of group IV. No significant differences ($P>0.01$) were observed in body weights before the treatment with injected iron solution and at the days of sacrifice.

Observations of hepatic and splenic sections from all groups of control animals reveal apparently normal morphological structures compared to some published results obtained in similar experimental conditions [42,43].

The hepatic parenchyma of all groups iron-injected animals present a normal architecture of the liver, being relevant the presence of ordered arrays of hepatocytes and normal cellular details. However, the last period injected animals reveals some changes in the hepatocytes, being the nuclei strongly stained with normal features (Figure 4.8).

Splenic sections of iron-injected mice are similar to those of related control groups (Figure 4.9a). Nevertheless at the last administration period, some morphological changes were seen among the stroma. The capsule evidences regular thickness and morphology and trabeculae are also seen (Figure 4.9b). Clear

differences are also noted between red and white pulp (Figure 4.9c). However, depletion of extensive areas among the red pulp was also documented.

No structural damage was evidenced in the renal sections obtained from the control group of animals (Figure 4.10a). The overall structure of both glomeruli as well as renal tubules is apparently normal. In addition, the sections obtained from 7 days injected mice evidenced no alterations being very similar to the control. Histological sections from mice sacrificed by 14 day exhibited minor morphological changes in the distal convoluted tubules as evidenced in Figure 4.10b. Furthermore a large number of mildly to moderately affected renal tubules were found by 21 days of sacrifice (Figure 4.10c). Kidney of the last group of animals, namely those sacrificed by 28 days evidenced remarkable degenerative features being compared to the previous group (Figure 4.10d).

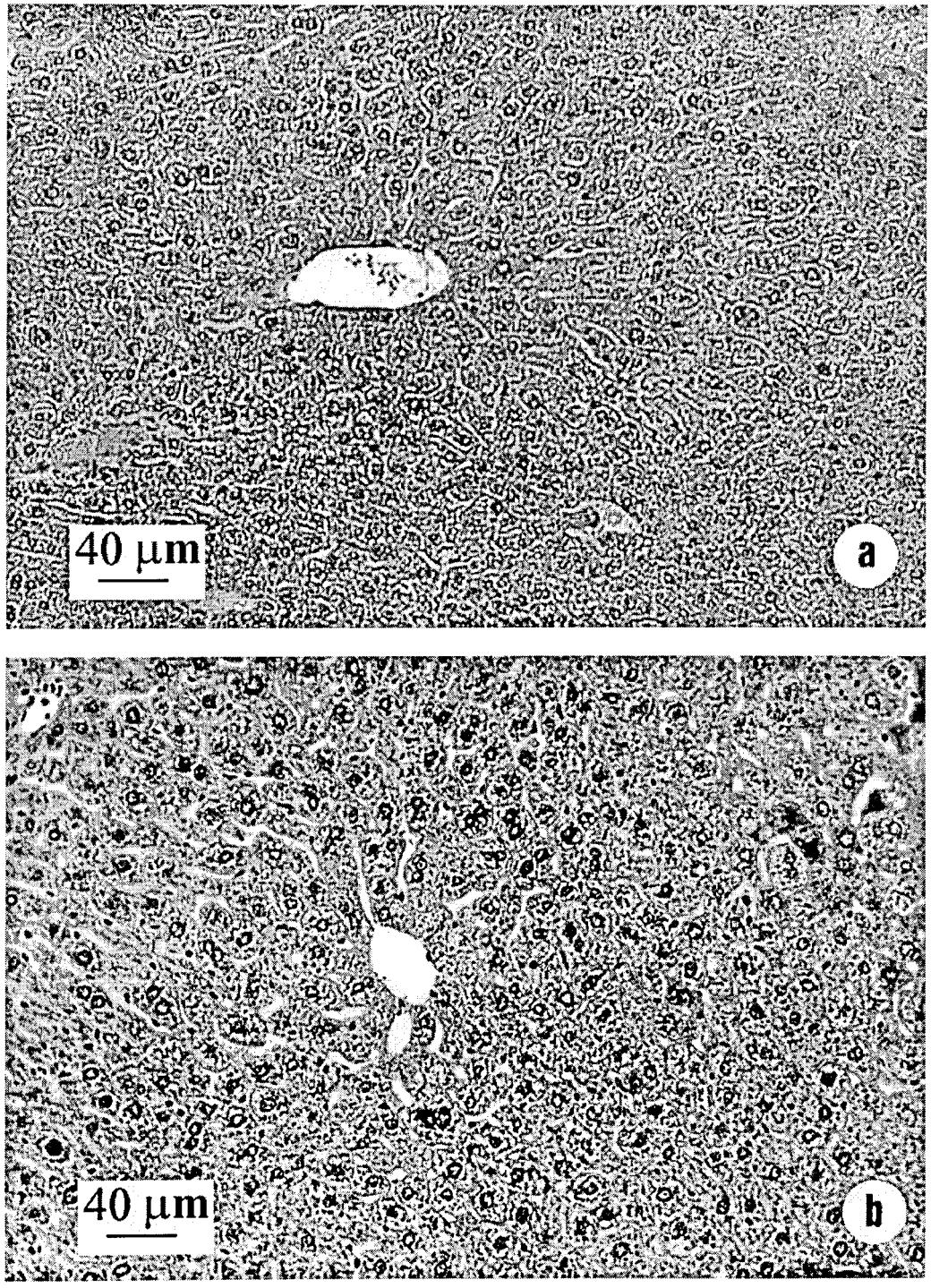

Figure 4.8. Histological features from: a) control and b) 21-days-iron-administered. Mice liver presenting some morphological differences. Although arrays of hepatocytes are well evidenced in both groups, hypercromatic nuclei are clearly seen in the last period dosing.

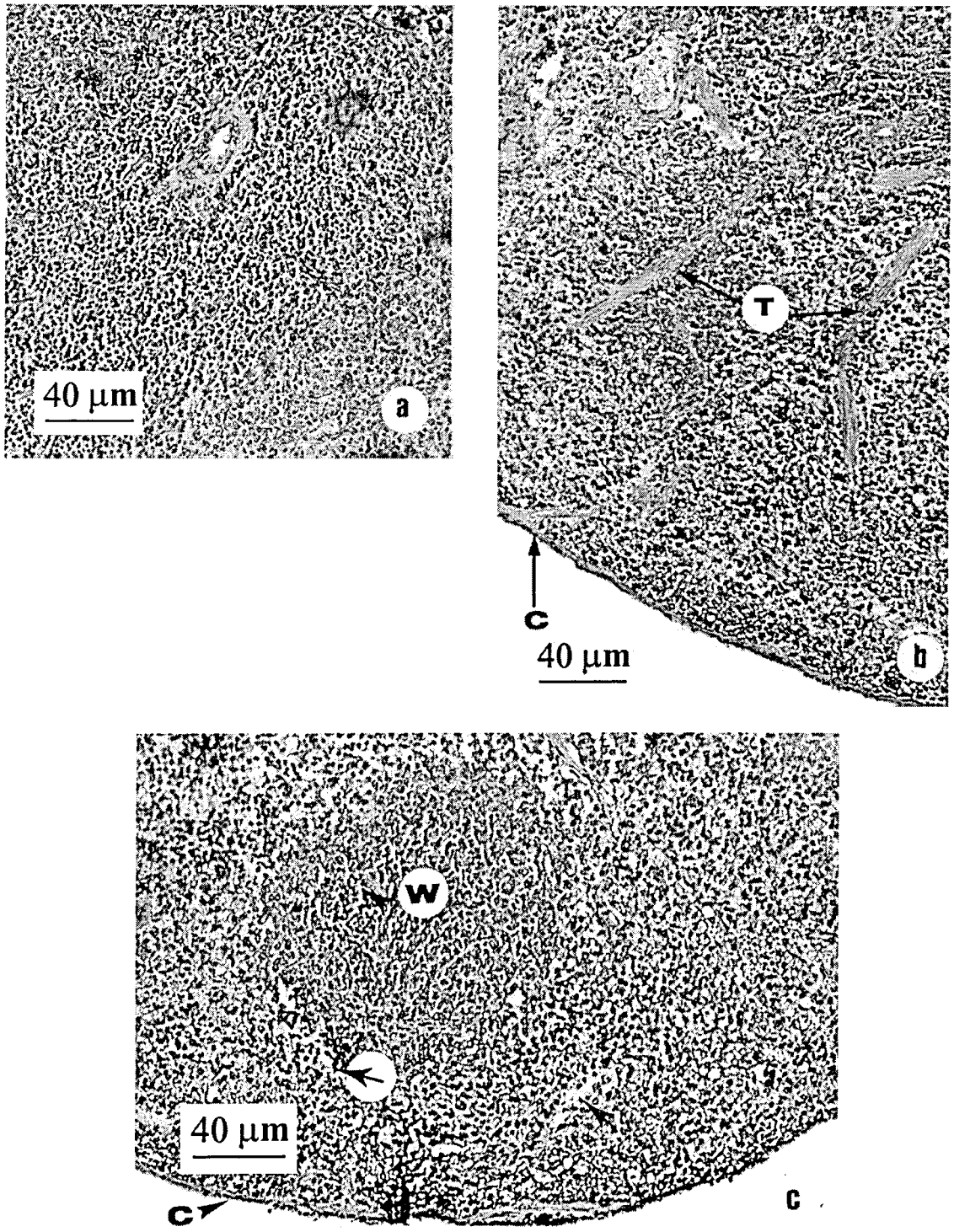

Figure 4.9. Splenic histological features from: a) control and b, c) 21-days-iron-administered mice. Capsule (C) and trabeculae (T) display regular features. Cell deflection is clearly shown (arrows). (W) white pulp.

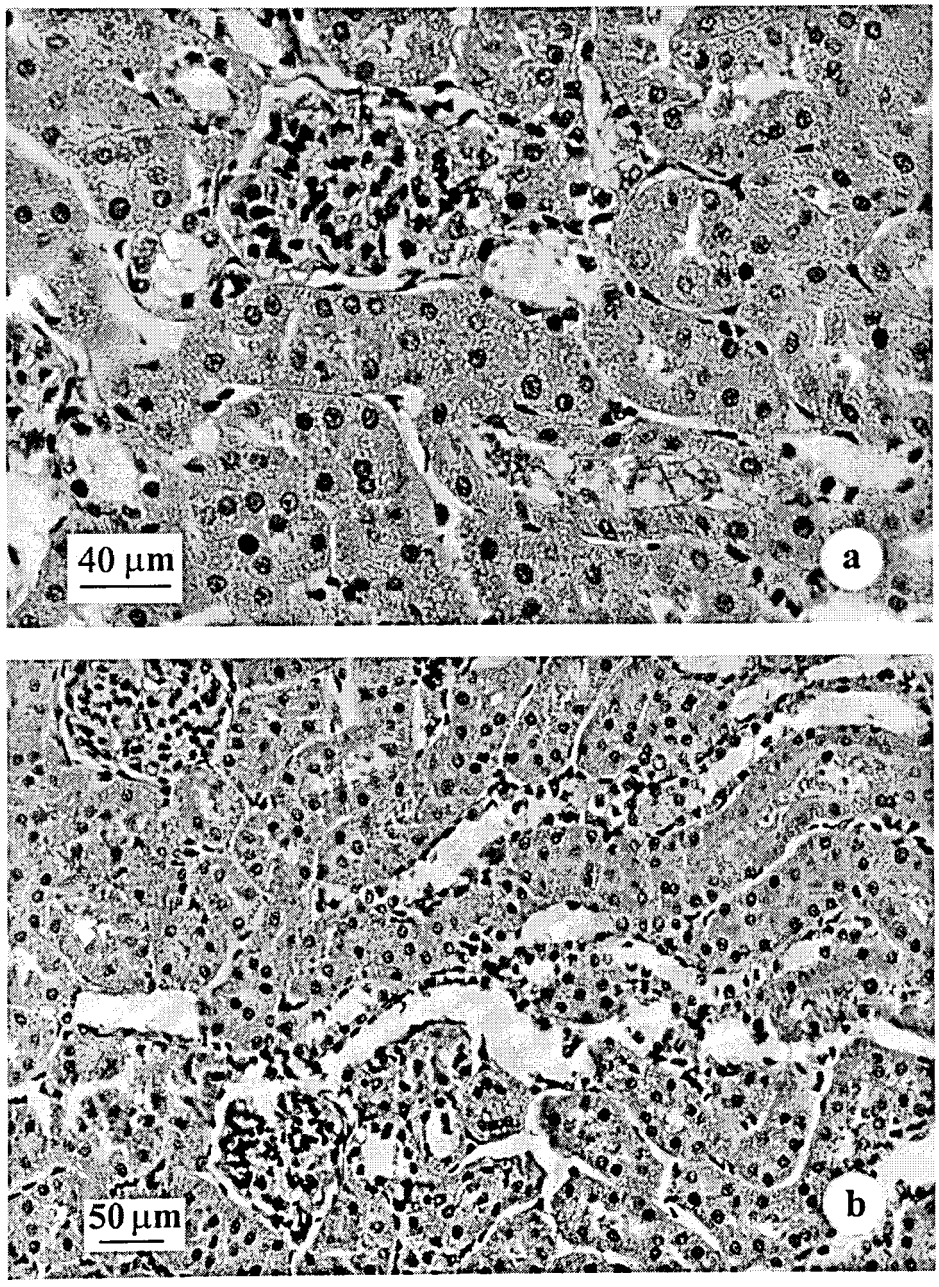

Figure 4.10. a) Histological section of a control kidney through the cortex area showing a typical glomerulus and different aspects of renal tubules with normal morphology. b) Histological features of the kidney from a 14 day injected mouse, showing minor changes in the distal convoluted tubules. Glomeruli and proximal convoluted tubules are apparently normal.

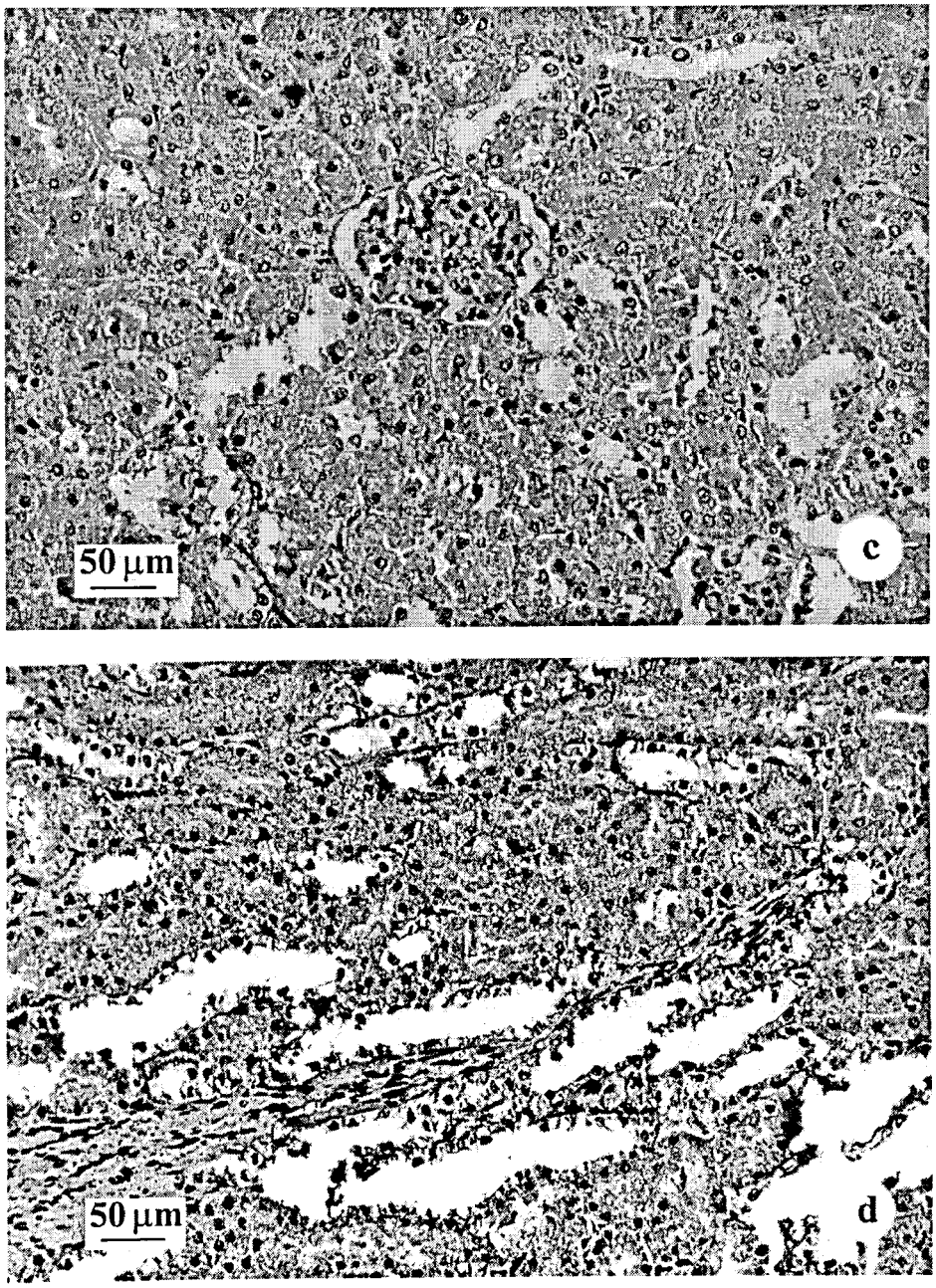

Figure 4.10. c) Several changes are observed in a renal section from a mouse sacrificed after 21 days. The typical histology is characterised by degeneration and necrosis of the epithelium lining the renal tubules. However, glomerulus seems to be preserved. d) Similar degenerative changes are observed in the kidney of the last dosing group of mice. Disruption of the epithelium in the renal tubules is clearly evidenced.

DISCUSSION

The accuracy and reproducibility of the iron results obtained by both methods, *i.e.*, AdSV in combination with the MFM using catechol as the complexing agent and AAS, give credence to the proposed method. The differences between the two methods were within 0.90-4.32%.

The detection limit obtained by this electrochemical method is adequate for the iron quantification in numerous biological materials such as liver, spleen, lung and body fluids. It is only needed a small sample quantity for reliable results once this is the metal most abundant in biological materials [23].

One inconvenient of using flameless atomic absorption spectrometry is that it is necessary a considerable amount of sample to work in the range of few mg/L. Using the graphite furnace the dilution factors applied to the biological samples are enormous and can lead to erroneous results.

The success of the AdSV technique is only achieved with a complete destruction of the organic matter. If residues of organic matter remained, they adsorb onto the mercury surface negating the access of the metal ion in analysis. However, one limitation of the AdSV techniques is the relative selectivity of the complexing agents for other ions present in solution. Catechol complexes simultaneously with copper giving a very sensitive peak at -0.220 V near the iron peak [44].

AdSV using microelectrodes reduces considerably the sample volume and also the analysis time is dramatically diminished when compared to the conventional electrodes and this is confirmed by previous studies done by the same group [35,45].

The large number of significant differences in iron concentrations of the liver, kidney and spleen found in the animals injected compared with the control groups give credence to the fact that this metallic element appears in the tissues far from the place of the injection which are significantly greater than the normal. The values found for iron concentration in the studied organs from control groups are very similar in magnitude to previous values reported by Smith and Black [46] in experimental studies with male New Zealand white rabbits.

From what is known about corrosion in patients who carries stainless steel implants, the tissues surrounding the alloy, may have an iron concentration that ranges between 300 to 3200 mg/L [9] or even higher some cases more. It is very complicated to predict the corrosion rate of implants once there are several factors that affect this phenomenon [5,47]. Normally, the estimated corrosion rates are very small [46,48]. In this study, the quantity of iron injected in mice was overestimated, considering an implanted area relatively large and suffering from accelerated corrosion.

Calculations were done to determine the percentage of metal that was injected and that is accumulated in the three organs and interesting results were obtained. After one week from the first injection (group I), the quantity of iron that was accumulated in liver, spleen and kidney was approximately 86 μg per animal in contrast with the quantity initially injected that was 269 μg. The quantity that is retained in the three organs is approximately 30% in group I and after the four weeks of treatment is nearly 22%. This means that iron enters in the normal metabolism and is accumulated in the body.

From the histological analysis, the presence of the iron excess during the treatment time compared with the control groups does not seem to induce significant damage in the tissues. It is obvious that these organs have a strong ability to accumulate the excess of iron in the body. In a normal human being 30% of the total body iron is stored in the form of ferritin and hemosiderin, primarily in the liver, spleen and bone marrow [49].

The major accumulation of this metal was seen in the liver. This organ has shown a variation in the iron content with time. The small changes observed in hepatocytes suggest that iron is confined to that cells [50].

Apparently the spleen exceed its capacity to store iron. In this organ, the iron from haemoglobin is recovered and temporarily stored in cells. This iron is supplied in accordance with the organic needs, being employed in the formation of

new haemoglobin. As demonstrated by histological data some cell depletion was observed among the red pulp at the last iron-administration period. This result may be related to the high concentration of iron in this organ, as revealed by the present analytical studies.

The kidney was the organ more affected by the presence of the iron excess [51]. There was a significant increase during the treatment time. At day 28 the iron concentration decreased significantly compared to the other sacrifice days suggesting that the iron accumulated starts to be eliminated, but at that time the metal induced remarkable degenerative features.

It is important to extend this study with longer periods of time to see if the high accumulations of iron induce deleterious alterations with time in the studied organs, once its behaviour showed to be dependent of the organ involved and of the duration of injections.

CONCLUSIONS

The application of square wave voltammetry using adsorptive collection of iron-catechol onto a MFM demonstrated to be an adequate method to quantify iron in biological samples.

The analytical results shown an increase of iron concentration in the liver, kidney and spleen compared with the control animals.

Iron was distributed from the site of injections throughout the body due to the fact that 20 to 30% of the total iron initially administered to mice appeared in the liver, kidney and spleen during the time of the experience.

During this time the organs showed a significant iron accumulation with the spleen to exceed its capacity to retain this metal.

No significant damage of the morphological aspect of tissues were observed during the treatment time, even so the kidney was the organ more affected by the presence of the accumulated iron.

REFERENCES

[1] J. B. Rheinold, *Clinical Chemistry*, **21** (1975) 476.

[2] R. R. Crichton and R. J. Ward, "*Iron and Human Diseases*", R. B. Lauffer (ed.), CRC Press, (1992), 23.

[3] S. R. Lynch, D. A. Lipschitz, T. H. Bothwell, R. W. Charlton, "*Iron in Biochemistry and Medicine*", A. Jacobs, M. Worwood (eds.), Academic Press, London, (1974) 563.

[4] J. Black, "*Biological Performance of Materials: Fundamentals of Biocompatibility*", Biomedical Engineering and Instrumentation, R. Plonsey and J. L. Katz (eds.), Marcel Dekker, New York, **8** (1981) 158.

[5] E. J. Sutow and S. R. Pollack, "*Biocompatibility of Clinical Implant Materials*", D. F. Williams (ed.), CRC Press, Boca Raton, Florida, (1981) 77.

[6].G. D. Winter, *J. Biomed. Mater. Res. Symposium*, **5** (1974) 11.

[7] G. D. Winter, "*Biocompatibility of Implant Materials*", D. F. Williams (ed.), London, (1976) 28.

[8] A. B. Ferguson Jr, P. G. Laing and E. S. Hodge, *J. Bone Joint Surg.*, **42A**, (1960) 77.

[9] O. E. M. Pohler, "*Biomaterials in Reconstructive Surgery*", L. R. Rubin (ed.), The C. V. Mosby Company, (1983) 196.

[10] F. Lux and R. Zeisler, *J. Radioanal. Chem.*, **19**, (1974) 289.

[11] M. Traisnel, D. Le Maguer H. F. Hildebrand and A. Iost, , *Clin. Mater.*, **5**, (1990) 309.

[12] K. Merritt, S. A. Brown, N. A. Sharkey, *J. Biomed. Mater. Res.*, **18** (1984) 991.

[13] K. Merritt, S. A. Brown, "*Corrosion and Degradation of Implant Materials: Second Symposium*", A. C. Fraker, C. D. Griffin, (eds.), American Society for Testing and Materials, Philadelphia, (1985) 195.

[14] K. Merritt, S. A. Brown, "*Clinical Applications of Biomaterials*", John Wiley & Sons, (1982) 85.

[15] J. L. Woodman, J. Black, S. Jimenez, "*Biomaterials 1980*", G. D. Winter, D. F. Gibbons, H. Plenk, Jr. (eds.), John Wiley & Sons, (1982) 245.

[16] K. Merritt, T. D. Growe, S. A. Brown, *J. Biomed. Mater. Res.*, **23** (1989) 845.

[17] B. A. I. Schafer, R. G. Cheron, R. Dluhy, B. Cooper, R. E. Gleason, J. S. Soeldner and H. F. Bunn, *N. Engl. J. Med.*, **304** (1981) 319.

[18] I. Bernat, "*Iron Metabolism*", Plenum Press, New York, (1983) 215.

[19] E. Gosztonyi, "*Iron Metabolism*", Plenum Press, New York, (1983) 339.

[20] E. D. Weinberg, "*Iron and Human Deseases*", R. B. Lauffer (ed.), CRC Press Inc., (1992) 179.

[21] C. L. Chakrabarti, C. C. Wan and W. C. Li, *Spectrochimica Acta*, **35B** (1980) 93.

[22] K. Nakamura, H. Watanabe and H. Orii, *Anal. Chim. Acta*, **120** (1980) 155.

[23] S. Lugowski, D. C. Smith and J. C. Van Loon *J. Biomed. Mater. Res.*, **21** (1987) 657.

[24] H. van Beek, H. C. A. Greefkes and A. J. Baars, *Talanta*, **34** (1987) 580.

[25] D. B. van Wyck, R. B. Schifman, J. Ruiz and D. Martin, *Clin. Chem.*, **43** (1988) 1128.

[26] D. Chakraborti, M. Burguera and J. L. Burguera, *Fresenius J. Anal. Chem.*, **347** (1993) 233.

[27] K. Brainina and E. Neyman, "*Electroanalytical Stripping Methods*", J. D. Winefordner (ed.), John Wiley & Sons, New York, (1993) 71.

[28] B. J. Basu and S. R. Rajagopalan, *Analyst*, **117** (1992) 1623.

[29] S. B. Adeloju, A. M. Bond and M. H. Briggs, *Anal. Chim. Acta*, **164** (1994) 181.

[30] R. M. Wightman, *Anal. Chem.*, **53** (1981) 1125A.

[31] D. Pletcher, "Microelectrodes. Theory and Applications", M. I. Montenegro, M. A. Queirós and J. L. Daschbach (eds), Nato-ASI, Kluwer Academic Publishers, The Netherlands, (1991) 3.

[32] M. Wojciechowski, W. Go and J. Osteryoung, *Anal. Chem.*, **57** (1984) 155.

[33] R. Kalvoda and M. Kopanica, *Pure & Appl. Chem.*, **61** (1989) 97.

[34] J. Wang, "*Stripping Analysis*", VCH Publishers, (1985) 9.

[35] M. C. Pereira, J. L. Faria, M. L. Reis and J. P. Sousa, *Electroanalysis,* **9** (1997).

[36] C. M. G. van den Berg and Z. Q. Huang, *J. Electroanal. Chem.*, **177** (1984) 269.

[37] S. Morais, G. S. Carvalho and J. P. Sousa, *Electroanalysis*, **10** (1997).

[38] J. Wang and S. Mannino, Analyst, **114** (1989) 643.

[39] G. Capodaglio, C. M. van den Berg and G. Scarponi, *J. Electroanal. Chem.*, **235** (1987) 275.

[40] C. M. G. van den Berg, *Anal. Chim. Acta*, **164** (1984) 195.

[41] J. N. Miller, *Analyst*, **116** (1991) 3.

[42] M. L. Pereira, M. C. Pereira and J. P. Sousa, *Biomedical Letters*, **52** (1995) 235.

[43] M. C. Pereira, M. L. Pereira, J. P. Sousa, in press *J. Biomed. Mater. Res.* (1997).

[44] M. C. Pereira and J. P. Sousa, *Portugaliae Electrochimica Acta*, **14** (1996) 273.

[45] M. C. Pereira, M. L. Pereira and J. P. Sousa, *Electroanalysis*, **9** (1997) 941.

[46] G. K. Smith and J. Black, "*Corrosion and Degradation of Implant Materials: Second Symposium*", A. C. Fraker and C. D. Griffin (eds)., American Society for Testing and Materials, Philadelphia, (1985) 223.

[47] M. A. Barbosa, "*Biomaterials Degradation*", M. A. Barbosa (ed.), Elsevier Science Publisher, The Netherlands, (1991) 227.

[48] S. G. Steinemann, "*Evaluation of Biomaterials*", G. D. Winter et al. (eds.), United Kingdom, (1980) 1.

[49] G. K. Smith, "*Biomaterials in Reconstructive Surgery*", L. R. Rubin (ed.), The C. V. Mosby Company, (1983) 229.

[50] R. S. Britton, G. A. Ramm, J. Olynyk, R. Singh, R. O'Neill and B. R. Bacon, "*Progress in Iron Research*", C. Hershko et al. (eds.), Plenum Press, New York, (1994) 239.

[51] M. C. Pereira, M. L. Pereira and J. P. Sousa, submitted to *Journal of Trace Elements in medicine and Biology*, (1997).

Chapter 5

CONCLUSIONS

5

CONCLUSIONS

A summary of the principal conclusions that can be drawn from the results discussed in chapters 2, 3 and 4 is presented in this chapter, and are the following:

Electrochemical method proposed

The application of mercury film microelectrodes with the stripping techniques available are very easy to implement and is a promising technique to complement with the AAS for evaluation and monitoring the uptake of metals by the organism.

However, the major limitation of the stripping analysis is the number of elements that could be quantified by this technique.

AdSV using MFM was the electrochemical method proposed to quantify the iron, chromium and nickel contents in the studied mice organs. Adequate methodology was developed and was found to give reliable and reproductive results. This technique also offers the advantage of attaining very low detection limits and proved its ability for monitoring essential and toxic elements in biological samples.

The ligands that were more appropriate to be used with this type of samples were: dimetylglioxime, DTPA and catechol to complex with nickel, chromium and iron, respectively.

The sample treatment, *i.e.*, the digestion procedure is a step of crucial importance for the success of the proposed electrochemical method. During the mineralisation process some proteins lead to the formation of the *p*-nitrobenzoic acid that strongly adsorbs on the mercury electrode surface inhibiting the metals signals and they are only destroyed in the presence of the perchloric acid.

The methodology proposed for the determination of the major elements of the stainless steel alloy in the digested biological samples does not differ essentially

from those suggested for analysis of natural and sea waters. This clearly demonstrates that the salts resulting from the complete destruction of the organic matter do not interfere with the metals determination and the major interferences arising from other metals that compete with the ligands chosen once they are present in very high concentrations.

The high accuracy of the analysis results for iron, chromium and nickel obtained by coupling MFM with AdSV was confirmed by the AAS analysis, for which no statistically significant discrepancies between both techniques were found.

Accumulation and histological effects in mice

The metallic elements in study appear in the tissues far from the place of the injections once after the injection schedule all animal groups have a significant increase of chromium, iron and nickel when compared with the values found in the control groups.

During the first two weeks of treatment normal morphology was seen in the liver, kidney and spleen for the three metals studied. At the fourth week, mice

groups presented some morphological alterations induced by the presence of the nickel and iron.

The quantity of nickel that remained in the studied organs were less than 1% compared with the quantity of this metal initially injected. Nevertheless, nickel was the metal that provoked more relevant morphological alterations in the studied organs.

Chromium behaved in a similar way to nickel being almost totally eliminated by the organism. Moreover, the quantity that remained in the local organs was indicative of a strong accumulation. However, no morphological changes in tissues were observed after four weeks of treatment.

20 to 30% of the iron initially injected was accumulated in the studied organs provoking a rise in the iron levels compared to the control animals. Only slight changes were observed in the morphology of the tissues and the kidney was the organ more affected by the presence of so high iron levels.

PRACTICAL CONTRIBUTIONS OF THIS WORK

With this work it is hopped to give a valid contribution to the increase use of microelectrodes in combination with adsorptive stripping techniques in studies of trace metals in biological and/or other types of samples, once they have demonstrated to be very flexible to adapt to the electrochemical equipment associated with low costs and having a rapid response with high sensitivity.

The animal model used to study the effects provoked by the stainless steel corrosion products *per si*, was performed in mice and lead to a better understanding of the potential metal effects in organs of vital importance such as the liver and the kidney. It is important to remember that potentially negative effects due to the metal ions release may only be detectable after several years. However, the results from the present thesis are potentially important and serve as an encouragement for controlled studies considering relatively longer periods of time.

APPENDIX

Histological technique

Optimised programs for AAS

HBSS composition

Histological technique

1. Dissection and fixation

After mice dissection, pieces (3-5 mm thick) of the collected organs: liver, kidney and spleen, were quickly fixed in Bouin's Solution for 24 h. This technique avoids the destruction of cells by their own enzymes or bacteria, besides to harden the tissues, becoming more resistant to the subsequent steps of the histological technique.

2. Dehydration, impregnation and inclusion

After fixation the tissues are not firm enough to enable thin sections and, therefore, they must be embedded in a medium which completely infiltrates and surrounds the tissue giving hardness. For normal preparations paraffin wax is used. The water content present in tissues do not permit the infiltration of the paraffin and it is necessary to dehydrate the tissues.

The elimination of the water content present in the tissues was done by successive passages in bathing of ethanol with crescent grades:

ethanol 70°	24 h
ethanol 90°	1 h
ethanol 100°	1 h
ethanol 100°	30'

Furthermore, the pieces were submitted to one passage with ethanol and benzol in equal parts during 30 minutes and finally with pure benzol during 1hour and 30 minutes.

The following stage is the tissue impregnation with paraffin wax (Melting Point 52-55°C). The pieces were immersed in a bath of melted paraffin wax for complete penetration in all tissue cavities.

3. Sectioning and staining

Sections of 3-5 μm thick were cut with a Leitz 1512 microtome. These sections were placed on a glass slide containing albuminous water.

Routine staining of paraffin sections requires dewaxing and was done with xilol baths. The rehydrating was processed with:

ethanol 100°	5'

ethanol 95°	5'
ethanol 75°	5'
ethanol 50°	5'
tap water	15-30'

The purpose of staining is to differentiate the tissue elements to be recognised and examined under the light microscope.

Heamatoxylin and eosin were employed as general stains and the procedure was the following:

heamatoxylin	15'
tap water	15'
eosin	2'

The staining of these sections with heamatoxylin and eosin evidences the nuclei in violet blue, the cytoplasm in more or less intense rose and the elastic fibres in rose. This technique, also permits good conservation of cell morphology.

Once again it was necessary to dehydrate the pieces and is processed through ascending ethanol grades.

ethanol 95° (passage)

ethanol 100° (passage)

Sometimes, the histological pieces have stain in excess and it was necessary to clearing the preparation to become more transparent and this was done with xilol.

4. Mounting and drying

Mounting consist in the placement of the material in conditions to be observed by the microscope. The sections were mounted with Canada balsam after which the lamella is placed up avoiding air bubbles. The balsam solidify making adherence between the lamina and lamella. The balsam dryness is slow and the preparations were placed in the stove at 60 °C during 3-5 days to verify the complete dryness.

Optimised programs for AAS

The programs presented in Tables I and II apply to a spectrometer Perkin Elmer Model 4100ZL and were optimised for the digested mice organs samples using the procedures recommended by the manufacturer. Pyrolytic graphite tubes were used for sample atomisation.

Table I. Furnace program for determination of nickel in the digested mice organs samples.

		Time, s	
Stage	**Temp, °C**	**Ramp**	**Hold**
Drying	110	1	20
Drying	130	5	30
Pyrolysis	1400	10	20
Atomisation	2300	0	5
Clean-out	2400	1	2

Table II. Furnace program for determination of chromium in the digested mice organ samples.

		Time, s	
Stage	**Temp, °C**	**Ramp**	**Hold**
Drying	110	1	20
Drying	130	5	30
Pyrolysis	1200	10	20
Atomisation	2400	0	5
Clean-out	2500	1	2

The injection volume was 20 μL, the injection temperature at 20 °C. and the flow gas was argon 250 mL/min. During the atomisation step the flow gas is stopped.

In Table III is presented the instrumental parameters used in the flame atomic absorption for the determination of iron using a spectrometer Model GBC 904AA as well as the optimised parameters for the digested mice organs samples.

Table III. Instrumental parameters for the determination of iron in the digested mice organ samples.

Wavelength (nm)	248.3
Lamp current (mA)	7.0
Flame type	Air-Acetylene (oxidising)
Acetylene flow	2.10
Air flow	12.2
Working range (ppm)	0.50 - 4.0

HBSS composition

Table IV. Composition of HBSS Hanks' Balanced Salt Solution (Sigma)

COMPONENT	g/L
Inorganic salts	
Sodium Chloride	8.0
Potassium Chloride	0.40
Sodium Bicarbonate	0.35
Calcium chloride.2H2O	0.185
Magnesium Sulfate (anhydrous)	0.10
Potassium Phosphate (anhydrous)	0.06
Sodium Phosphate (anhydrous)	0.05
Other	
D-Glucose	1.0
Specification	
pH at RT (with sodium bicarbonate)	7.3±0.3